INFORMATION TO USERS

This manuscript has been reproduced from the microfilm master. UMI films the text directly from the original or copy submitted. Thus, some thesis and dissertation copies are in typewriter face, while others may be from any type of computer printer.

The quality of this reproduction is dependent upon the quality of the copy submitted. Broken or indistinct print, colored or poor quality illustrations and photographs, print bleedthrough, substandard margins, and improper alignment can adversely affect reproduction.

In the unlikely event that the author did not send UMI a complete manuscript and there are missing pages, these will be noted. Also, if unauthorized copyright material had to be removed, a note will indicate the deletion.

Oversize materials (e.g., maps, drawings, charts) are reproduced by sectioning the original, beginning at the upper left-hand corner and continuing from left to right in equal sections with small overlaps.

Photographs included in the original manuscript have been reproduced xerographically in this copy. Higher quality 6" x 9" black and white photographic prints are available for any photographs or illustrations appearing in this copy for an additional charge. Contact UMI directly to order.

ProQuest Information and Learning
300 North Zeeb Road, Ann Arbor, MI 48106-1346 USA
800-521-0600

Université d'Ottawa · University of Ottawa

USE OF PC12 CELLS TO CHARACTERIZE PAFR-GPCR-MEDIATED ACTIVITY IN NEURAL PRECURSORS

Cynthia Brewer

A Thesis submitted to
the Faculty of Graduate and Postdoctoral Studies
in partial fulfillment of the requirements for the degree of
Master of Science

Department of Biochemistry, Microbiology and Immunology

University of Ottawa,
Ottawa, ON, Canada

THESIS ABSTRACT

Platelet activating factor (PAF: 1-*O*-alkyl-2-acetyl-*sn*-glycero-3-phosphocholine) is a biologically active phospholipid mediator produced by neurons and glial cells. In adult central nervous system (CNS), physiological concentrations of PAF have been shown to mediate long-term potentiation, the purported cellular basis of mammalian learning and memory. Elevated levels of PAF are implicated in the pathophysiology of a number of neurodegenerative diseases, ischemia-reperfusion injury, human immunodeficiency virus-1 (HIV-1) associated dementia, and the developmental brain disorder Miller-Dieker Syndrome (MDS). Three neuropathologies are associated with sustained PAF exposure. Following ischemic attack or HIV-1 infection, PAF is implicated in neuronal loss in both adult and developing brain. In MDS, defective PAF catabolism is associated with inappropriate neural precursor proliferation and incomplete neuronal migration.

It is not clear how these PAF-mediated effects are initiated in CNS. A seven transmembrane G-protein coupled receptor (PAFR-GPCR) has been cloned and mRNA is expressed in CNS. In addition, distinct intracellular receptor isoforms (iPAFRs) in rodent cortical extracts have been characterized pharmacologically. It is not known which of these PAF binding proteins initiate PAF-mediated neuropathology. Our ability to detect PAF receptors is further hindered by a lack of commercial PAF antibodies. To address these issues, in this thesis, I sought to:

(1) Identify a neural precursor cell line capable of differentiating between PAFR-GPCR and iPAFR-initiated biological activity,

(2) Determine the effect of PAFR-GPCR activation on differentiation of neural precursors to a neuronal phenotype, and

(3) Characterize a new PAFR-GPCR antibody to facilitate localization of protein in CNS and CNS cell lines.

These studies were performed using the rodent pheochromocytoma PC12 cell line; a culture system widely employed as a model of neuronal differentiation, signal transduction, and cell death. In Chapter 1, experimental data is presented demonstrating that PAF triggers apoptotic cell loss independently of PAFR-GPCR. PC12 cells do not express PAFR-GPCR but are capable of responding to ligand. Apoptosis was confirmed by four different techniques assessing PAF-induced nuclear and chromatin condensation, DNA strand breaks, DNA fragmentation into histone-associated oligonucleosomes, and nuclear disintegration into apoptotic bodies. Cell death was PAF-specific, in that it was not elicited by *lyso*-PAF, the immediate metabolite and precursor of PAF. The kinetics of cell death was dependent upon activity of functional PAF acetylhydrolases expressed by PC12 cells, capable of inactivating PAF ligand. Apoptosis was receptor-mediated, in that, it could be blocked by five different PAF antagonists and could not be attributed to physicochemical effects on the plasma membrane. PC12 cells, lacking endogenous rodent PAFR-GPCR expression, were transfected with a constitutively active human PAFR-GPCR construct. Unexpectedly, PAFR-GPCR expression in PC12 cells protected cells

from PAF-induced apoptosis. We propose that a novel binding protein (possibly an iPAFR) triggers apoptotic loss of PC12 cells whereas PAFR-GPCR activation may promote cell survival.

In Chapter 2, studies were performed to determine whether sustained PAFR-GPCR activation impacts upon pathological neural precursor proliferation or migration consistent with the MDS phenotype. Data indicate that transfected clones fail to undergo relative growth arrest when differentiated to a neuronal phenotype. Evidence is also presented to justify speculation that PAF is synthesized during differentiation. PAFR-GPCR activation by endogenous PAF stimulates neural precursor proliferation but does not affect neuronal migration. These data imply that chronic exposure to PAF *in vivo* may delay the ability of neural precursors expressing PAFR-GPCR to exit the cell cycle and thereby inhibit the appropriate timing of migration of neurons characteristic of MDS.

Finally, in Chapter 3, characterization of a novel PAFR-GPCR antibody is presented to assist in protein analysis *in vitro* and *in vivo*.

In summary, PAFR-GPCR is likely involved in aberrant neural precursor proliferation. Other PAF receptors, not yet identified at the molecular level, are responsible for initiating PAF-mediated neuronal death.

ACKNOWLEDGMENTS

I would like to thank my supervisor Dr. Steffany Bennett, for giving me the opportunity to work on this challenging project. I am grateful for the time, energy, enthusiasm, support and patience, which was in generous supply over the past two years. I would also like to thank the members of my thesis advisory committee Dr. D. Franks, Dr. H. C. Birnboim and Dr. M. Sikorska-Walker for all their helpful suggestions and comments. In particular a special thank you to Dr. D. Franks for the use of the microscopy equipment and advice in immunohistochemistry.

In addition, I would like to express my appreciation to the Bennett Lab members (present and past) who contributed in part to collection of the data reported in this thesis: Fanny Bonin, Jen Morin and Marie-Christine Nault. Finally, I wish to extend my gratitude to all the members of the Bennett laboratory for their technical assistance and encouragement. Thank you all very much.

TABLE OF CONTENTS

THESIS ABSTRACT ii
ACKNOWLEDGMENTS v
TABLE OF CONTENTS vi
LIST OF FIGURES viii
LIST OF TABLES x
LIST OF ABBREVIATIONS xi
CHAPTER 1: GENERAL INTRODUCTION 1
Platelet Activating Factor: Overview 1
PAF Anabolic and Catabolic pathways 2
PAF Signal Transduction in the Adult Central Nervous System 4
Signaling events initiated by PAFR-GPCR 5
Neurotoxic effects of PAF 8
PAF and Neuronal Differentiation 9
Objective 14
CHAPTER 2: CHARACTERIZATION OF AN *IN VITRO* MODEL TO STUDY PAF LIGAND/PAFR-GPCR INTERACTION 15
Introduction 15
Objective 15
Materials and Method 16
Cell Culture 16
Generation of hPAFR-GPCR and empty vector stable transfectants 17
RT-PCR 17
Northern analysis 19
Western blot analysis 20
PAF acetylhydrolase activity assay 21
Cell survival and cell death assays 21
Statistical analysis 23
Results 24
WT-PC12 cells lack endogenous PAFR-GPCR RNA expression 24
Characterization of stable hPAFR-GPCR and empty vector transfectants 24
PAFAH1b expression and activity 26
Acute PAF administration induces WT-PC12 cell loss 30
Sustained exposure to PAF agonist exacerbates cell loss 33
PAF-induced cell death is not mediated by downstream metabolites 35
PAF-induced cell loss is attenuated by selected PAF antagonists 36
PAF elicits nuclear condensation, DNA strand breaks, and oligonucleosomal DNA fragmentation 36
Expression of PAFR-GPCR protects cells from PAF-induced apoptosis 42
Discussion 44
CHAPTER 3: EXPRESSION OF hPAFR-GPCR RESULTS IN INCREASED PROLIFERATION DURING NEURONAL DIFFERENTIATION 51
Introduction 51
Objective 52
Model System 52

Materials and Method ____ 53
Cell Culture ____ 53
In vitro Cell Migration Assays ____ 53
Cell Proliferation Assays ____ 54
Immunohistochemistry ____ 55
PAF acetylhydrolase activity assay ____ 55
Statistical analysis ____ 56
Results ____ 56
Undifferentiated and NGF-differentiated Growth Analysis ____ 56
Expression of low, medium and high levels of hPAFR-GPCR protein has no effect on growth of undifferentiated cultures ____ 57
Expression of hPAFR-GPCR results in increased proliferation during NGF-induced differentiation to a neuronal phenotype ____ 61
Proliferation of hPAFR-GPCR transfected cells during NGF-induced differentiation is inhibited by the PAFR-GPCR specific antagonist CV3988 64
Exogenous PAF administration stimulates proliferation of hPAFR-GPCR expressing cells in low serum media ____ 67
In vitro migration assay ____ 67
PAF acetylhydrolase activity increases during NGF-induced differentiation 71
Discussion ____ 73
CHAPTER 4: CHARACTERIZATION OF A NEW PAFR-GPCR ANTIBODY DEVELOPED IN THE BENNETT LABORATORY ____ **81**
Introduction ____ 81
Materials and Methods ____ 81
Production of polyclonal anti-hPAFR-GPCR antiserum ____ 81
Generation of WT-PC12 expressing GFP-hPAFR-GPCR fusion construct 82
Western Blot analysis of hPAFR-GPCR antibody ____ 83
Proteomics performed on GFP-hPAFR-GPCR fusion protein ____ 83
Results ____ 84
Biochemical analysis of GFP-hPAFR-GPCR stably transfected into WT-PC12 cells and validation of hPAFR-GPCR polyclonal antibody ____ 84
Proteomic analysis of GFP-hPAFR-GPCR ____ 84
Discussion ____ 87
CHAPTER 5: GENERAL DISCUSSION AND CONCLUSIONS ____ **90**
REFERENCES ____ **94**
APPENDIX A ____ **110**

LIST OF FIGURES

Figure 1.1: The chemical structure of PAF and a summary of the anabolic and catabolic PAF pathways. 3
Figure 1.2: PAFR-GPCR structure-function relationships. 7
Figure 2.1: RT-PCR analysis of WT-PC12 cells demonstrates that undifferentiated and NGF-differentiated cells do not express PAFR-GPCR mRNA. 25
Figure 2.2: WT-PC12 cells were transfected with pcDNA3.1/GS containing the cDNA for hPAFR-GPCR. 27
Figure 2.3: Analysis of hPAFR-GPCR-V5 fusion protein expression using anti-V5 antibody. 28
Figure 2.4: RT-PCR analysis demonstrates mRNA expression of PAFAH1b subunits (LIS-1, PAFAH1b α1, PAFAH1b α2) in both undifferentiated and NGF-differentiated WT-PC12 cells. 29
Figure 2.5: PAF induces cell loss in WT-PC12 cells following acute administration. 32
Figure 2.6: Sustained exposure to PAF agonist exacerbates cell loss. 34
Figure 2.7: PAF-induced cell loss is not mediated by the PAF metabolite lyso-PAF. 37
Figure 2.8: Chemical structures of the PAF antagonists used in this study. 38
Figure 2.9: WT-PC12 cell survival is afforded by a variety of PAF antagonist following challenge with PAF. 39
Figure 2.10: WT-PC12 cells undergo apoptosis following PAF administration. 40
Figure 2.11: Expression of hPAFR-GPCR renders WT-PC12 cells impervious to PAF-induced cytotoxicity. 43
Figure 3.1: WT-PC12 cells reduce proliferation and extend neurites following NGF treatment. 58
Figure 3.2: Growth kinetics of WT-PC12, empty vector pGS-2 and hPAFR-GPCR expressing clone. 59
Figure 3.3: Expression of hPAFR-GPCR has no effect on growth of undifferentiated cultures. 60
Figure 3.4: Transfection of hPAFR-GPCR results in increased proliferation during NGF-induced differentiation to a neuronal phenotype. 62
Figure 3.5: Expression of the neuronal intermediate filament MAP2 following NGF-induced differentiation is not significantly affected by hPAFR-GPCR expression. 63
Figure 3.6: NGF elicits cell proliferation in hPAFR-GPCR expressing cells. PCNA is expressed more intensely in HPAFR-7 cells. 65
Figure 3.7: Increased cell proliferation during NGF-induced differentiation is mediated by PAF/PAFR-GPCR interaction. The PAFR-GPCR specific antagonist CV3988 blocks increased proliferation during NGF-induced differentiation in HPAFR-7. 66
Figure 3.8: Proliferation is dependent upon PAF/PAFR-GPCR interaction. 68

Figure 3.9: Exogenous PAF administration elicits cell proliferation in hPAFR-GPCR expressing cells. PCNA is expressed more intensely in HPAFR-7 cells. 69
Figure 4.1: Characterization of an hPAFR-GPCR antibody raised against a synthetic peptide corresponding to residues 125-138 of the human PAFR-GPCR. 86

LIST OF TABLES

Table 2.1: PAF acetylhydrolase activity in cytosolic fractions from undifferentiated cultures. 31
Table 3.1: Effect of hPAFR-GPCR expression on the net migration of differentiating PC12 cells. 70
Table 3.2: Comparison of PAF acetylhydrolase activity in cytosolic fractions from undifferentiated cultures. 72

LIST OF ABBREVIATIONS

ANOVA	analysis of variance
bp	base pair
BrdU-	5-Bromo-2'-deoxy-uridine
BSA	bovine serum albumin
CMV	cytomegalovirus promoter
CNS	central nervous system
DIG	digoxigenin
DMSO	dimethyl sulfoxide
DTNB	5,5'-dithiobis(2-nitrobenzoic acid); Ellman's reagent
DTT	dithiothreitol
EDTA	ethylenediamine tetraacetic acid
EthD-1	ethidium bromide homodimer
EtOH	ethanol
HIV-1	human immunodeficiency virus-1
HPAFR	WT-PC12 cells transfected with pcDNA3.1/GS/hPAFR-GPCR
hPAFR-GPCR	human sequence of PAFR-GPCR
IP	intraperitoneal
kD	kilodaltons
MAP	microtubule associated protein
MAPK	mitogen activated protein kinase
mc-PAF	PAFAH resistant PAF analog
MDS	Miller-Dieker Syndrome
NGF	nerve growth factor
PAF	platelet activating factor or 1-*O*-alkyl-2-acetyl-*sn*-glycero-3-phosphocholine
PAFAH	PAF acetylhydrolase
PAFR-GPCR	cloned seven transmembrane G-protein coupled PAF receptor
iPAFR	intracellular PAF receptor isoform
PAGE	polyacrylamide gel electrophoresis
PBS	phosphate buffered saline
pGS	WT-PC12 cells transfected with pcDNA3.1/GS
PLA_2	phospholipase A_2
PCNA	proliferating cell nuclear antigen
PVDF	polyvinylidene difluoride
RAS	Ribi adjuvant system
RNA	ribonucleic acid
ROS	reactive oxygen species
RT-PCR	reverse transcriptase-polymerase chain reaction
SDS	sodium dodecylsulfate
SSC	sodium chloride/sodium citrate
TUNEL	terminal deoxynucleotidyl transferase (TdT) dUTP nick end labeling

CHAPTER 1: GENERAL INTRODUCTION

Platelet Activating Factor: Overview

Platelet activating factor (PAF) or 1-*O*-alkyl-2-acetyl-*sn*-glycero-3-phosphocholine is a biologically active phospholipid mediator demonstrated to exert diverse physiological and pathological effects on a wide variety of cells and tissues. Perhaps best characterized for its involvement in inflammatory processes, PAF is also involved as a mediator in the endocrine, gastrointestinal, reproductive, cardiovascular systems and, salient to this thesis, the nervous system (for reviews see, Braquet and Rola-Pleszczynski, 1987; Braquet et al., 1987; MacLennan et al., 1996).

During the 1970s, Benveniste et al. (1972) described a lipid extract capable of stimulating platelet aggregation. Independently Muirhead et al. (1976) described a lipid extract capable of lowering blood pressure. Subsequent structural analysis revealed that both these compounds were PAF (Demopoulos et al., 1979; Blank et al., 1979; Benveniste et al., 1979). PAF is, in fact, a generic acronym used to refer to the family of structurally similar PAF-like compounds (for a review see, Pinckard et al., 1994). Based upon the chemical linkage at the *sn*-1 position, the ligand family is separated into three subclasses: alkyl-, alkenyl- and acyl-PAF. The predominant and most potent molecular species are alkyl-$C_{16}H_{33}$ or $C_{18}H_{37}$ PAF (Figure 1.1) (Pinckard et al., 1994). For the remainder of this thesis, I will use the acronym PAF to refer specifically to these two molecular species unless otherwise stated. Essential features of the chemical structure of PAF, required for maximum biological activity, are an alkyl ether moiety at the

sn-1 position, an acetyl group at the *sn*-2 position, and phosphocholine at the *sn*-3 position. Subtle structural changes are sufficient to cause significant decrease or the complete abolishment of all biological activities (Snyder, 1995). The requirement of an acetyl group at the *sn*-2 position is essential for the specificity and biological activity of PAF and is underlined by the complete loss of biological activity when PAF is converted to *lyso*-PAF through the actions of PAF acetylhydrolase (PAFAH) (Snyder, 1995).

PAF Anabolic and Catabolic pathways

The concentration of PAF present in biological systems is regulated by (1) synthesis via one of two possible pathways and (2) rapid degradation by the action of PAF acetylhydrolase. PAF can be synthesized via the *de novo* or remodeling pathways, both of which have been reviewed extensively (see Snyder, 1994, 1995) (Figure 1.1). The *de novo* pathway is a three enzymatic step pathway beginning with an intermediate in the synthesis of ether-linked phospholipids (Figure 1.1). The remodeling pathway is a two enzymatic step pathway, whereby a resident membrane phospholipid precursor of PAF is transformed into PAF (Figure 1.1).

Protracted exposure to high concentrations of PAF has been implicated in a variety of pathologies (Braquet et al.,1987; MacLennan et al., 1996). The half-life of PAF is regulated by a family of PAF acetylhydrolases (PAFAHs). Although

Figure 1.1: The chemical structure of PAF and a summary of the anabolic and catabolic PAF pathways.

The general chemical structure of PAF is represented in grey. The predominant and most potent molecular species are indicated by the R group at the *sn*-1 position as alkyl- $C_{16}H_{33}$ or $C_{18}H_{37}$ PAF. In this thesis, the acronym PAF refers specifically to these two molecular species unless otherwise stated. PAF biosynthesis occurs via two independent pathways. The *de novo* pathway begins with the precursor lipid alkylglycerophosphate, an intermediate in the synthesis of ether-linked phospholipids. Alkylglycerophosphate is transformed into alkylacetylglycerophosphate by a specific acetyltransferase. Alkylacetylglycerophosphate is converted to PAF by sequential actions of a phosphohydrolase to yield alkylacetylglycerol, followed by a specific phosphocholinetransferase. The remodeling pathway produces PAF from alkylacylglycerophosphocholine, a phospholipid present in membranes. This phospholipid is transformed into lyso-PAF by PLA_2, which in turn is converted into PAF by lyso-PAF acetyltransferase. Note that PAF catabolism by PAF acetylhydrolase also yields lyso-PAF, which can be recycled to alkylacylglycerophosphocholine by acyltransferase. (adapted from Bazan, 1998; Francescangeli et al., 2000)

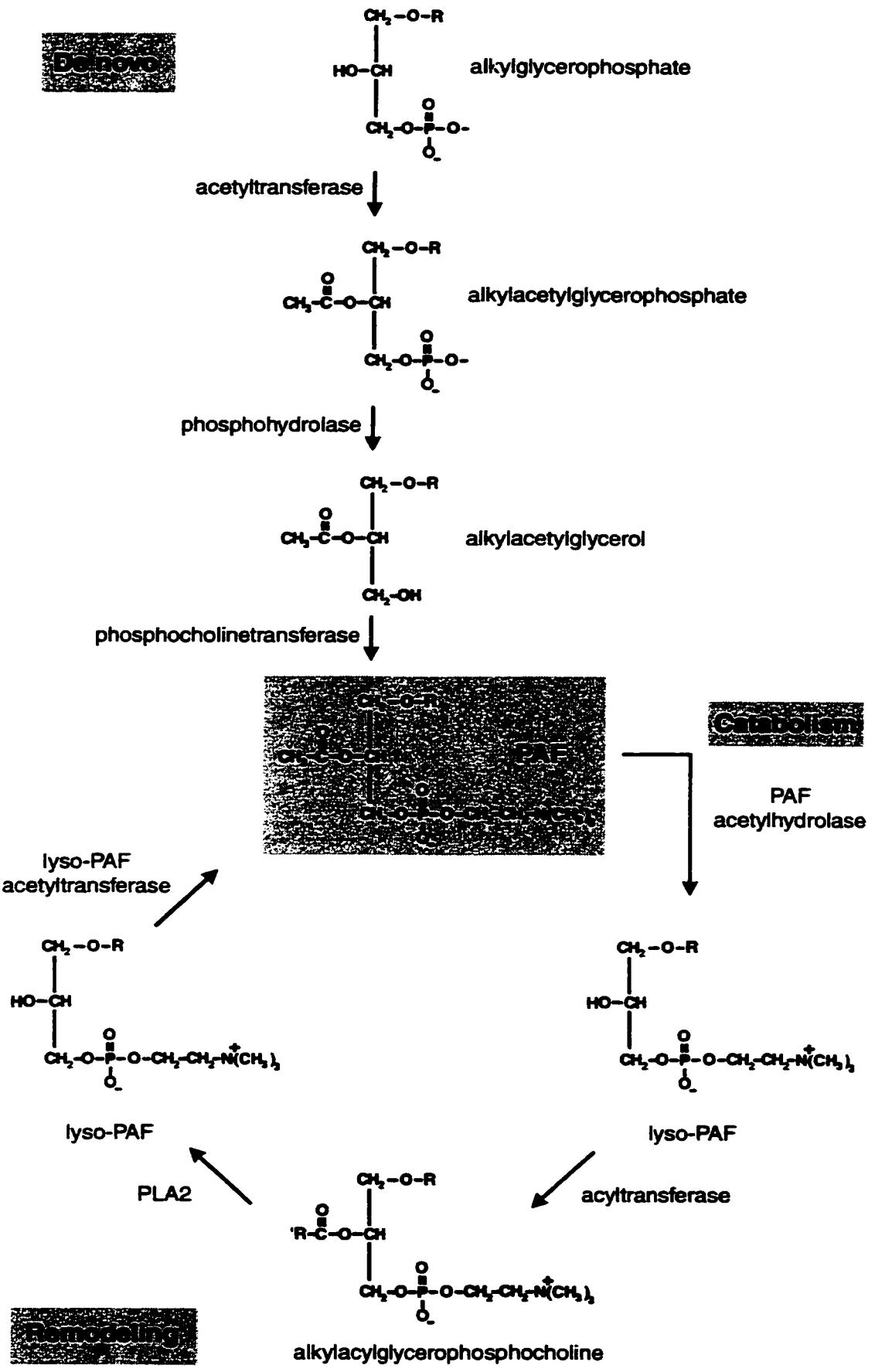
De novo
alkylglycerophosphate
acetyltransferase
alkylacetylglycerophosphate
phosphohydrolase
alkylacetylglycerol
phosphocholinetransferase
PAF
Catabolism
PAF
acetylhydrolase
lyso-PAF
acetyltransferase
lyso-PAF
lyso-PAF
PLA2
acyltransferase
alkylacylglycerophosphocholine
Remodeling

PAFAHs are structurally diverse isoenzymes, each enzyme is capable of catalyzing the hydrolysis of the acetyl group at the sn-2 position of PAF to generate the biologically inactive molecule *lyso*-PAF (Figure 1.1). Plasma PAFAH and two intracellular forms (Ib and II) of PAFAH, encoded by distinct genes, have been characterized (for a review see Stafforini et al., 1997; Prescott et al., 2000). Both the plasma PAFAH and intracellular PAFAH II isoforms are single polypeptide enzymes capable of PAF hydrolysis and the hydrolysis of oxidatively fragmented PAF-like lipids containing relatively long *sn*-2 acyl chains (Hattori et al., 1995; Stremler et al., 1991). In contrast, intracellular PAFAH Ib (the brain-specific PAFAH) is a heterotrimeric enzyme complex. This isoform is PAF-specific and does not recognize oxidized phospholipids as substrates (Hattori et al., 1993).

PAF Signal Transduction in the Adult Central Nervous System

PAF is a potent neuromodulator. The presence of PAF in the CNS has been demonstrated and its synthesis by neurons and glia is analogous to its synthesis in peripheral cells (Francescangeli et al., 2000; Baker, 1995). The biological activities of PAF are receptor-mediated and are not the result of physicochemical effects on the plasma membrane of target cells (for a review see Prescott et al. 2000). One PAF receptor, a G-protein coupled receptor (PAFR-GPCR), has been cloned and is expressed in CNS (Mori et al., 1997). Two high affinity binding sites, localizing to intracellular membranes (iPAFRs), and a low affinity binding site, localizing to the plasma membrane, have been

identified pharmacologically from rodent cortical protein extracts (Marcheselli et al., 1990). Note that receptor heterogeneity in the CNS is consistent with the pharmacological characterization of iPAFRs in the periphery (Shukla, 1992; Hwang, 1990). Both neurons and glia (astrocytes and microglia) respond to PAF. Compiled data from various studies indicate that PAF stimulates intracellular calcium mobilization (Wang et al., 1999; Yue et al., 1992; Catalan, 1992; Bito et al., 1992), glutamate release (Clark et al., 1992), increases in cyclic GMP levels (Calcerrada et al., 1999c), activation of MAP kinases (Mukherjee et al., 1999), modulation of protein kinase C isoforms (Calcerrada et al., 1999a), phosphoinositide turnover (Shi et al.,1996; Catalan et al., 1992), protein tyrosine phosphorylation (Calcerrada et al., 1999b), and cytokine induction (Wang and Sun, 2000). These intracellular signaling events have been demonstrated by examining the effects of exogenously added PAF, by determining endogenous PAF levels following treatment with other agonists, or by examining the modulatory effects of a wide range of PAF antagonists on neuronal, microglial, or astrocytic signal transduction.

Signaling events initiated by PAFR-GPCR

PAF was the first lipid molecule for which a protein receptor was identified. The receptor was first cloned by Honda et al. (1991) from guinea pig lung. Human, mouse, rat, bovine, and pig homologs were subsequently identified (Bito et al.,1994; Ishii et al., 1996; Nakamura et al., 1991; Ye et al., 1991; Kunz et al., 1992; Horn et al., 1998). The human PAFR-GPCR gene is driven by two

separate promoters that splice to the same open reading frame, contains no introns, and is located on chromosome 1p35-p34.3 (Mutoh et al., 1993; Seyfried et al., 1992; Chase et al., 1996).

PAFR-GPCR has been identified as a member of the GPCR superfamily based on sequence analysis and computer modeling (Shukla, 1992; Kajihara et al., 1994). Bioinformatic analysis and detailed site-directed mutagenesis studies have revealed several structure-function relationships (refer to Figure 1.2). GPCRs constitute the largest group of membrane bound receptor proteins involved in signal transduction (Morris and Malbon, 1999; Horn et al., 1998; Probst et al., 1992). Salient to a role for PAF as a neuromodulator in addition to its proinflammatory actions in the periphery, it is well established that the vast majority of neurotransmitters and neuromodulators in the visual, olfactory, hormonal, and opiate systems mediate their physiological effects by binding to their respective GPCRs (Morris and Malbon, 1999; Milligan, 2000; Watson and Arkinstall, 1994). Members of the GPCR superfamily share a similar structure consisting of 7 transmembrane domains. Receptor activation leads to binding and activation of heterotrimeric G-proteins that, in turn, activate downstream signaling events. PAFR-GPCR can interact with multiple G-proteins, leading to simultaneous stimulation of distinct signaling pathways as assessed by the ability of pertussis toxin to inhibit some, but not all, PAF-induced effects in rat basophilic RBL-2H3 cells (Haribabu et al., 1999; Ali et al., 1994), chinese hamster ovary cells, CHO (van Biesen et al., 1996; Honda et al., 1994), immortalized

Figure 1.2: PAFR-GPCR structure-function relationships.

The mutagenesis studies cited have identified critical regions in PAFR-GPCR responsible for ligand binding, intracellular signaling and receptor desensitization. This figure is based upon bioinformatic analysis performed in our laboratory and the detailed studies of Le Gouill et al., 1997, Parent et al., 1996a,b,c, Ishii et al., 1997, Carlson et al., 1996, Takano et al., 1994, Ali et al., 1997, Prescott et al., 2000, Probst et al., 1992. The PAFR-GPCR receptor backbone was obtained from the GPCR database (Horn et al., 1998).

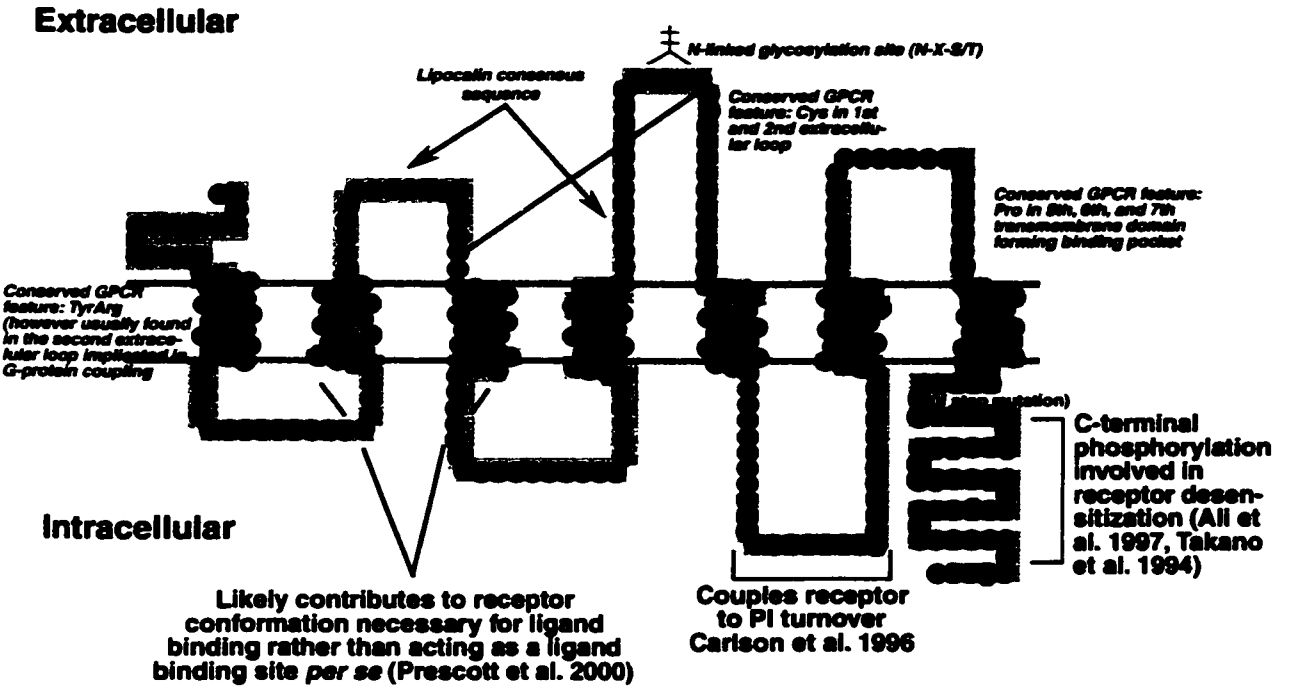

Receptor affinity

- F97, F98
  adjacent phenylalanines
  important for structural stability
  Parent et al. 1996b
- H188, H248, H249, Q252,Q276,T278
  Mutation decreases PAF ligand affinity.
  H188, 248, 249 hypothesized to form a
  binding pocket for PAF phosphate group.
  Ishii et al. 1997
- Lipid-binding consensus sequences common to the lipocalin family of lipid-binding proteins
- C90-C163 Disulfide bridge, C95, N285, K298stop
  Mutation stops ligand binding and
  results in intracellular expression
  Le Gouill et al. 1997, Parent et al. 1996b
- N58, D63, N100, T101,S104, D289
  Mutation increases PAF ligand affinity.
  N100A mutant renders receptor responsive to lyso-PAF.
  Parent et al. 1996a,b, Ishii et al. 1997
- H303-stop, Serine/Threonine residues in c-terminal tail
  Mutations in guinea pig PAFR block ligand-induced receptor
  internalization and ligand resensitization (but not desensitization)
  C317(stop), N285 in human PAFR blocks internalization.
  Ishii et al. 1998, Le Gouill et al. 1997

Receptor function

- D63, D289, Y293
  Mutation prevents G-protein coupling
  Le Gouill et al. 1999, Parent et al. 1996a
- Conserved GPCR features
  (Probst et al. 1992)
- PAFR consensus sequences conserved in all PAFR species homologs

hippocampal HN33.11 cells (Shi et al., 1996), and primary rodent hippocampal cultures (Clark et al., 2000).

Neurotoxic effects of PAF

As reviewed above, PAF acts as a potent neuromodulator in postnatal CNS. Notably, PAF has been shown to mediate long-term potentiation, the molecular mechanism purported to underly memory formation and neuronal plasticity (Clark et al., 1992; Kato et al., 1994; Wieraszko et al., 1993; Grassi et al., 1998; Bliss and Collingridge, 1993). Excessive levels of PAF, however, contribute to neuronal cell injury following stroke and seizures (Kumar et al., 1988; Domingo et al., 1994; Nishida and Markey, 1996; Yue and Feuerstein, 1994; Marcheselli and Bazan, 1994), the pathogenesis of neurodegenerative diseases such as HIV-1-associated dementia (Gelbard et al., 1994; Nishida et al., 1996), and may play a role in Alzheimer's disease (Hershkowitz and Adunsky, 1996). PAF-mediated neurotoxicity has been directly demonstrated *in vitro* (Kornecki and Ehrlich, 1988; Gelbard et al., 1994; Westmoreland et al., 1996). In our laboratory, Dr. Bennett's group has demonstrated that, *in vivo*, PAFR-GPCR is expressed by neurons undergoing apoptosis in both rat hippocampus following excitotoxic challenge and rat retina following hypoxia (Bennett et al., 1998, Bennett et al., submitted). These results have led to the hypothesis that PAFR-GPCR initiates PAF-induced apoptosis. However, the effect of PAFR-GPCR stimulation on PAF-mediated neurotoxicity has not been defined.

PAF and Neuronal Differentiation

It is important to devote a substantial section of this review to the potential involvement of PAF in neuronal differentiation given studies described in Chapter 3. The study of PAF in CNS development is an exploding field and subject to controversy. The first reports implicating PAF in neuronal differentiation demonstrated that exposure of NG108-15 and murine neuroblastoma NB-2a cells to low concentrations of PAF induced neuronal differentiation (Herrick-Davis et al., 1991; Kornecki and Ehrlich, 1988). A similar phenomenon was reported using primary cultures from embryonic rat cerebra (Ved et al., 1991). Furthermore, in a quantitative study of PAF in the rat brain, an age-dependent decrease in PAF concentration has been reported, providing circumstantial evidence that PAF signaling is maximal during cerebral development (Tokumura et al., 1992).

Certainly, PAF has been implicated in pathological CNS development. Sustained exposure to high levels of PAF is hypothesized to be one of the signaling defects responsible for the genetic disorder Miller-Dieker Syndrome (MDS). Linked with defective PAF degradation, MDS is a rare disorder categorized as classical or type I lissencephaly (development of a smooth cortical surface) and clinically classified as a neuronal migration disorder (Aicardi, 1994; Barth, 1987). The brains of patients with MDS are often smaller with a four-layered as opposed to a six-layered cerebral cortex. The cortex is thicker with little white matter (fibre tracts) and the cerebral ventricles are enlarged (Dobyns et al., 1991). Afflicted individuals present with severe mental

retardation, recurring epileptic seizures, and face a reduced life expectancy. Described in the 1960s, MDS was believed to be an autosomal recessive disorder (Miller, 1963; Dieker et al., 1969). Cytogenetic and molecular genetics studies have since identified the genetic determinant as a hemizygous deletion or mutation in the LIS-1 gene located at chromosome 17p13.3 (Reiner et al., 1993; Dobyns et al., 1993; Chong et al., 1997). A link between defective PAF metabolism and MDS was first proposed in 1994 when the beta subunit of bovine brain PAFAH1b was reported to be the bovine homolog to the human Lis-1 protein (Hattori et al., 1994). The heterotrimeric PAFAH1b enzyme complex is composed of two homologous catalytic subunits alpha 1 (29 kD) and alpha 2 (30 kD) and a non-catalytic beta subunit (45 kD subunit) (herein referred to as Lis-1)[1]. Recent evidence demonstrates that the Lis-1 subunit likely regulates PAFAH1b activity (Shmueli et al., 1999). All human LIS-1 mutations examined to date diminish or abrogate the capacity of Lis-1 to interact with alpha 1 and alpha 2 subunits (Sweeney et al., 2000). As reviewed above, PAFAH1b specifically inactivates PAF lipids (Hattori et al., 1993). Maximal activity in the developing brain is observed during neuronal migration (Albrecht et al., 1996). The inability of the Lis-1 protein in MDS to recognize PAF and its alpha 1 and alpha 2 partners likely impedes the ability of PAFAH1b to inactivate its substrate thereby impairing neuronal migration (Sweeney et al., 2000). In support of this hypothesis, sustained PAF exposure *in vitro* has been shown to collapse

---

[1] There are two nomenclatures in the literature for PAFAH1b subunits. A second system refers to the catalytic subunits as the β and γ subunit and Lis-1 as the α subunit.

neuronal growth cones (Clark et al., 1995), elicit cytoskeletal alterations (McNeil et al., 1999), and inhibit neuronal motility (Bix and Clark, 1998; Adachi et al., 1997). Lis-1 may also directly transmit a PAF-mediated signal to the cytoskeleton in addition to its role in the PAFAH1b trimer. Lis-1 amino acid sequence analysis has revealed that it is a member of the WD-40 repeat family of proteins recognized for multiple protein-protein interactions (Garcia-Higuera et al., 1996; Wang et al., 1995; Neer et al., 1994). Reported interactions with tubulin and the microtubule network have earned Lis-1 the designation as an unconventional microtubule-associated protein (MAP) and suggest that Lis-1 may participate directly in the control of neuronal motility and migration (Sapir et al., 1997, 1999; Faulkner et al., 2000; Liu et al., 2000; Smith et al., 2000; Sasaki et al., 2000; Niethammer et al., 2000; Feng et al., 2000). This hypothesis has yet to be empirically tested.

The multiplicity of Lis-1 interactions raises the dilemma about how haplo-insufficency of LIS-1 might cause lissencephaly. Central to this issue is whether there is a functional relationship between PAFAH1b and the MDS phenotype. Do elevated PAF levels during cerebral development lead to MDS? A low concentration of PAF has been shown to induce neuronal cell differentiation in culture (Herrick-Davis et al., 1991; Kornecki and Ehrlich, 1988), while high concentrations are toxic (Kornecki and Ehrlich, 1988; Gelbard et al., 1994; Westmoreland et al., 1996), suggesting that PAF levels may be crucial for neuronal differentiation as well as affect cell viability. Given that PAFAH1b activity peaks when neurons begin migration, it is possible that a sharp reduction

in PAF concentration is necessary to initiate or sustain migration. As the Lis-1 protein is only one subunit of a heterotrimeric enzyme complex, hemizygosity of the LIS-1 gene may lead to reduced levels of assembled, functional enzyme resulting in continuous PAF signaling. Identification of PAFAH1b as a non-traditional G-protein like trimer and Lis-1 as a MAP family member has also led to speculation that Lis-1 participates in signaling downstream of PAF hydrolysis (Ho et al., 1997; Sapir et al., 1999). Conformational changes in the heterotrimeric PAFAH1b complex elicited by PAF hydrolysis may permit Lis-1 subunit to interact directly with cytoskeletal proteins (Sapir et al., 1997, Whynshaw-Boris and Gambello, 2001). Although this hypothesis remains to be experimentally validated, empirical evidence clearly demonstrates the importance of PAFAH1b activity during cortical development. A recent report demonstrated that hemizygosity of the alpha 1 subunit led to manifestation of mental retardation, atrophy of the brain, ataxia, and seizures in a female patient (Nothwang et al., 2001). The disrupted alpha 1 gene encoded for a truncated, catalytically inactive protein that lost the ability to interact with Lis-1 (Nothwang et al., 2001).

Murine models will provide useful tools to determine the role of Lis-1 in the developing nervous system. Two independent groups have recently demonstrated that, in mice, homozygotic deletion of the LIS-1 gene is embryonic lethal and have successfully developed LIS-1 +/- mutant mice (Cahana et al., 2001; Hirotsune et al., 1998). Initial characterization of these animals have revealed brain abnormalities similar to those of human type I lissencephaly. Enlargement of the ventricles is apparent as well as cortical, hippocampal, and

olfactory bulb disorganization as a result of aberrant neuronal migration (Cahana et al 2001; Hirotsune et al 1998). In addition, 5-Bromo-2'-deoxy-uridine (BrdU)-labeling has unveiled an intriguing increase in neural precursor proliferation LIS-1 heterozygotes between embryonic days E11-14.5. Specifically, an increase in the number of neurons born between E11-14.5 migrating to layer III of the neocortex (Hirotsune et al., 1998), the cortical plate (Cahana et al., 2001), and the CA1 subfield of the hippocampus (Fleck et al., 2000) has been observed. Although the mechanisms responsible for this enhanced neural precursor proliferation is unknown, PAF has repeatedly been demonstrated to trigger *in vitro* proliferation in a variety of non-neuronal cells. Examples include human T and B lymphocytes (Behrens and Goodwin, 1990; Leprince et al., 1991), human and guinea pig bone marrow cells (Denizot et al., 1996; Kato et al., 1988; Kudo et al., 1991), human lung fibroblasts (Roth et al., 1996), rodent lung pericytes (Khoury and Langleben, 1996), and primary rodent and human fibroblasts (Bennett and Birnboim, 1997, Bennett et al., 1993). The mitogenic effects of PAF have also been reported in a number of human breast cancer cell lines (Bussolati et al., 2000), the human K562 erythroid cell line (Dupuis et al., 1997), and the endometrial adenocarcinoma cell line HEC-1A (Bonaccorsi et al., 1997). These data implicate PAF in the growth of neuronal precursors and the regulation of neuronal migration.

Objective

Given the critical effects of PAF on neuronal differentiation, signaling, and viability, it is essential to identify the molecular mechanisms responsible for initiating PAF-mediated signal transduction. The overall objectives of this thesis are:

1. Identify a cell culture model capable of differentiating the effects of PAFR-GPCR and other PAF binding proteins and
2. Characterize biological activity initiated by PAFR-GPCR activity in neural precursors.

The present thesis is divided into the following three sections designed to address the overall objectives:

1. Characterization of an *in vitro* model to study PAF ligand/PAFR-GPCR receptor interaction.
2. Examination of the effect of PAF/PAFR-GPCR interaction during differentiation to a neuronal phenotype.
3. Characterization of a new human PAFR-GPCR antibody developed in our laboratory.

CHAPTER 2: CHARACTERIZATION OF AN *IN VITRO* MODEL TO STUDY PAF LIGAND/PAFR-GPCR INTERACTION

Introduction

As reviewed in Chapter 1, PAF is a potent neuromodulator. Transient PAF stimulation mobilizes intracellular calcium, inhibits ionotropic GABA receptor activation, and elicits glutamate synthesis in primary neuronal culture (Bito et al., 1992; Clark et al., 1994; Chen and Bazan, 1999). Sustained PAF exposure triggers neuronal cell loss following ischemia-reperfusion injury, epileptiform seizure, and HIV-1 infection (Yue and Feuerstein, 1994; Bazan, 1998; Gelbard et al., 1994; Nishida et al., 1996; Marcheselli and Bazan, 1994).

It has yet to be established how PAF-mediated cytotoxicity is initiated. A single seven-transmembrane spanning G-protein coupled PAF receptor (PAFR-GPCR) has been cloned and is expressed by neurons, astrocytes, and microglia (Bennett et al., 1998; Mori et al., 1997; Mori et al., 1996; Bito et al., 1992). The cytotoxic effects of PAF are commonly attributed to activation of this receptor (PAFR-GPCR) in non-neuronal cells (Kuijpes et al., 2001; Berthou et al., 2000; Barber et al., 1998) but this relationship has not been empirically tested in neurons or neural precursors.

Objective

As a means of improving our understanding of the physiological and pathophysiological roles of PAF and PAFR-GPCR in the CNS we used the PC12

cell model to test the hypothesis that PAF-induced cell death is mediated by PAFR-GPCR. Expression and functional activity of PAFR-GPCR and the trimeric components of brain PAFAH1b (LIS-1, PAFAH1b α1, PAFAH1b α2) were determined. Stable PC12 cell lines overexpressing human PAFR-GPCR cDNA (hPAFR-GPCR) under the regulation of the cytomegalovirus promoter (CMV) were developed. In this series of experiments, PAF elicited apoptotic cell loss of PC12 cells but apoptosis occurred independently of PAFR-GPCR activation. Overexpression of hPAFR-GPCR and functional PAFAH1b activity protected against PAF-induced apoptosis.

Materials and Method

Cell Culture

A clonal line, PC12-AC of rodent pheochromocytoma PC12 cells (American Tissue Culture Collection), derived in the Bennett laboratory was used in all cell culture manipulations and is hereinafter referred to as WT-PC12 cells. WT-PC12 and HPAFR clones were maintained in 10 cm tissue culture dishes at 37^0C and 5% CO_2/95% air atmosphere. Cells were cultured in complete medium (RPMI 1640 supplemented with 10% horse serum and 5% newborn calf serum, streptomycin and penicillin at 100 units/mL; Invitrogen). Stock cultures were fed with complete medium every 2-3 days and passaged when sub-confluent. In addition, transfected cell lines received 200 µg/mL Zeocin (Invitrogen) during feeding.

Generation of hPAFR-GPCR and empty vector stable transfectants

WT-PC12 cells were transfected with empty vector (pcDNA3.1/GS) or pcDNA3.1/GS containing the 1029 bp hPAFR-GPCR open reading frame tagged at the C-terminus with six histidine residues and the V5 epitope (Invitrogen). Transfections were performed using Transfast reagent according to the manufacturer's specifications (Promega). Clonal lines (HPAFR and pGS empty vector) resistant to 400 µg/ml Zeocin were expanded after 14 days of culture and maintained in 200 µg/ml Zeocin.

RT-PCR

All reagents were from Invitrogen except where indicated. Total cellular RNA was extracted from cultures using TRIzol reagent according to the protocol provided by the manufacturer. Ten µg of total ribonucleic acid (RNA) was treated with RQ1-DNAse as described by the manufacturer (Promega). RNA was ethanol (EtOH) precipitated and re-dissolved in nuclease free H_2O (Promega). Template RNA was random-primed with 10 pmol pdN_6 (Promega). RNA and primer were heated for 10 min at 70°C. dNTPs (125 µM each, Promega), dithiothrietol (DTT: 10 mM), 5X first strand buffer (50 mM Tris-HCl (pH 8.3), 75 mM KCl, 3 mM $MgCl_2$), and 200 U of Superscript II RT were added in a total volume of 20 µl. Reactions were incubated at 25°C for 10 min, 42°C for 1 h, and 50°C for 30 min. Control reactions were carried out in the absence of Superscript II RT. Two µl of the cDNA RT reaction mix were PCR amplified in a total volume of 50 µl containing 1 mM $MgCl_2$, 1X PCR buffer (20 mM Tris-HCl (pH 8.4), 50

mM KCl), dNTPs (200 μM each, Promega), 5 U of *Taq* DNA polymerase, and 25 pmol per primer for PAFR-GPCR, LIS-1, PAFAH1b α1, PAFAH1b α2, or 10 pmol per primer for GAPDH. The reaction mixture was denatured at 95°C for 30 sec, annealed at 55°C for 90 sec, and extended at 72°C for 120 sec. Priming occurred over 35 cycles for PAFR-GPCR, LIS-1 and PAFAH1b α2 and 30 cycles for PAFAH1b α1 and GAPDH. Primers used were (1) 5'-CACTTATAACCGC TACCAGGCAG-3' (forward) and 5'-AAGACAGTGCAGACCATCCACAG-3' (reverse) defining a 381 bp amplicon of both rodent and human PAFR-GPCR, (2) 5'-GCATCCTACTTCCTCATCCT-3' (forward) and 5'-ACTTCAGTGACCGTA TCCGT-3' (reverse) defining a 538 bp amplicon of human PAFR-GPCR, (3) 5'-CTGCTTCAGAGGATGCTACA-3' (forward) and 5'-ATCAGAGTGCCGTCC TGATT-3' (reverse) defining a 373 bp amplicon of rodent LIS1, (4) 5'-GACGGACGCTGGATGTCTCT-3' (forward) and 5'-AGACGAAGCAGC AAGGAGTG-3' (reverse) defining a 587 bp amplicon of rodent PAFAH1b α1, (5) 5'-TGCAGCAGTACGAGATATGG-3' (forward) and 5'-AACATGTCGTGG CAGGAGAT-3' (reverse) defining a 418 bp amplicon of rodent PAFAH1b α2, and (6) 5'-TGGTGCTGAGTATGTCGTGGAGT-3' (forward) and 5'-AGTCTTCTGA GTGGCAGTGATGG-3' (reverse) defining a 292 bp amplicon of rodent GAPDH. The absence of genomic DNA contamination and reagent contamination was demonstrated by performing appropriate parallel control reactions (i.e., RT reactions carried out in the absence of enzyme to detect genomic DNA contamination in the RNA template, no template to detect reagent contamination, no primers to detect false priming artifacts). The PCR products and PCR

markers (Promega) were size-fractionated by electrophoresis on a 1.2% (w/v) agarose gel, stained with ethidium bromide, and digitized under UV light using AlphaImager-1220 software (Alpha Innotech Corporation).

Northern analysis

Total RNA (30 µg), isolated as described above, was denatured with formaldehyde, electrophoretically separated on a 1.2% (w/v) agarose gel containing 0.2 M formaldehyde, and transferred to Hybond-N nylon membrane (Amersham-Parmacia) as described in (Bennett et al., 1994). Blots were hybridized at 50°C for 16 h in DIG Easy Hyb solution (Roche). Probes were a 538 bp DIG-labelled cDNA amplicon of the human leukocyte PAFR-GPCR gene in pCDM8 (Kunz et al., 1992) (kindly provided by Dr. N Gerard, Harvard Medical School) or a 292 bp DIG-labelled cDNA amplicon of the GAPDH gene in pGAPDH (Piechaczyk et al., 1984) (kindly provided by Dr. C Birnboim, University of Ottawa). Probes were prepared using a DIG-PCR kit and the corresponding primers described above, according to the protocol provided by the manufacturer (Roche). Blots were washed twice for 5 min at 65°C in 2X SSC/0.1% SDS, twice for 15 min at 65°C in 0.1X SSC/0.1% SDS, once for 5 min at room temperature in 1X DIG washing solution (Roche) and once for 1 h in 1X DIG blocking solution (Roche). Signal was detected using an anti-DIG-HRP antibody (1:5000; Roche) diluted in 1X DIG blocking solution, visualized using CDP-Star according to the protocol provided by the manufacturer (Roche) and exposed to Biomax X-Ray film (Kodak).

Western blot analysis

Total protein lysates were prepared from sub-confluent cultures in RIPA buffer (10 mM phosphate buffer, 1% Nonidet P-40, 0.5% sodium deoxycholate, 0.1% SDS, 30 µl/ml aprotinin, 1mM sodium orthovanadate, 0.1 mg/ml phenylmethysulfonyl fluoride). After removal of cellular debris by centrifugation, protein content was determined using BioRad's Protein Assay DC kit with bovine serum albumin (BSA) as standard. Total protein lysate (30 µg) was separated by SDS-polyacrylamide gel electrophoresis (SDS-PAGE) under reducing conditions on 10% SDS-polyacrylamide gels and electroblotted to polyvinylidene difluoride (PVDF) membranes (Millipore). Western analysis was performed using monoclonal anti-V5 (1:5000; Invitrogen) as primary antibody and detected by horseradish peroxidase-conjugated goat anti-mouse IgG (1:2000; Jackson Immunolabs). Antibodies were diluted and membranes were blocked in 10 mM PBS containing 1% heat-denatured casein. After overnight incubation with the primary antibody at 4°C the secondary antibody was incubated at room temperature for 1 h. Membranes were washed repeatedly between incubations with PBS containing 0.05% Tween-20. Immunoreactive bands were visualized using SuperSignal West Pico (Pierce) chemiluminescent substrate according to the protocol provided by the manufacturer and exposed to Biomax X-Ray film (Kodak). Densitometric analysis of replicate immunoblots was performed using AlphaImager-1220 software.

PAF acetylhydrolase activity assay

The activity of cytosolic PAFAH was assayed using the commercially available PAF acetylhydrolase assay kit (Caymen Chemical). Undifferentiated WT-PC12, pGS empty vector and HPAFR-7 cytosolic fractions were prepared in 250 mM sucrose, 10 mM Tris-HCl (pH 7.4) and 1 mM EDTA from cells on day 5 of culture plated at an initial seeding density of 5 x 10^4 cells. Cell lysates were centrifuged at 600 X g for 10 minutes and at 100,000 X g for 60 minutes. The resulting supernatants were concentrated using an Amicon centrifuge concentrator with a molecular weight cut-off of 10,000 (Millipore). Protein content was quantitated as above. Samples containing 50 µg of cytosolic protein were incubated in the presence of 2-thio-PAF substrate for 30 minutes at room temperature. Hydrolysis of the thioester substate was measured spectrophotometrically at 405 nm by detection of the generated free thiols using 5,5'-dithiobis(2-nitrobenzoic acid) (DTNB; Ellman's reagent). In all assays, blanks without protein and no substrate controls with protein were run in parallel and subtracted from the experimental values.

Cell survival and cell death assays

PC12 cells (8.8x10^3 cells/ cm^2) were plated overnight in 6 cm diameter tissue culture plates. Cells were treated for 24 h with EtOH (0.1% or 10%), PAF (10 nM-10 µM, Biomol), mc-PAF (100 nM-10 µM, Biomol or Caymen Chemical) or *lyso*-PAF (10- 10 µM, Biomol) in low serum media (RPMI containing 0.5% heat-inactivated horse serum). A number of experiments included culture of

EtOH (0.1%) or PAF (1 μM) treated cells in the presence of DMSO (0.1%) or the PAF antagonists CV3988 (200 nM-20 μM, Biomol), CV6209 (10 nM-1μM, Biomol), BN52021 (1 μM-100 μM, Biomol), FR49175 (0.5 μM-5μM, Biomol), ONO-6248 (1 μM-100 μM), L659-989 (0.1 μM-10μM) or RP59227 (1 μM-100 μM). The PAF antagonists ONO-6248, L659-989, and RP59227 were kindly provided by Dr. TY Shen, University of Virginia.

After 24 hours of exposure cell survival and viability was assessed by hemocytometer cell counts of Trypan Blue excluding cells and using the WST assay according to the protocol provided by the manufacturer (Roche). Note that cleavage of the tetrazolium salt WST-1, by mitochondrial dehydrogenases in viable cells, to formazan product (measured at A_{450}-A_{690} nm) is directly proportional to the number of metabolically active cells. In addition, evaluation of oligonucleosomal fragmentation was performed using the Cell Death Detection ELISA kit according to the protocol provided by the manufacturer (Roche). Variations of the above experiments included: cells plated at lower cell densities treated with PAF (1 μM), cells (plated at $8.8x10^3$ cells/ cm^2) treated with a single dose of EtOH (0.1%), PAF (1 μM) or mc-PAF (1 μM) followed by cell survival assessment 24 h, 48 h, and 72 h post treatment. As well as cultures repeatedly treated with EtOH (0.1%) or PAF (1 μM) every 24 h for up to 144 hours followed by cell survival assessment at 24 h, 48 h, 72 and 168 h of culture. Low serum media was replaced at each treatment.

Microscopic investigations were performed to determine biochemical and morphological evaluation of apoptosis. In these studies, $8.8x10^3$ cells/ cm^2 were

plated in 10 cm diameter plates containing four 22 cm^2 glass coverslips coated with 0.1% gelatin. DNA fragmentation was determined by terminal deoxynucleotidyl transferase (TdT) dUTP nick end labeling (TUNEL) of cultures fixed for 20 min in 4% paraformaldehyde in 10 mM PBS (10 mM sodium phosphate buffer, pH 7.5, 154 mM NaCl) according to the protocol provided by the manufacturer (Roche). Negative controls included incubation with FITC–labeled dUTP in the absence of TdT. Cells were double-labeled with Hoechst 33258 (0.2 µg/ml, 20 min at room temperature) for morphological evaluation of apoptosis.

To differentiate between apoptotic and necrotic cell death, cultures were plated as above. Prior to fixation and TUNEL processing, cultures were incubated with ethidium bromide homodimer (0.75 µM) according to the protocol provided by the manufacturer (Molecular Probes). Ethidium bromide homodimer (EthD-1) is a membrane impermeant dye and can only enter cells if the plasma membrane has been compromised or artificially permeabilized. Positive necrotic controls were induced by treatment of WT-PC12 cells with 10% EtOH.

Statistical analysis

Data were analyzed using one-way factorial ANOVA tests or unpaired Student's *t*-tests, as applicable. Following detection of a statistically significant F value with respect to the effect of a given series of treatments, *post hoc* Dunnett's *t*-tests were used to identify which treatment condition differed statistically from control (vehicle-treated). P values of <0.05 were considered

statistically significant (shown as *); P values of <0.01 were considered highly statistically significant (shown as **).

Results

WT-PC12 cells lack endogenous PAFR-GPCR RNA expression

Endogenous expression of PAFR-GPCR was determined by RT-PCR using primers that generate a 381 bp amplicon of rodent or human template (Figure 2.1). Undifferentiated WT-PC12 cells and cultures differentiated to a neuronal phenotype for 7 days in the presence of nerve growth factor (NGF; NGF-PC12) do not express endogenous rodent PAFR-GPCR (Figure 2.1). Rat brain mRNA template (data not shown) and HPAFR-3, a clonal population of WT-PC12 cells transfected with hPAFR-GPCR, was amplified as a positive control (Figure 2.1, HPAFR-3). The same random-primed RT products were amplified for GAPDH to demonstrate template integrity (Figure 2.1). The absence of PAFR-GPCR RNA expression in WT-PC12 cells was corroborated by Northern analysis (Figure 2.2C; WT-PC12).

Characterization of stable hPAFR-GPCR and empty vector transfectants

WT-PC12 cells were transfected with pcDNA3.1/GS/hPAFR-GPCR or pcDNA3.1/GS to generate stable clonal lines expressing epitope-tagged human PAFR-GPCR driven by the CMV promoter or empty vector. Transgene expression was verified by RT-PCR in 5 hPAFR-GPCR transfectants (HPAFR clones 1-4, 7) using primers that detect a 538 bp amplicon of hPAFR-GPCR

Figure 2.1: RT-PCR analysis of WT-PC12 cells demonstrates that undifferentiated and NGF-differentiated cells do not express PAFR-GPCR mRNA.

Total RNA was extracted from WT-PC12 cells grown in complete media, from WT-PC12 cells differentiated to a neuronal phenotype for 7 days in low serum media containing 50 ng/ml NGF (NGF-PC12), and from a stable clonal line transfected with hPAFR-GPCR (HPAFR-3) grown in complete media. RT-PCR was performed using primers which recognize both human and rodent transcripts. A 381 pb amplicon was detected only in the positive control (HPAFR-3). The same templates were amplified with GAPDH specific primers to demonstrate template integrity.

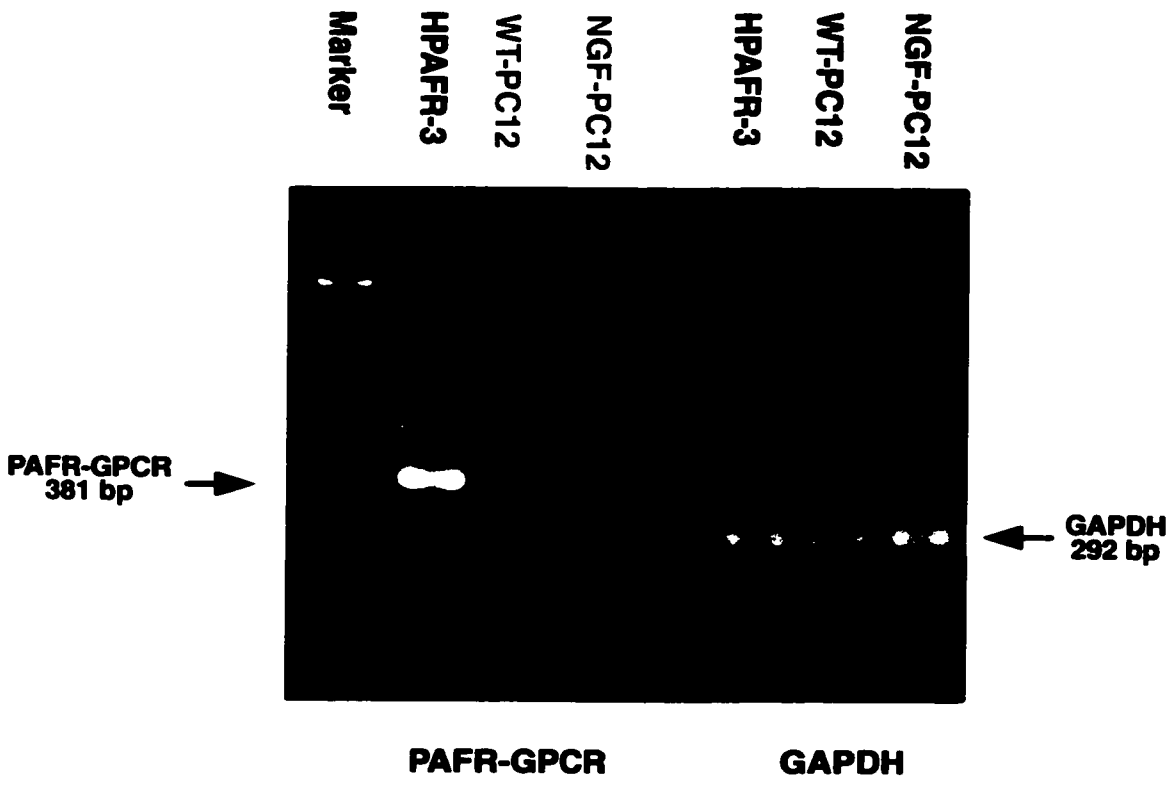
Marker
HPAFR-3
WT-PC12
NGF-PC12
HPAFR-3
WT-PC12
NGF-PC12
PAFR-GPCR
381 bp
GAPDH
292 bp
PAFR-GPCR
GAPDH

(Figure 2.2B). The same random-primed RT products were amplified for GAPDH to demonstrate template integrity (Figure 2.2B). Stable empty vector clonal transfectants were expanded based on their resistance to the selectable marker zeocin. Northern analysis of WT-PC12, two empty vector clones (pGS-1, pGS-2), and two hPAFR-GPCR transfectants confirmed that HPAFR-4 and HPAFR-7 alone uniquely expressed the transfected 1029 bp human PAFR-GPCR transcript (Figure 2.2C). Western analysis of hPAFR-GPCR stably transfected into WT-PC12 cells is shown in Figure 2.3. The monoclonal anti-V5 antibody, raised against the viral V5 epitope tagged to the C-terminus of hPAFR-GPCR, detected a single band at 68 kD in the screened HPAFR clones (Figure 2.3A). Densitometry of two independent immunoblots was performed to determine relative protein levels (Figure 2.3B). Clones were ranked as high (HPAFR-1, HPAFR-4), medium (HPAFR-2, HPAFR-7), or low (HPAFR-3) expressors of hPAFR-GPCR.

PAFAH1b expression and activity

Endogenous expression of PAFAH1b mRNA was determined by RT-PCR. Undifferentiated and NGF-differentiated WT-PC12 cells express PAFAH1b α1, PAFAH1b α2, and LIS-1 transcript (Figure 2.4). Total RNA was extracted from WT-PC12 cells grown in complete media, from WT-PC12 cells differentiated to a neuronal phenotype for 5 days in low serum media containing 50 ng/ml NGF (NGF-PC12). RT-PCR was performed using primers that recognize rodent

Figure 2.2: WT-PC12 cells were transfected with pcDNA3.1/GS containing the cDNA for hPAFR-GPCR.

(A) Expression construct used to generate hPAFR-GPCR transfectants. Empty vector, lacking hPAFR-GPCR insert was used to generate empty vector control clones. (B) Clones (HPAFR-1-4, 7) were screened for hPAFR-GPCR expression by RT-PCR using primers that detect a 538 pb amplicon corresponding to hPAFR-GPCR. The same random-primed RT products were amplified with GAPDH specific primers to demonstrate template integrity. (C) Northern analysis of WT-PC12, empty vector transfectants (pGS-1, pGS-2), and hPAFR-GPCR transfectants (HPAFR-4, HPAFR-7). The 1 kB transgene was detected in stable hPAFR-GPCR transfectants only.

A)

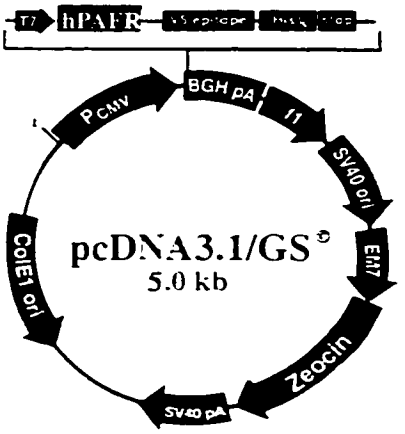
T7
hPAFR
BGH pA
f1
SV40 ori
EM7
Zeocin
SV40 pA
ColE1 ori
PCMV
pcDNA3.1/GS©
5.0 kb

B)

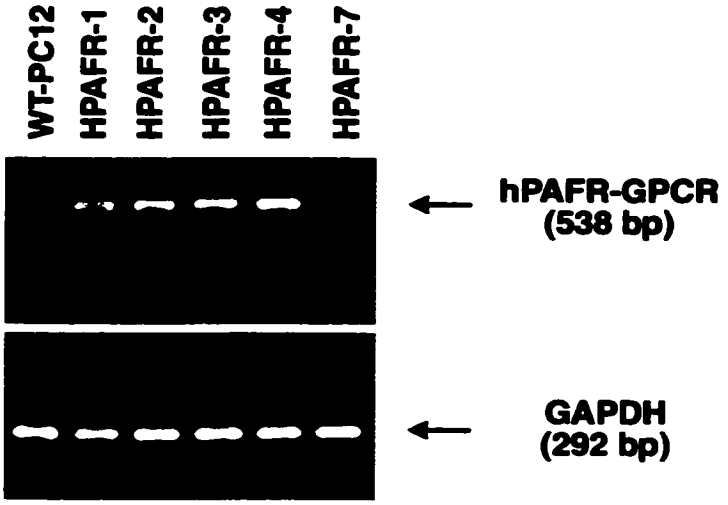
WT-PC12
HPAFR-1
HPAFR-2
HPAFR-3
HPAFR-4
HPAFR-7
hPAFR-GPCR
(538 bp)
GAPDH
(292 bp)

C)

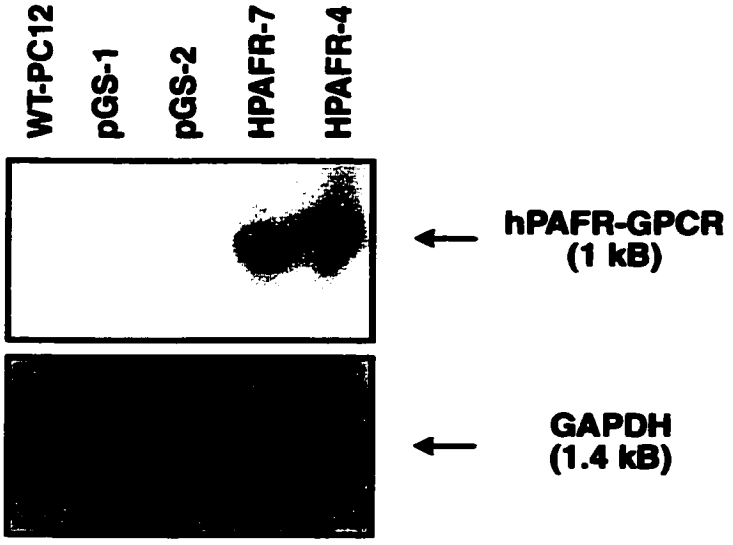
WT-PC12
pGS-1
pGS-2
HPAFR-7
HPAFR-4
hPAFR-GPCR
(1 kB)
GAPDH
(1.4 kB)

Figure 2.3: Analysis of hPAFR-GPCR-V5 fusion protein expression using anti-V5 antibody.

(A) Representative Western immunoblot of protein samples from undifferentiated WT-PC12 and a number of HPAFR clones. Total protein lysates were separated by SDS-PAGE, transferred to PVDF membrane and detected using monoclonal anti-V5 antibody as described in materials and methods. A single band representing hPAFR-GPCR was detected at ~68 kD in transfectants. (B) Densitometry of 2 replicate immunoblots identified clones expressing low (HPAFR-3), medium (HPAFR-2, HAPFR-7) and high (HPAFR-4, HPAFR-1) levels of hPAFR-GPCR.

A)

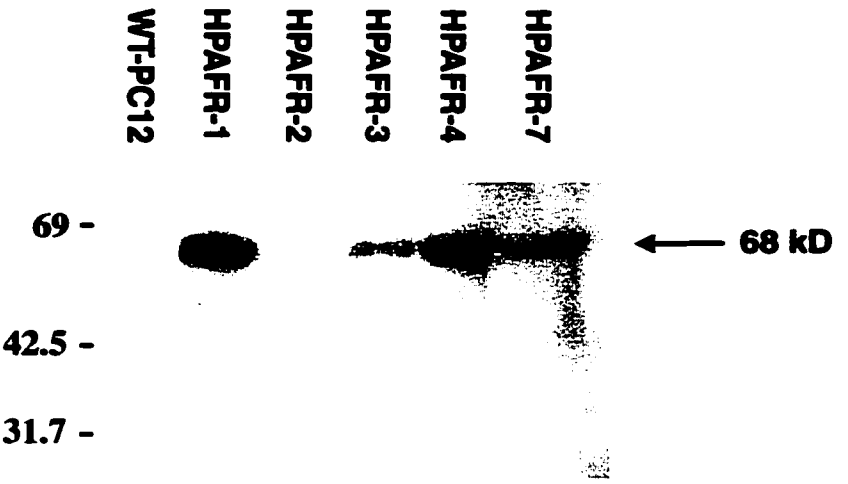
WT-PC12
HPAFR-1
HPAFR-2
HPAFR-3
HPAFR-4
HPAFR-7
69 -
42.5 -
31.7 -
68 kD

B)

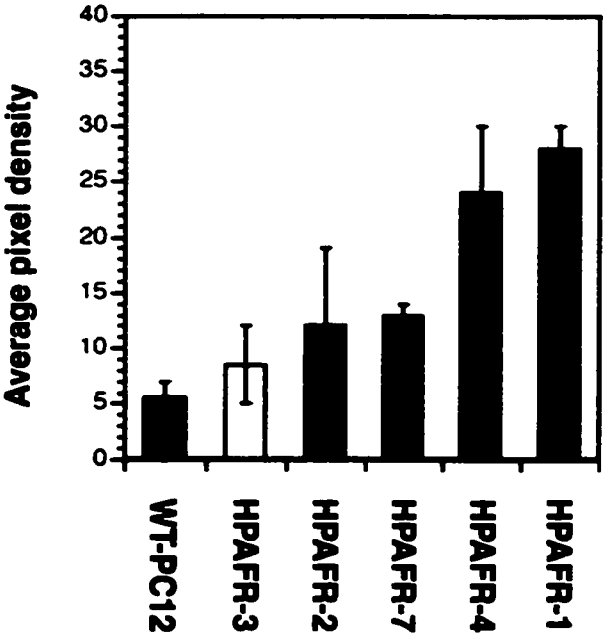
Average pixel density
40
35
30
25
20
15
10
5
0
WT-PC12
HPAFR-3
HPAFR-2
HPAFR-7
HPAFR-4
HPAFR-1

Figure 2.4: RT-PCR analysis demonstrates mRNA expression of PAFAH1b subunits (LIS-1, PAFAH1b α1, PAFAH1b α2) in both undifferentiated and NGF-differentiated WT-PC12 cells.

Total RNA was extracted from WT-PC12 cells grown in complete media and from WT-PC12 cells differentiated to a neuronal phenotype for 5 days in low serum media containing 50 ng/ml NGF (NGF-PC12). RT-PCR was performed using primers which recognize rodent transcripts for LIS-1, PAFAH α1, and PAFAH α2 defining amplicons of 373, 587, and 418 bp respectively. Corresponding PCR amplicons were detected in undifferentiated and NGF-differentiated RNA samples (lane 1). The absence of genomic DNA contamination and reagent contamination was demonstrated by performing appropriate parallel control reactions as follows: no reverse transcriptase during RT reaction, no template, no primers (lanes 2-4, respectively). Rodent cerebrum (lane 5) was used as a PAFAH1b positive control. The same templates were amplified with GAPDH specific primers to demonstrate template integrity.

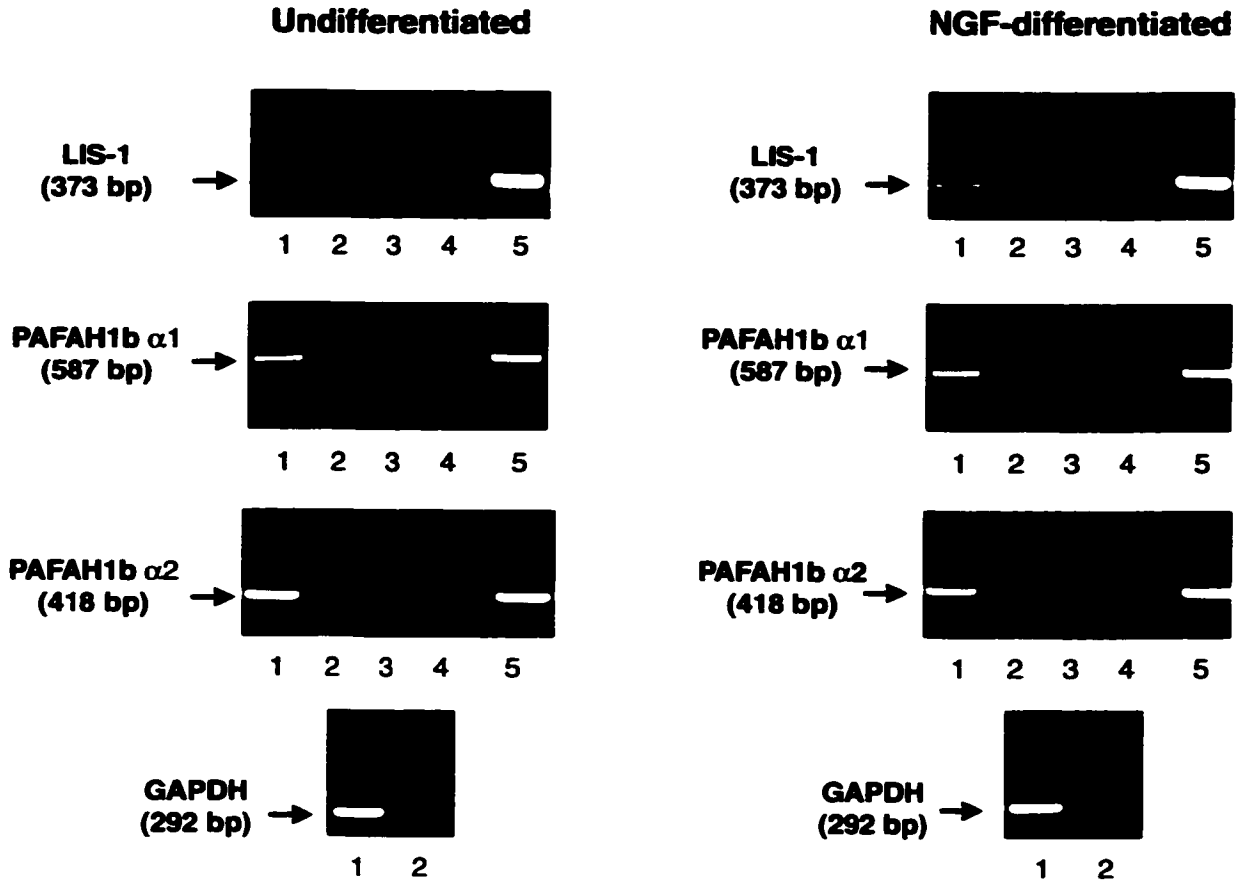
Undifferentiated
NGF-differentiated
LIS-1
(373 bp)
1 2 3 4 5
PAFAH1b α1
(587 bp)
1 2 3 4 5
PAFAH1b α2
(418 bp)
1 2 3 4 5
GAPDH
(292 bp)
1 2

transcripts for LIS1, PAFAH α1, and PAFAH α2 defining amplicons of 373, 587, and 418 bp respectively. The absence of genomic DNA contamination and reagent contamination was demonstrated by performing appropriate parallel control reactions. The same random-primed RT products were amplified for GAPDH to demonstrate template integrity. To test whether PAFAH1b is functional, PAFAH activity was measured in cytosolic fractions prepared from undifferentiated WT-PC12, pGS empty vector, and HPAFR-7 cells. PAFAH activity was detected in all cultures. Activity was not affected by hPAFR-GPCR expression (Table 2.1). In addition, active plasma PAFAH , known to be present in bovine serum, was detected in complete media but not low serum media preparations (data not shown).

Acute PAF administration induces WT-PC12 cell loss

PAF induced a dose-dependent decrease in cell number following acute administration (24 hours in low serum media). A 17%, 24%, and 44% reduction in cell number was observed following administration of 100 nM, 1 μM, and 10 μM PAF respectively (Figure 2.5A). An increased susceptibility to PAF was observed in cultures plated at low cell densities (900 cells/cm^2) with an overall 53% reduction in cell number following 1 μM PAF treatment (Figure 2.5B; 900 cells/cm^2). In comparison, cells plated at higher cells densities (Figure 2.5B; 1800-8800 cells/cm^2) demonstrated a comparable 24% cell loss following PAF treatment. Note that PAF-triggered cell loss in the absence of endogenous

Table 2.1: PAF acetylhydrolase activity in cytosolic fractions from undifferentiated cultures.

WT-PC12, pGS-2, and HPAFR-7 cytosolic fractions were prepared as described in materials and methods. The catalytic activity of samples containing 50 μg of cytosolic protein was measured using the PAF acetylhydrolase assay kit (Caymen Chemical). In all assays, blanks without protein and no substrate controls with protein were run in parallel and subtracted from the experimental values (n=6).

	WT-PC12	pGS-2	HPAFR-7
PAF acetylhydrolase activity (nmol/min/μg)	0.062	0.064	0.051
SEM	0.008	0.017	0.003

Figure 2.5: PAF induces cell loss in WT-PC12 cells following acute administration.

(A) WT-PC12 cells plated at 8800 cells/cm^2 were exposed for 24 h to different concentrations of PAF (0, 0.01, 0.1, 1, 10 μM) in low serum media. A dose dependent decrease in cell number was observed as assessed by trypan blue hemocytometer cell counts. (B) Cells plated at high and low cell densities were sensitive to PAF-induced cell loss following 1 μM treatment. An increase susceptibility to PAF was observed in cultures plated at the lowest cell density. Data are expressed as percent vehicle treated cultures. Results reported as means ± SEM (n=5-39 per data point) details as described in materials and methods. [*p<0.05, ** p<0.01; A, ANOVA, *post-hoc* Dunnett's *t*-test; B, Student's *t*-test]

A)

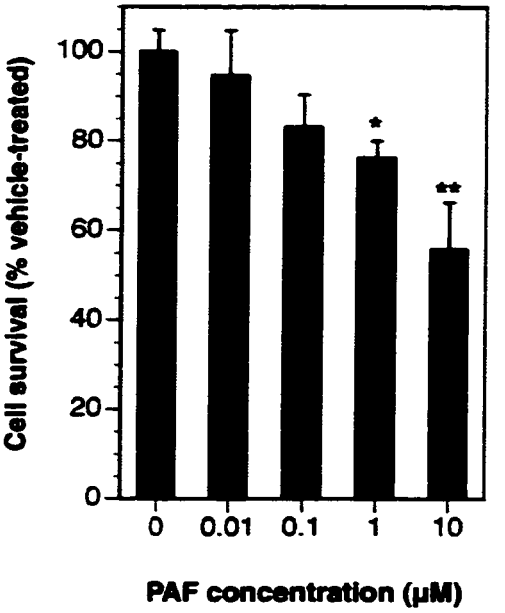
Cell survival (% vehicle-treated)
100
80
60
40
20
0
*
**
0
0.01
0.1
1
10
PAF concentration (μM)

B)

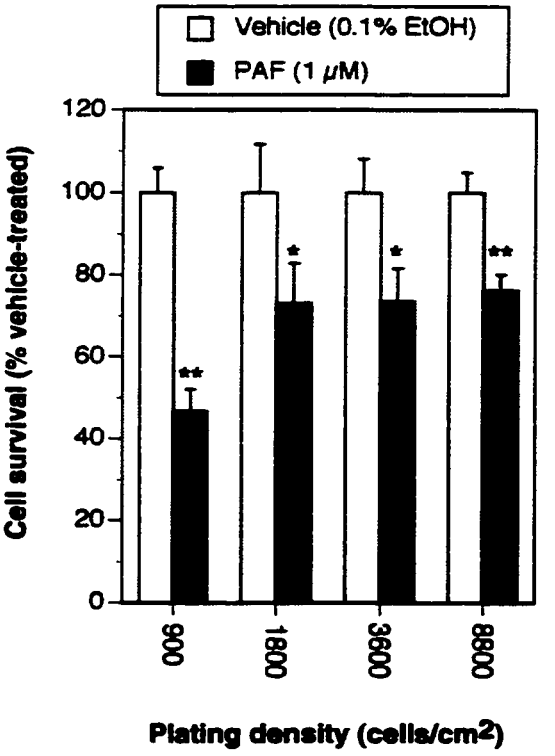
Vehicle (0.1% EtOH)
PAF (1 μM)
Cell survival (% vehicle-treated)
120
100
80
60
40
20
0
**
*
*
**
900
1800
3600
8800
Plating density (cells/cm2)

rodent PAFR-GPCR expression. Cytotoxicity was observed only when cells were cultured in low serum media and not in complete media (data not shown).

Sustained exposure to PAF agonist exacerbates cell loss

To determine whether PAFAHs alleviate PAF-induced cytotoxicity, WT-PC12 cells were treated with the synthetic PAF analog, mc-PAF (1-*O*-Hexadecyl-2-N-methylcarbamyl-*sn*-glycero-3-phosphocholine). The methyl-carbamyl group at the *sn*-2 position of mc-PAF is resistant to degradation by PAFAHs thus permitting prolonged PAF agonist activity (O'Flaherty et al., 1987).

mc-PAF elicited cell death comparable to that observed with PAF after 24 h of treatment. Cell loss was dose-dependent with observed 14%, 32%, and 38% reductions in WT-PC12 survival after treatment with 100 nM, 1 μM, and 10 μM mc-PAF relative to vehicle (0.1% EtOH) (Figure 2.6A). However, a single mc-PAF dose (1 μM) effectively extended the kinetics of cell loss compared to PAF (1 μM) (Figure 2.6B). Note that, in Figure 2.6, B, C, and D data are standardized to the number of untreated control cells cultured in low serum media to demonstrate the effect of vehicle on cell survival. PAF administration resulted in a 33% reduction in cell number relative to untreated cells after 24 h of treatment (Figure 2.6B; PAF). No additional reductions in cell number were observed at 48 and 72 h (Figure 2.6B; PAF). By contrast, mc-PAF triggered progressive cell loss. While a comparable 33% reduction in cell number was observed 24 h after treatment, 63% and 70% reductions in cell number was observed 48 h and 72 h after treatment respectively (Figure 2.6B; mc-PAF). WT-

Figure 2.6: Sustained exposure to PAF agonist exacerbates cell loss.

(A) Effect of the non-metabolizable PAF analog mc-PAF on WT-PC12 cell viability. WT-PC12 cells plated at 8800 cells/cm^2 were exposed for 24 h to different concentrations of mc-PAF (0, 0.1, 1, 10 μM) in low serum media. A dose dependent decrease in cell number was observed as assessed by trypan blue hemocytometer cell counts. Data are expressed as percent survival standardized to vehicle treated cultures. (B) Cell loss kinetics following a single dose of PAF (1 μM) or mc-PAF (1 μM). Panels (C, D) represent the effect of chronic PAF (1 μM) administration every 24 h. (C) determination of metabolic activity using the WST assay and (D) trypan blue hemocytometer cell counts. For (B, C, D) data are expressed as percent of untreated cells cultured in low serum media to demonstrate the effect of vehicle treatment. Results reported as means ± SEM (n= 6-18 per data point) details as described in materials and methods. [*$p<0.05$, ** $p<0.01$; A and B ANOVA, *post-hoc* Dunnett's *t*-test; C and D Student's *t*-test]

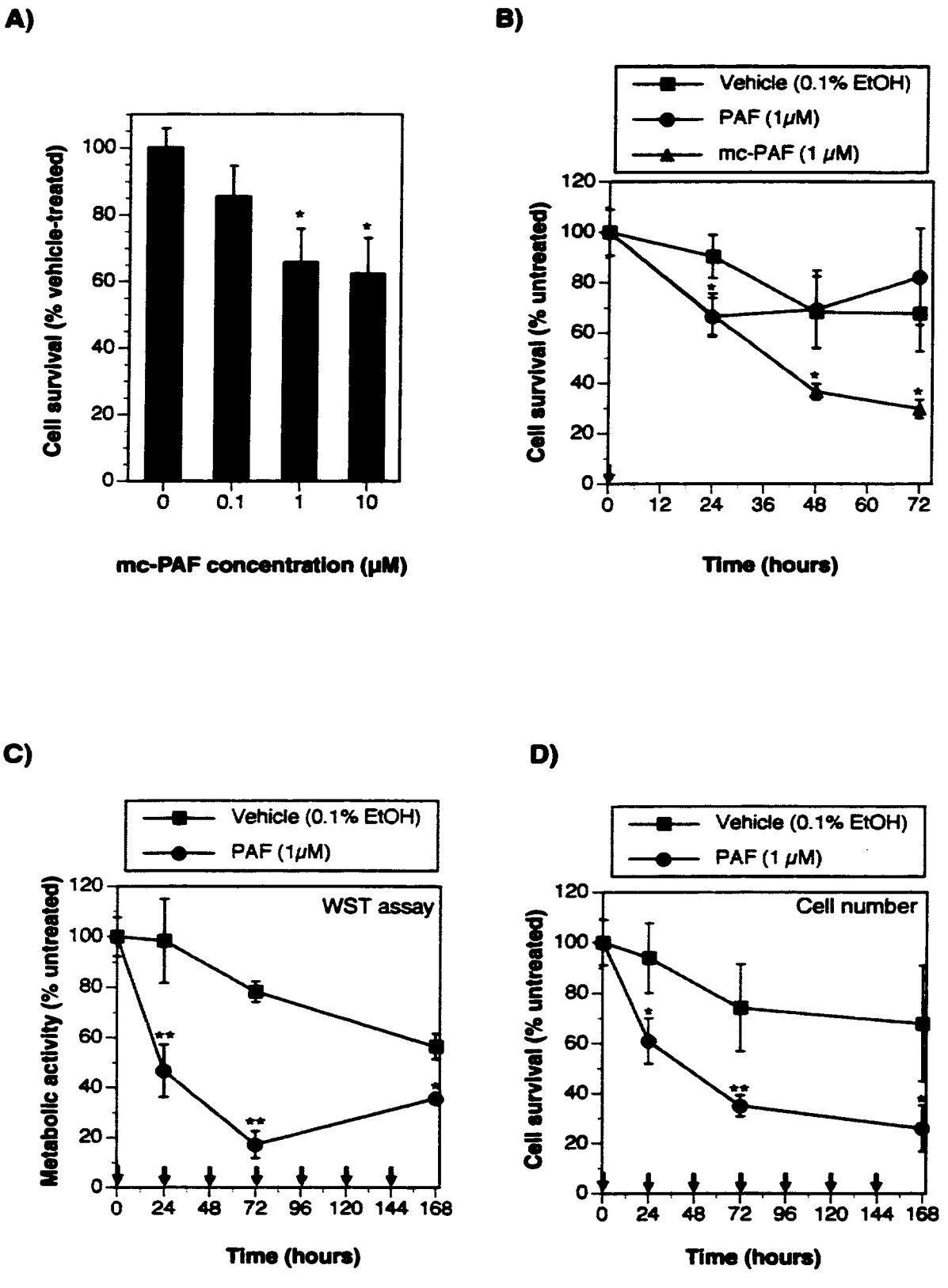
A)
Cell survival (% vehicle-treated)
100
80
60
40
20
0
0
0.1
1
10
mc-PAF concentration (μM)
B)
Vehicle (0.1% EtOH)
PAF (1μM)
mc-PAF (1 μM)
Cell survival (% untreated)
120
100
80
60
40
20
0
0
12
24
36
48
60
72
Time (hours)
C)
Vehicle (0.1% EtOH)
PAF (1μM)
WST assay
Metabolic activity (% untreated)
120
100
80
60
40
20
0
0
24
48
72
96
120
144
168
Time (hours)
D)
Vehicle (0.1% EtOH)
PAF (1 μM)
Cell number
Cell survival (% untreated)
120
100
80
60
40
20
0
0
24
48
72
96
120
144
168
Time (hours)

PC12 viability was also compromised by sustained EtOH exposure (0.1%). A 10% reduction in cell number relative to untreated cells was observed 24 h after treatment; a 33% cell loss was noted 48 h after treatment with no further reductions observed after 72 h of treatment (Figure 2.6B; vehicle).

To establish the effect of chronic PAF exposure on WT-PC12 viability, cells were repeatedly treated with PAF (1 μM) or vehicle (0.1% EtOH) every 24 h. Progressive impairment in the ability of WT-PC12 cells to reduce WST (Figure 2.6C) and an incremental loss in overall cell number (Figure 2.6D) were observed after chronic PAF treatment. The metabolic activity of WT-PC12 cells was reduced by 53% and 83% at 24 and 72 h, with a moderate recovery to 64% viable at 168 h (Figure 2.6C). This sustained compromise in mitochondrial respiration corresponded to a rapid 39% and 65% reduction in cell number after 24 and 72 h of treatment relative to cultures grown in low serum media (Figure 2.6D). A more subtle 7% loss in cell number was observed between 72 h and 168 h of treatment resulting in a 72% reduction in cell number (Figure 2.6D) consistent with the partial recovery in metabolic activity observed between 72 h and 168 h (Figure 2.6C).

PAF-induced cell death is not mediated by downstream metabolites

The observed mc-PAF data suggest PAF-induced cell death is dependent upon sustained ligand exposure. Given that cytosolic PAFAH activity was detected in WT-PC12 cultures, to determine whether PAFAHs protect WT-PC12 cells, the effect of *lyso*-PAF on cell survival was assessed. Various

concentrations of *lyso*-PAF, the immediate metabolite generated by PAFAH, had no effect on the survival of WT-PC12 cells at concentrations below 10 μM (Figure 2.7).

PAF-induced cell loss is attenuated by selected PAF antagonists

To establish that PAF-induced cell death is not simply the result of physicochemical effects on the plasma membrane, the ability of a panel of PAF antagonists to block PAF-induced cytotoxicity was examined (Figure 2.8). Treatment of WT-PC12 cell with PAF (1 μM) in the presence of non-structural PAF antagonists effectively blocked PAF-induced cell death (Figure 2.9B; BN52021, FR49175, L659-989, RP59227). In contrast, only one out of 3 structural PAF antagonist, afforded cell survival. The commercially available antagonists CV3988 and CV6209 were unable to alleviate PAF-induced cell loss while protection was provided by ONO-6248 (Figure 2.9B).

PAF elicits nuclear condensation, DNA strand breaks, and oligonucleosomal DNA fragmentation

To evaluate whether PAF elicits apoptotic cell death, nuclear and biochemical indices of apoptosis were assessed. PAF elicited nuclear changes and DNA strand breaks consistent with apoptotic cell loss (Figure 2.10). After 24 h of PAF (1 μM) treatment, WT-PC12 nuclei were smaller and more brightly stained with Hoescht 33258 (Figure 2.10B) compared to vehicle-treated cells

Figure 2.7: PAF-induced cell loss is not mediated by the PAF metabolite *lyso*-PAF.

WT-PC12 cells plated at 8800 cells/cm^2 were exposed for 24 h to different concentrations of *lyso*-PAF (0, 0.01, 0.1, 1, 10 μM) in low serum media. *Lyso*-PAF the immediate metabolite generated by PAFAH had no effect on the survival of WT-PC12 cells at concentrations below 10 μM as assessed by trypan blue hemocytometer cell counts. Data are expressed as percent vehicle treated cultures. Results reported as means ± SEM (n= 5 per data point) details as described in materials and methods. [*$p<0.05$, ANOVA, *post-hoc* Dunnett's *t*-test]

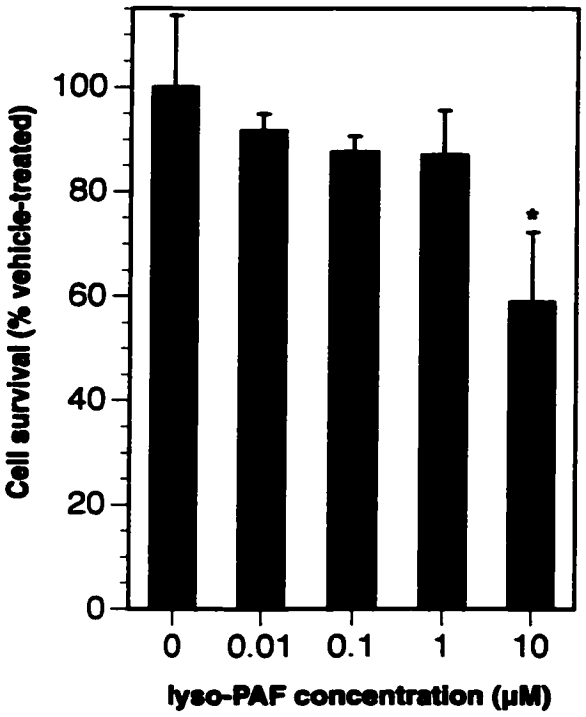
Cell survival (% vehicle-treated)
100
80
60
40
20
0
*
0
0.01
0.1
1
10
lyso-PAF concentration (μM)

Figure 2.8: Chemical structures of the PAF antagonists used in this study.

(A) Structural PAF analogs as PAF antagonists (CV-3988, CV-6209, ONO-6248).
(B) Non-structural PAF antagonists (BN52021, RP59227, L659-989, FR49175).

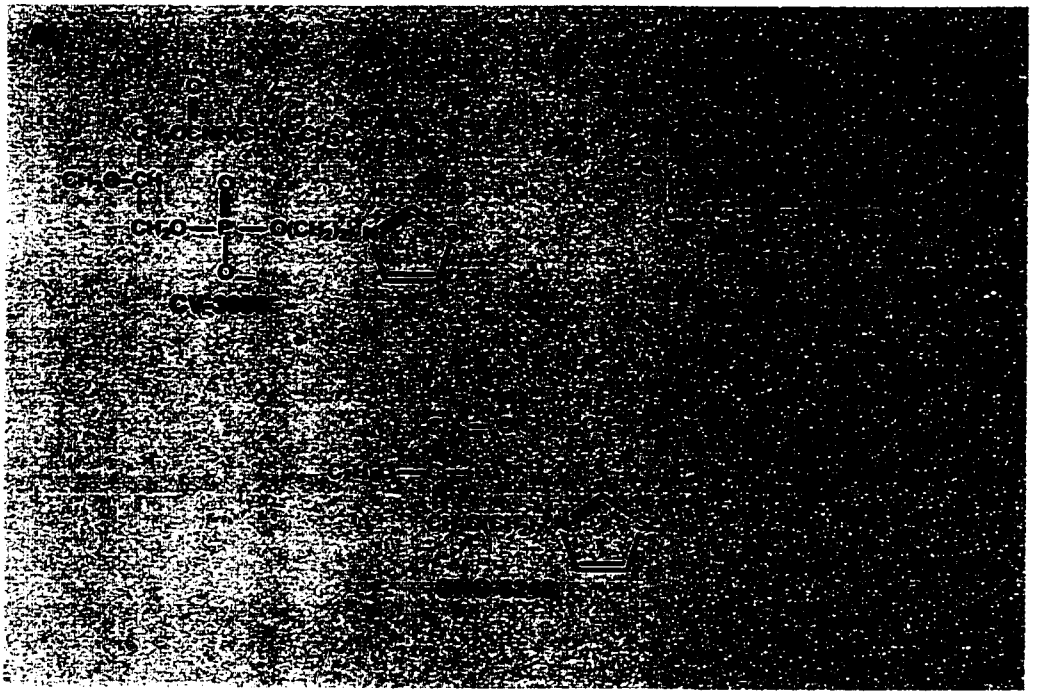

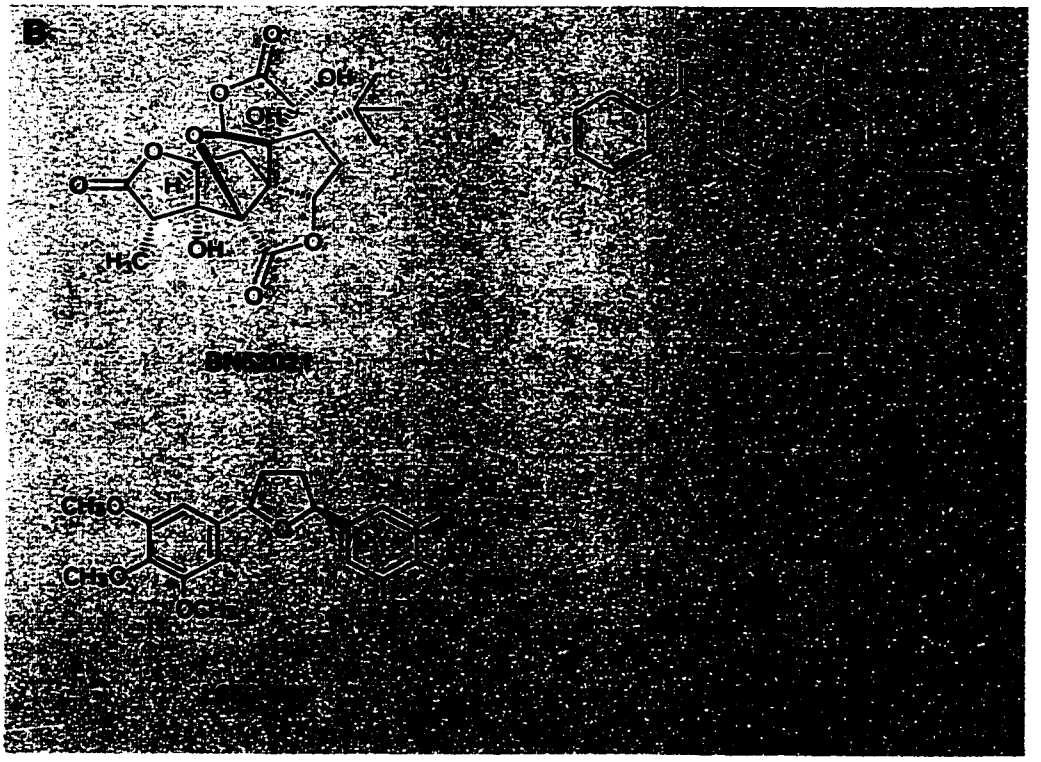

Figure 2.9: WT-PC12 cell survival is afforded by a variety of PAF antagonist following challenge with PAF.

(A) Effect of a panel of PAF antagonists on WT-PC12 cell viability. WT-PC12 cells were exposed for 24 h to different concentrations of PAF antagonists in low serum media. (B) Effect of a panel of PAF antagonists on PAF-induced cell loss. WT-PC12 cells were exposed for 24 h to PAF (1 μM) in the presence of PAF antagonist in low serum media. The PAF antagonists used were (from left to right) none (vehicle), CV6209, CV3988, ONO6248, BN52021, FR49175, L659989, RP59227. Note that the PAF antagonists ONO6248, BN52021, FR49175, L659989, RP59227 afforded protection against PAF-induced cell loss. Cell survival in (A and B) was assessed by trypan blue hemocytometer cell counts. Data are expressed as percent of vehicle treated cultures. Results reported as means ± SEM (n= 5-47 per data point) see text for details. [**$p<0.01$, significant reduction in cell survival compared to vehicle treatment; † $p<0.05$, †† $p<0.01$, significant protection relative to PAF-treated cultures; ANOVA, *post-hoc* Dunnett's *t*-test]

A)

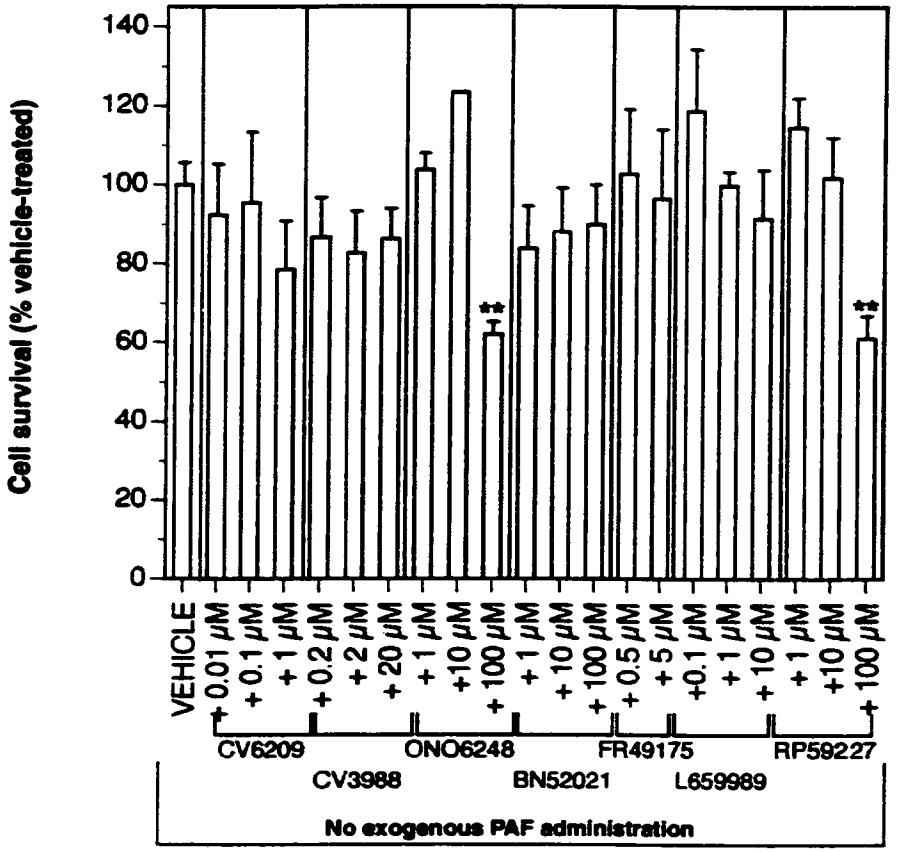
Cell survival (% vehicle-treated)
140
120
100
80
60
40
20
0
VEHICLE
+ 0.01 μM
+ 0.1 μM
+ 1 μM
+ 0.2 μM
+ 2 μM
+ 20 μM
+ 1 μM
+10 μM
+ 100 μM
+ 1 μM
+ 10 μM
+ 100 μM
+ 0.5 μM
+ 5 μM
+0.1 μM
+ 1 μM
+ 10 μM
+ 1 μM
+10 μM
+ 100 μM
CV6209
ONO6248
FR49175
RP59227
CV3988
BN52021
L659989
No exogenous PAF administration

B)

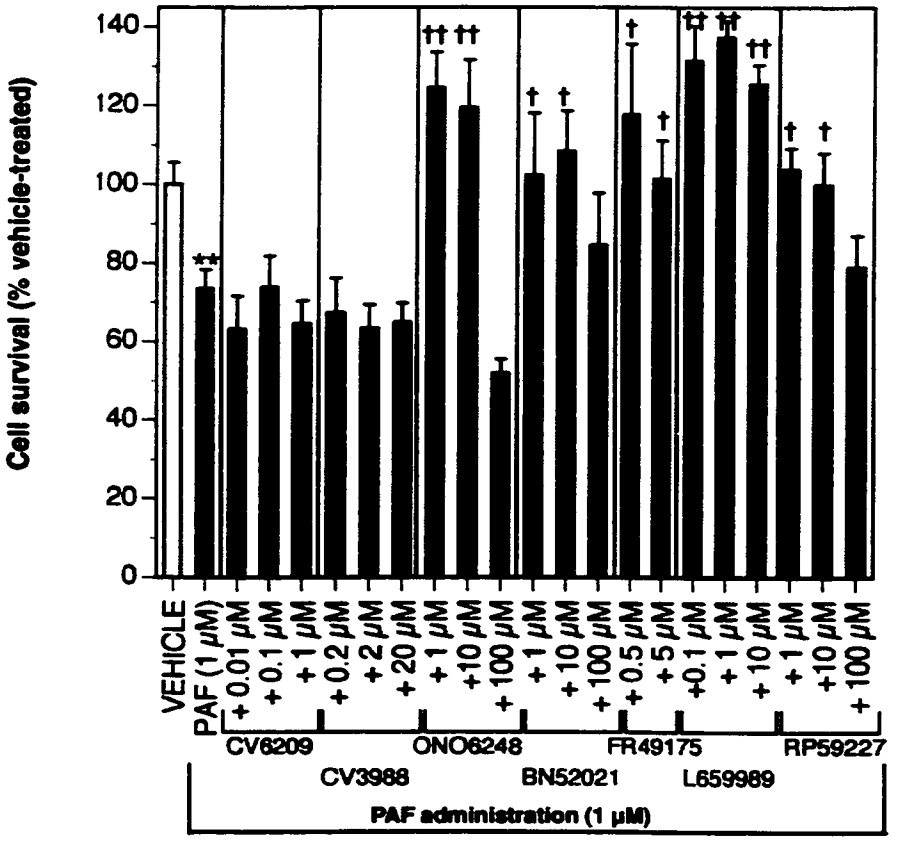
Cell survival (% vehicle-treated)
140
120
100
80
60
40
20
0
VEHICLE
PAF (1 μM)
+ 0.01 μM
+ 0.1 μM
+ 1 μM
+ 0.2 μM
+ 2 μM
+ 20 μM
+ 1 μM
+10 μM
+ 100 μM
+ 1 μM
+ 10 μM
+ 100 μM
+ 0.5 μM
+ 5 μM
+0.1 μM
+ 1 μM
+ 10 μM
+ 1 μM
+10 μM
+ 100 μM
CV6209
ONO6248
FR49175
RP59227
CV3988
BN52021
L659989
PAF administration (1 μM)

Figure 2.10: WT-PC12 cells undergo apoptosis following PAF administration.

PAF elicits nuclear condensation, DNA strand breaks and oligonucleosomal DNA fragmentation. All photomicrographs are representative images of cultures treated with vehicle (0.1% EtOH) (A, C), 10% EtOH (E, F) or PAF (1 μM)(B, D, G, H). (A-D) nuclei double-labeled with Hoechst and TUNEL. Note the rare TUNEL positive cells detected in vehicle-treated cultures (arrows, C). Multiple TUNEL positive cells are evident in PAF treated cultures (D). PAF treatment also elicited chromatin condensation (asterisks, B), nuclear blebbing (arrows, B), and nuclear fragmentation into apoptotic bodies (arrowhead, B). DNA fragmentation occurs prior to loss of plasma membrane integrity as assessed by EthD-1 staining. Cultures treated with 10% EtOH were both EthD-1 and TUNEL positive (E, F). PAF treated cultures were TUNEL positive but not EthD-1 positive (G, H). Scale bar, 10 μm. Panel I, demonstrates quantitative *in vitro* determination of cytoplasmic histone-associated DNA fragments after PAF treatment (n=9). There was a 37% increase in DNA fragmentation. This difference failed to reach statistical significance.

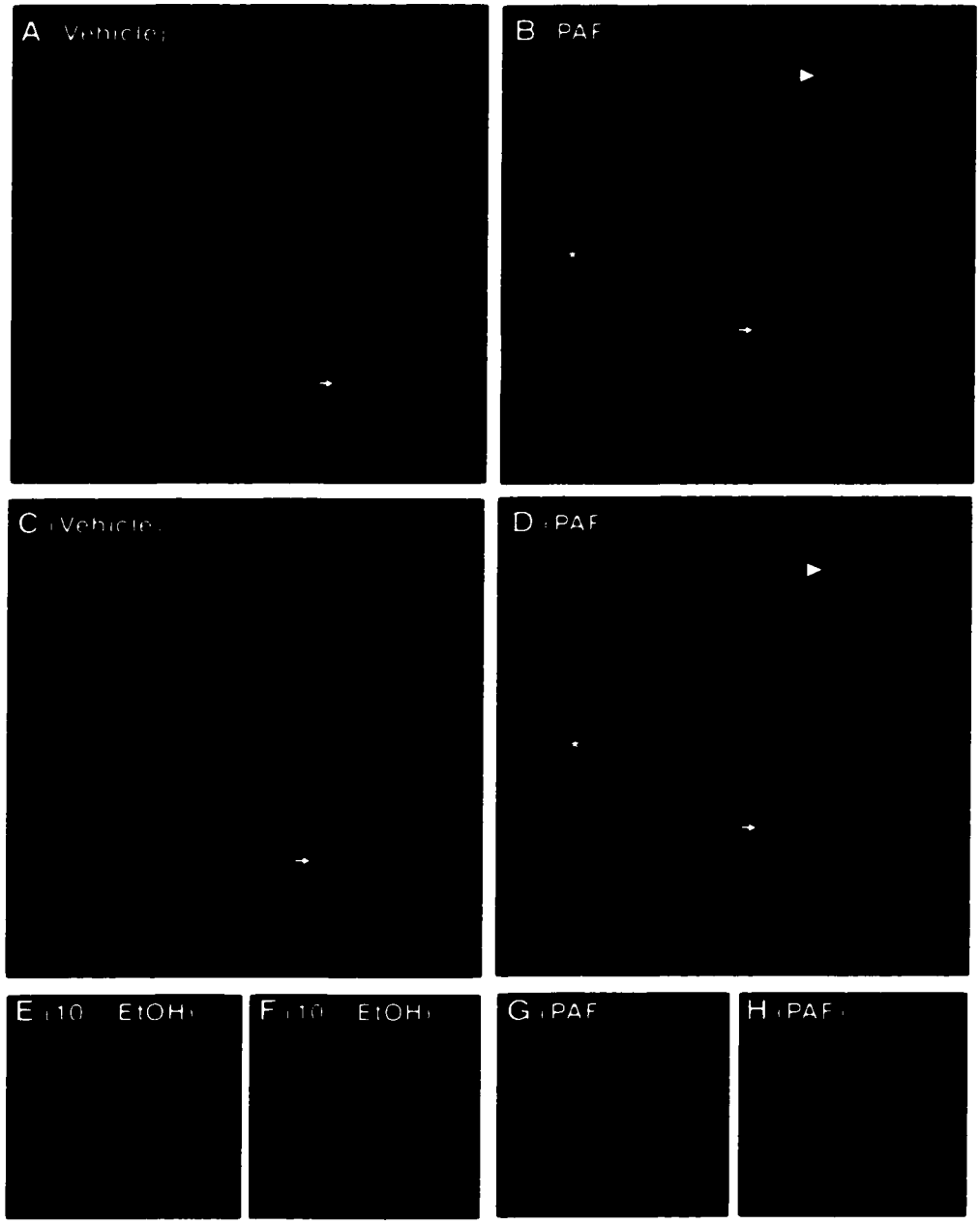
A (Vehicle)
B PAF
C (Vehicle)
D (PAF
E (10 EtOH)
F (10 EtOH)
G (PAF
H (PAF)

I)

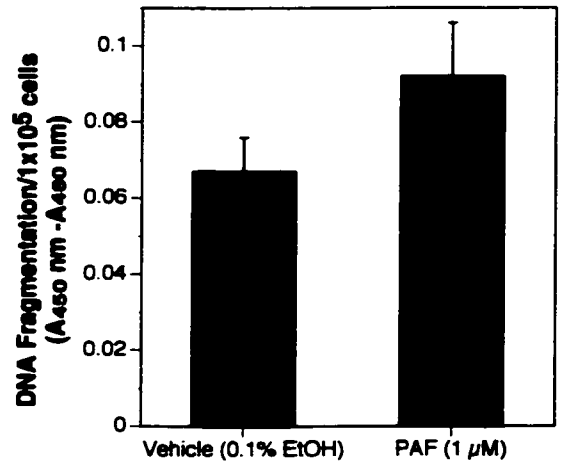
DNA Fragmentation/1x10^5 cells
(A450 nm -A490 nm)
0.1
0.08
0.06
0.04
0.02
0
Vehicle (0.1% EtOH)
PAF (1 μM)

(Figure 2.10A)-characteristics consistent with nuclear and chromatic condensation. Rare TUNEL-positive cells indicative of DNA fragmentation were detected in vehicle-treated cultures (arrows, Figure 2.10C). Multiple TUNEL-positive cells were observed in PAF-treated cultures (Figure 2.10D). Because TUNEL can detect both oligonucleosomal fragmentation characteristic of apoptotic cell death and random DNA damage associated with necrotic cell loss, the morphology of nuclei double-labeled with Hoechst and TUNEL was scored. Condensation of damaged chromatin at the nuclear periphery (asterisks, Figure 2.10B), nuclear blebbing (arrows, Figure 2.10B), and nuclear fragmentation into apoptotic bodies (arrowhead, Figure 2.10B) were detected in PAF but not vehicle-treated cultures.

To determine whether PAF-treated cells undergo DNA fragmentation before or after loss of plasma membrane integrity, cultures were stained with EthD-1 prior to fixation and processing for TUNEL reactivity. To elicit necrotic cell death by membrane disruption (positive control), cultures were treated for 24 h with 10% EtOH, which were both EthD-1 and TUNEL postive (Figure 2.10E,F). In contrast, TUNEL-positive PAF (1 μM)-treated cells (Figure 2.10H) were not stained with EthD-1 (Figure 2.10G). When cells were treated with higher concentrations (10 μM) of PAF or *lyso*-PAF, membrane permeability as indicated by EthD-1 staining was readily apparent in TUNEL-positive cells (data not shown). Thus, it is likely that, at physiologically relevant concentrations of PAF, DNA fragmentation precedes loss of plasma membrane integrity indicative of apoptotic loss. At extremely high concentrations of lipid, both PAF and *lyso*-PAF

likely exert lytic detergent effects on plasma membrane leading to necrotic cell death.

To quantify apoptotic DNA damage triggered by PAF, histone-associated DNA fragments were measured using a commercial ELISA. A 37% increase in oligonucleosomal fragmentation was detected following PAF (1 μM) treatment relative to vehicle (0.1% EtOH) treatment (Figure 2.10I).

Expression of PAFR-GPCR protects cells from PAF-induced apoptosis

To evaluate the effect of PAFR-GPCR expression on PAF-induced apoptosis empty vector pGS-2 and HPAFR-7 cells were treated for 24 h in low serum media with PAF (1 μM). Comparable to WT-PC12 cells (Figure 2.5), PAF elicited a 27% loss of pGS-2 cells (Figure 2.11). In contrast, expression of PAFR-GPCR protected cells from PAF-induced cell death. No change in viability of HPAFR-7 cells was observed following PAF treatment relative to vehicle-treated cultures.

Figure 2.11: Expression of hPAFR-GPCR renders WT-PC12 cells impervious to PAF-induced cytotoxicity.

Empty vector pGS-2 and HPAFR-7 cells were exposed for 24 h to PAF (1 μM) in low serum media. Cell survival was assessed by trypan blue hemocytometer cell counts. Empty vector alone was susceptible to PAF-induced cell loss. HPAFR-7 cell viability was unaffected by PAF treatment. Data are expressed as percent vehicle treated cultures. Results reported as means ± SEM (n= 7 per data point) details as described in materials and methods. [*$p<0.05$, students *t*-test]

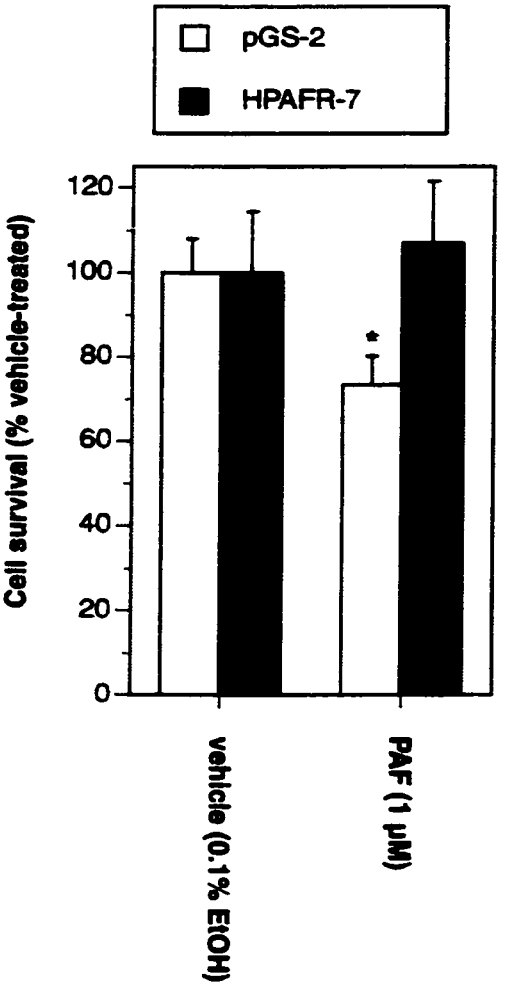
pGS-2
HPAFR-7
Cell survival (% vehicle-treated)
120
100
80
60
40
20
0
*
vehicle (0.1% EtOH)
PAF (1 μM)

Discussion

The proinflammatory lipid PAF is hypothesized to be a principle initiator of neuronal dysfunction and death in HIV-dementia and a secondary mediator of neuronal loss in ischemia and epilepsy (Yue and Feuerstein, 1994; Bazan, 1998; Gelbard et al., 1994; Nishida et al., 1996; Marcheselli and Bazan, 1994; Feuerstein et al., 1990; Schifitto et al., 1999). The mechanisms underlying PAF-induced cell death have only begun to be elucidated. The presented data demonstrates that PAF triggers apoptotic loss of WT-PC12 cells but that neurotoxicity is not initiated by PAFR-GPCR.

Apoptotic cell loss was confirmed by four different assays evaluating nuclear changes associated with apoptosis. PAF-induced nuclear and chromatin condensation, DNA strand breaks, DNA fragmentation into histone-associated oligonucleosomes, and nuclear disintegration into apoptotic bodies. *Lyso*-PAF, the biologically inactive PAF metabolite, had no effect on WT-PC12 viability at physiological concentrations. These findings demonstrate that apoptosis is PAF-specific and is not elicited by downstream lipid metabolites. Cell death is mediated by PAF receptors in that it is blocked by five different PAF antagonists (ONO-6248, L659-989, FR41975, RP59227, BN52021) and cannot be attributed to physicochemical effects on cell membranes. Surprisingly, PAF-induced apoptosis occurred in the absence of PAFR-GPCR. WT-PC12 cells do not express PAFR-GPCR. Transfection of hPAFR-GPCR protected PC12 cells from PAF-induced cell death. We propose that a novel binding protein (i.e., an iPAFR) triggers apoptotic loss of PC12 cells whereas PAFR-GPCR activation may

promote cell survival. Our data are consistent with repeated demonstrations that PAF is neurotoxic (Kornecki and Ehrlich, 1988; Gelbard et al., 1994; Westmoreland et al., 1996) and support the growing consensus that targeting PAF signal transduction may reduce the rate of cell death in HIV-dementia, ischemia/reperfusion injury, and epileptic seizures (Schifitto et al., 1999; Langley et al., 1999; Akisu et al., 1998; Loucks et al., 1997; Gilboe et al., 1991; Panetta et al., 1987; Birkle et al., 1988).

A total of seven PAF antagonists (CV3988, CV6209, ONO-6248, L659-989, FR41975, RP59227, BN52021) were screened for their ability to inhibit PAF-induced neuronal apoptosis. Five PAF antagonists (ONO-6248, L659-989, FR41975, RP59227, BN52021) effectively blocked PAF-induced apoptosis. This panel of antagonists can be subdivided into PAF analogs (CV3988, CV6209, ONO-6248) and non-structural PAF antagonists (L659-989, FR41975, RP59227, BN52021). The PAF analogs screened in this study all share the glycerol backbone with varying degrees of similarities and substitutions of the side chain moieties (Figure 2.8). CV3988 and CV6209 were among the first PAF antagonists to be identified and used as reference standards for inhibition of PAF/PAFR-GPCR interaction (Terashita et al., 1983; Terashita et al., 1986). Neither of these reagents provided protection against PAF-induced neurotoxicity in the present study. Given the absence of endogenous PAFR-GPCR, these results are in agreement that these antagonists demonstrate specificity for PAFR-GPCR. Conversely, the structural analog ONO-6248 effectively inhibited PAF-induced apoptosis. It has been reported that ONO-6248 is more potent

than CV3988 in common screening assays (Shen et al., 1987). The present study suggest that this reported increase in potency likely reflects the ability of this compound to effectively displace PAF from uncharacterized PAF binding proteins. All of the non-structural antagonists blocked PAF-induced cell loss. Note the dissimilarities of these compounds (Figure 2.8). The synthetic lignan L659-989 (Hwang and Lam, 1991), FR49175, a derivative of the fungal metabolite gliotoxin (Okamoto et al., 1986), and the pyrrolo-thiazole derivative RP59227 (Lave et al., 1990) inhibited PAF-induced cell death. Finally, BN52021, also known as ginkolide B, effectively reduced cell loss following apoptogenic challenge with PAF. This terpenoid extract from the leaves of the *Ginkgo biloba* tree deserves special mention. Experimental evidence has demonstrated that this compound prevents PAF-induced glutamate release and protects neurons from ischemia-reperfusion injury (Akisu et al., 1998; Nogami et al., 1997; Clark et al., 1992; Birkle et al., 1988, Panetta et al., 1987). The potential clinical applications of this compound have recently been reviewed (DeFeudis and Drieu, 2000; Yoshikawa et al., 1999). In addition to classification as a PAF antagonist, BN52021 also has an antioxidant action as a free radical scavenger (Yoshikawa et al., 1999). This additional biological effect of BN52021 is particularly intriguing for several reasons: (1) reactive oxygen species (ROS) are implicated in apoptotic signaling cascades (for a review see Carmody and Cotter, 2001) and (2) increasing evidence is emerging that PAF contributes to tissue injury via ROS generation (Yildirim et al., 2000; Yamakawa et al., 2000; Goldman et al., 1999; Matsuo et al., 1996; Alloatti et al., 1994). Thus, the ability of BN52021 to block

PAF-induced apoptosis may result from its ability to inhibit PAF-induced oxyradical production in concert with competitive interaction for a novel PAF receptor. These results combined with the increasing evidence of PAF receptor heterogeneity demonstrate the ambiguity of pharmacological characterization of PAF antagonists and emphasizes the need for additional screening protocols. While the signaling mechanisms underlying PAF-mediated apoptosis must be identified, the ability of multiple PAF antagonists to inhibit PAF-induced cell death imply a receptor-mediated mechanism.

Because PAF is a phosopholipid, we tested the possibility that cytotoxicity is simply the result of physicochemical effects on the plasma membrane. Necrotic cell death can result from non-specific lytic detergent actions on the plasma membrane observed when lipid levels exceed their critical micelle concentration. The critical micelle concentration of PAF is estimated to be 2.5 - 3 μM (Blank et al., 1981). To test this hypothesis, we evaluated whether a breakdown in plasma membrane precedes DNA damage. Membrane disruption characteristic of necrotic cell loss was apparent when PC12 cells were treated with 10% EtOH, 10 μM PAF or 10 μM *lyso*-PAF but not when cells were exposed to lower concentrations of PAF. PAF- and *lyso*-PAF-mediated necrosis elicited by artificial lipid concentrations are not inhibited by PAF antagonists. When cells were treated with PAF (100 nM-1 μM) but not not *lyso*-PAF (100 nM-1 μM), apoptotic-like DNA damage was observed in cells with intact plasma membrane. Thus, while artificial concentrations of PAF (10 μM) elicit necrotic cell death, exposure to high but physiologically relevant concentrations of PAF (100 nM-1

μM) triggers nuclear changes and DNA damage consistent with apoptotic cell death. These data support our hypothesis that PAF-mediated apoptosis is not simply the result of physicochemical effects on plasma membrane but is mediated by a novel PAF binding protein/iPAFR expressed by PC12 cells.

The duration of PAF-induced apoptosis was found to be dependent upon chronic exposure to active ligand. A single exposure to PAF in serum-reduced media resulted in a 24% reduction in WT-PC12 cell number within 24 h. No further cell loss was observed. However, repeated exposure to PAF, or a single administration of PAFAH resistant mc-PAF, triggered persistent apoptotic cell death over a 72 h time period resulting in approximately an overall 70% reduction in cell number. These results provide circumstantial evidence for the hypothesis that PAFAHs attenuate PAF-mediated neurotoxicity. Recall that an acetyl group at the *sn*-2 position is essential for the specificity and biological activity of PAF (Snyder, 1995). PAFAHs hydrolize PAF at the *sn*-2 position thereby inactivating the ligand. Three isoforms of PAF acetylhydrolase (Ib, II, and plasma-type) have been identified. Isoforms 1b and II are intracellular; the plasma-type isoform is secreted (Chapter 1). Note that PAF-mediated apoptosis was not detected when cells were cultured in complete media with high serum content. In the present study, detectable PAFAH activity was evident in complete (serum-containing) but not serum-depleted media. Although the identity of these isoforms was not determined at the molecular level, it is likely that the enzyme present in complete media is plasma PAFAH. We also conclude that PAF is likely metabolized by the PAFAH1b enzyme complex in PC12 cells. This conclusion is based upon

expression of the PAFAH1b subunits (alpha 1, alpha 2, and LIS-1) by PC12 cells, the detection of PAFAH activity in cell lysates, and the observation that the majority of neural PAFAH activity is attributed to the PAFAH1b isozyme (Hattori et al., 1993). This marks the first demonstration of PAFAH activity in this cell line and it is likely that PAFAH1b limits the apoptogenic effect of PAF on PC12 cells. Furthermore, these data are consistent with recent studies demonstrating that administration of recombinant plasma PAF-acetylhydrolases or transfection of plasma PAF-acetylhydrolase protects neurons from apoptotic death (Perry et al., 1998; Hirashima et al., 2000; Ogden et al., 1998).

Although the neurotoxic effects of PAF have repeatedly been demonstrated, it has not been definitively established how PAF initiates cell death. Our data indicate that PAF-mediated apoptosis is initiated by a novel PAF binding protein. To date, a single PAF receptor has been cloned and identified as a GPCR (Chapter 1). Dr. Bennett's group have previously shown that PAFR-GPCR is expressed by apoptotic neurons in the hippocampal formation after excitotoxic injury and epileptic seizure *in vivo* (Bennett et al., 1998). These data led us to hypothesize that PAF acts through PAFR-GPCR to initiate cell death. In the present study, we found that PAF triggers PC12 cell death independently of PAFR-GPCR. Unexpectedly, PAFR-GPCR expression in PC12 cells afforded protection to PAF-induced cell death. Although it is acknowledged that further experimentation is required to ascertain whether (1) activation of PAFR-GPCR generates anti-apoptotic signals or (2) PAFR-GPCR competes for PAF binding thus preventing interaction with iPAFRs and subsequent generation of apoptotic

cascades. Regardless, these data point to the existence of additional PAF binding protein(s) capable of transducing a PAF-initiated apoptotic signal. Our laboratory has also demonstrated that the susceptibility of hNT cells to PAF-induced neurotoxicity occurs in the absence of PAFR-GPCR expression (unpublished observation, Westmoreland et al., 1996). Marcheselli et al. (1990) pharmacologically characterized iPAFRs in primary neuronal cultures, which localized to microsomal membranes. Stimulation of iPAFRs has been implicated in signal transduction leading to neuronal loss following epileptiform seizure and ischemic attack (Bazan, 1998). However, it is not known whether iPAFRs are coded by a novel PAF receptor gene(s) or represent internalized PAFR-GPCR. The present study provides phenotypic data to support the hypothesis that at least one iPAFR is a novel receptor protein. PC12 cells do not express PAFR-GPCR transcript and, as a result, sensitivity to PAF cannot be attributed to internalized PAFR-GPCR isoforms. The PAF antagonist, BN50730, has been identified as a specific antagonist of brain microsomal PAF binding sites (Marcheselli and Bazan, 1994). While this antagonist is not commercially available, we have agreed to work in cooperation with collaborators to determine whether BN50730 inhibits PAF-induced apoptosis in this cell line.

In summary, these data represent an initial step in providing a mechanistic understanding of the PAF-mediated cytotoxicity observed in HIV-dementia, ischemia-reperfusion injury, and epileptic seizure through interaction with a receptor other than PAFR-GPCR and support the hypothesis that PAF antagonists may reduce neuronal damage associated with these conditions.

CHAPTER 3: EXPRESSION OF hPAFR-GPCR RESULTS IN INCREASED PROLIFERATION DURING NEURONAL DIFFERENTIATION

Introduction

The physiological importance of signal transduction in the control of developmental processes such as cell proliferation and differentiation is well established. Precedents in the literature indicate that PAF and PAFAH1b play important roles in neuronal differentiation and proliferation (Chapter 1). From a biochemical perspective, demonstration of LIS-1 mutation as the genetic determinant for MDS has led to the hypothesis that decreased functional PAFAH1b results in sustained PAF signaling during corticogenesis. In mice, homozygotic deletion of LIS-1 is embryonic lethal while haplo-insufficiency results in cerebral malformation caused by impaired neuronal migration and an increase in neural precursor proliferation between embryonic days 11-14.5 (Hirotsune et al., 1998; Fleck et al., 2000; Cahana et al., 2001). In Chapter 2, it was demonstrated that PAFR-GPCR expression reduces PAF-mediated cytotoxicity. We have yet to determine whether PAF/PAFR-GPCR interaction triggers anti-apoptotic signaling pathways or whether receptor activation stimulates WT-PC12 cell proliferation thereby masking reduction in cell number attributed to apoptotic cell loss. Previous studies have shown that PAF triggers proliferation of non-neuronal cultures and influences neuronal migration and motility *in vitro* (Chapter 1). It is not known whether sustained PAFR-GPCR activation impacts on pathological neural precursor proliferation or migration consistent with the MDS phenotype.

Objective

To elucidate the role of PAF/PAFR-GPCR interaction in neuronal differentiation and migration, we used the PC12 cell model to test the hypothesis that PAF triggers neuronal precursor proliferation and/or inhibits neuronal migration. In this series of experiments, the data indicate that hPAFR-GPCR activation blocks the relative growth arrest associated with differentiation to a neuronal phenotype in PC12 cells.

Model System

Widely used as a model of neuronal differentiation and signal transduction, PC12 cells, a rodent pheochromocytoma-derived cell line, can be differentiated to a neuronal-like phenotype by exposure to nerve growth factor (NGF) in the presence of low serum media (Greene and Tischler, 1976). Hallmark features of this model are twofold; PC12 cells extend neurites and undergo relative growth arrest in comparison to undifferentiated cultures. In parallel with these morphological changes, PC12 cells develop expression of neuron-specific markers and biological activity over the course of NGF treatment (Levi and Alema, 1991). The biochemical pathways that lead to PC12 differentiation are still under investigation.

Materials and Method

Cell Culture

WT-PC12, empty vector, and HPAFR clones were cultured as described in Chapter 2. Cells were differentiated to a neuronal phenotype on rat tail collagen type 1 (Roche)-coated 10 cm dishes. Differentiation was induced 24 hours after plating by rinsing with PBS and replacing the complete media with low serum media (RPMI 1640 supplemented with 1% heat-inactivated horse serum; Invitrogen) in the presence of 50 ng/ml NGF 7S (Sigma or Invitrogen) and 0.1% EtOH.

In vitro Cell Migration Assays

Cell migration and motility was assessed as described in (Adachi et al., 1997). Cells were plated in complete media on collagen coated 10 cm tissue culture dishes at an initial seeding density of $5x10^4$ cells. Differentiation was induced as described above 24 hours after plating and cell colonies of similar size (average of 6-7 cells) were randomly selected for analysis. Photomicrographs were taken and colony locations were mapped for subsequent observation. Each colony was located on day 5 of culture and photomicrographs were taken. The migration index per cell was defined as described in (Adachi et al., 1997) using the following calculation: (diameter of colony at day 5 (μm)/diameter of colony on day 0 (μm))/ total number of cells in colony on day 5. Experiments were conducted in replicate, values are given as mean migration index ± SEM.

Cell Proliferation Assays

For all growth assessment studies $5x10^4$ cells were plated in complete media in 10 cm dishes and cultured in complete media (undifferentiated) or low serum media supplemented with NGF (NGF-differentiated) as described above. The media was replaced on day 3, 5, and 7 of culture. To ensure that the same number of cells was accurately plated in each experiment, plating control counts were performed 24 h after initial seeding. Growth kinetics in complete media and during NGF-induced differentiation were established over a 10 day period by hemocytometer cell counts of Trypan Blue excluding cells and the WST cell proliferation assay (described in Chapter 2). To block hPAFR-GPCR activation during differentiation the PAF antagonist CV3988 (0.2-2 μM, Biomol) was added to the differentiation media at each feeding. PAF-specific effects were ascertained by culture in low serum media containing PAF (0.01-1 μM, Biomol), lyso-PAF (0.1-1 μM, Cayman Chemical), or vehicle (0.1% EtOH). Note the latter experiments were performed in the absence of NGF.

Immunohistochemistry

Cells were seeded at 1.2 x 10^3 cells per well on collagen-coated 4-well culture glass slides (Becton Dickinson) in complete media. Twenty-four hours after plating, cultures were incubated in low serum media in the presence of NGF (50 ng/ml) and 0.1% ethanol or PAF (100 nM) in the absence of NGF. The media was replaced on day 3 of culture and processing commenced on day 5 of culture. Cells were rinsed with 10 mM PBS and fixed in 3.7% formaldehyde for 10 minutes. Following repeated PBS washes the primary monoclonal proliferating cell nuclear antigen (PCNA) antibody (1:6000; Sigma) or microtubule associated protein (MAP) 2 antibody (1:500; Sigma) was applied and incubated at 4^0C. Note MAP2 immunohistochemistry was performed on NGF-differentiated cultures only. Following repeated PBS washes immunopositive cells were visualized with a Cy3-conjugated goat-anti mouse secondary antibody (1:800; Jackson Immunolabs). Antibodies were diluted in Ab buffer (10 mM PBS, 3% BSA, 0.3% Triton-x, pH 7.2). Vectashield mounting medium (Vector Laboratories) was applied and cells were examined. The mean fluorescent intensity/number of cells per field ±SEM was determined using Northern Exposure imaging and analysis software and standardized to the mean fluorescent intensity of control empty vector cultures.

PAF acetylhydrolase activity assay

The activity of PAFAH was assayed using the commercially available PAF acetylhydrolase assay kit (Chapter 2). Cytosolic fractions were prepared and

assayed as described in Chapter 2 from NGF-differentiated WT-PC12, pGS-2 empty vector, and HPAFR-7 cells on day 5 of culture plated at an initial seeding density of $5x10^4$ cells.

Statistical analysis

Data were analyzed using one-way factorial ANOVA tests or unpaired Student's *t*-tests, as applicable. Following detection of a statistically significant F value with respect to the effect of a given series of treatments, *post hoc* Dunnett's *t*-tests were used to identify which treatment condition differed statistically from control (vehicle-treated, depending on the experiment). P values <0.05 were considered statistically significant differences (shown as *); P values of <0.01 were considered highly statistically significant differences (shown as **).

Results

Undifferentiated and NGF-differentiated Growth Analysis

Growth rates over a 10 day period were determined by hemocytometer counts of Trypan blue excluding cells and WST metabolic assay. WT-PC12 control cultures were untransfected parental cells cultured for the same number of passages as transfectants. Data were standardized to these controls and expressed as percent cell number or fold increase in WST absorbance. WT-PC12 cells extend neurites and demonstrate relative growth arrest when differentiated to a neuronal phenotype following treatment with NGF in low serum

media. (Figure 3.1; A, B). Note that WT-PC12 cells do not terminally differentiate in response to NGF, which results in measurable increases in cell number over the course of the experiment albeit reduced relative to growth of undifferentiated cultures. WT-PC12, pGS-2 empty vector, and HPAFR-7 cells displayed similar growth profiles when cultured in complete media (undifferentiated) (Figure 3.2A). Empty vector, pGS-2 transfected cells demonstrated a comparable reduction in growth following NGF-induced differentiation (Figure 3.2B). However, HPAFR-7 cells, a medium expressor of transfected hPAFR-GPCR (Chapter 2), continued to proliferate during the course of NGF-induced differentiation. A significant increase in cell number was observed as early as 3 days after initial NGF treatment (Figure 3.2B). To confirm these results, a panel of empty vector and hPAFR transfectants were screened using day 5 of culture as the end point for further studies.

Expression of low, medium and high levels of hPAFR-GPCR protein has no effect on growth of undifferentiated cultures

There was no effect on the proliferative response of PC12 cells transfected with hPAFR-GPCR in complete media. After 5 days of culture, total cell number and metabolic activity of WT-PC12 cells, pGS-2 empty vector, and a panel of HPAFR clones (HPAFR-3, HPAFR-7 and HPAFR-4 low, medium and high expressors of hPAFR-GPCR protein respectively, Chapter 2) were comparable (Figure 3.3; A, B). Data were standardized against WT-PC12 cells and expressed as percent cell number (cell counts) or fold increase in metabolic activity (WST assay).

Figure 3.1: WT-PC12 cells reduce proliferation and extend neurites following NGF treatment.

Cells were seeded at the same density and cultured in complete media (undifferentiated) or low serum media supplemented with 50 ng/ml NGF (NGF-differentiated). Note WT-PC12 cells do not terminally differentiate in response to NGF, which results in measurable increases in cell number over the course of treatment. Hallmark feature of this *in vitro* model are twofold: following NGF-induced differentiation (A) WT-PC12 cells demonstrate relative growth arrest and (B) extend neurites (arrow) and develop a neuronal-like phenotype in comparison to undifferentiated cultures.

A)

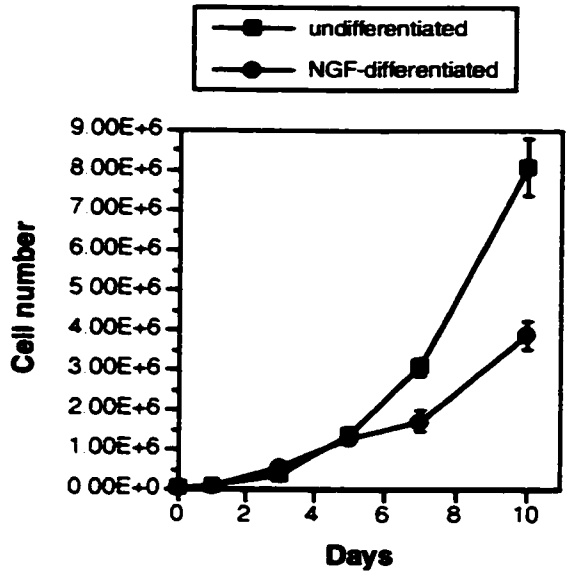

B)

Day 5 of culture

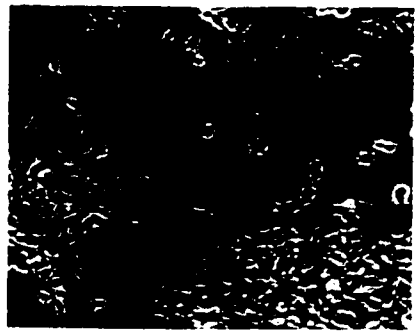

Undifferentiated Cells

NGF-differentiated cells

Figure 3.2: Growth kinetics of WT-PC12, empty vector pGS-2 and hPAFR-GPCR expressing clone.

Growth kinetics in complete media and during NGF-induced differentiation were established over a 10 day period by hemocytometer cell counts of trypan blue excluding cells. (A) Undifferentiated cultures (B) NGF-differentiated cultures. No difference in cell growth was observed in complete media. Note HPAFR-7, a medium expressor of transfected hPAFR-GPCR (Chapter 2), continued to proliferate during the course of NGF-induced differentiation. A significant increase in cell number is apparent as early as 3 days following NGF-treatment. Results reported as means ± SEM (n= 5-60 per data point) details as described in materials and methods. [*$p<0.05$, ** $p<0.01$, ANOVA, *post-hoc* Dunnett's *t*-test]

A)

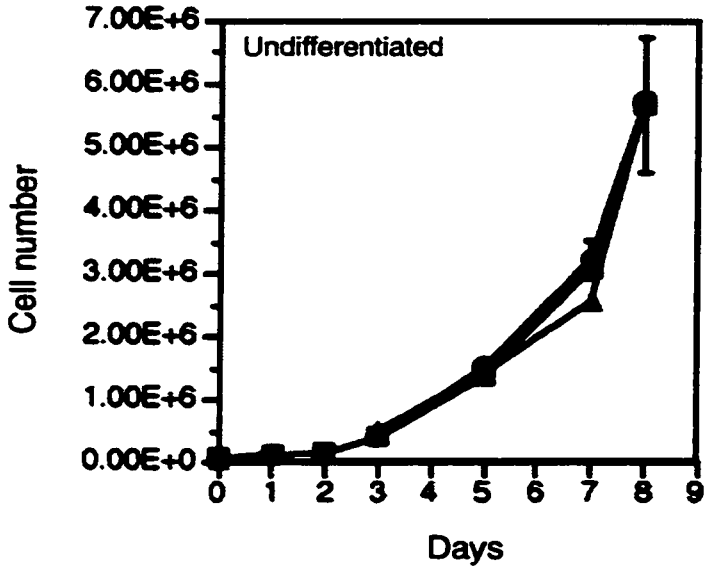
Undifferentiated
Cell number
7.00E+6
6.00E+6
5.00E+6
4.00E+6
3.00E+6
2.00E+6
1.00E+6
0.00E+0
0 1 2 3 4 5 6 7 8 9
Days

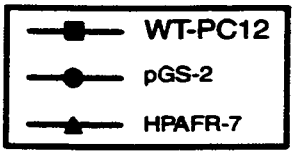
WT-PC12
pGS-2
HPAFR-7

B)

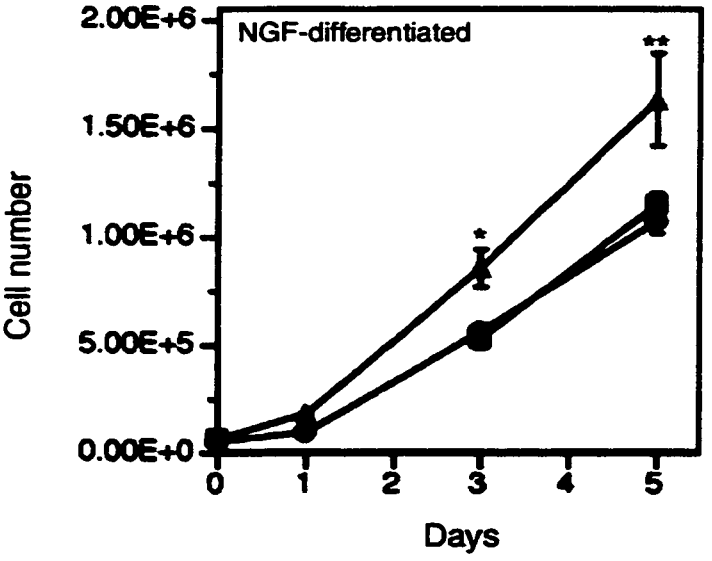
NGF-differentiated
Cell number
2.00E+6
1.50E+6
1.00E+6
5.00E+5
0.00E+0
*
**
0 1 2 3 4 5
Days

Figure 3.3: Expression of hPAFR-GPCR has no effect on growth of undifferentiated cultures.

Cell number was assessed on day 5 of culture by (A) trypan blue hemocytometer cell counts and by (B) WST cell proliferation assay to measure metabolic activity. Data are standardized against control cultures to represent percent (A) and fold (B) changes in cell proliferation relative to untransfected control WT-PC12 cells. No significant variance among cultures was observed. Results reported as means ± SEM (n= 5 per data point) details as described in materials and methods.

A)

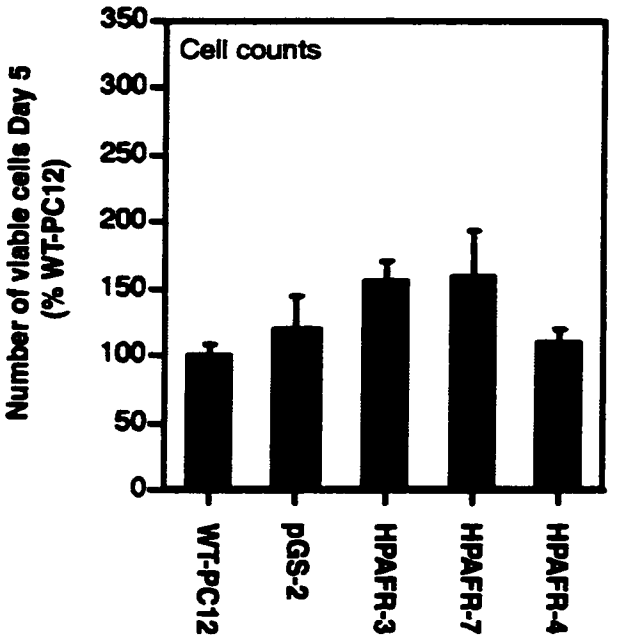
Cell counts
Number of viable cells Day 5
(% WT-PC12)
350
300
250
200
150
100
50
0
WT-PC12
pGS-2
HPAFR-3
HPAFR-7
HPAFR-4

B)

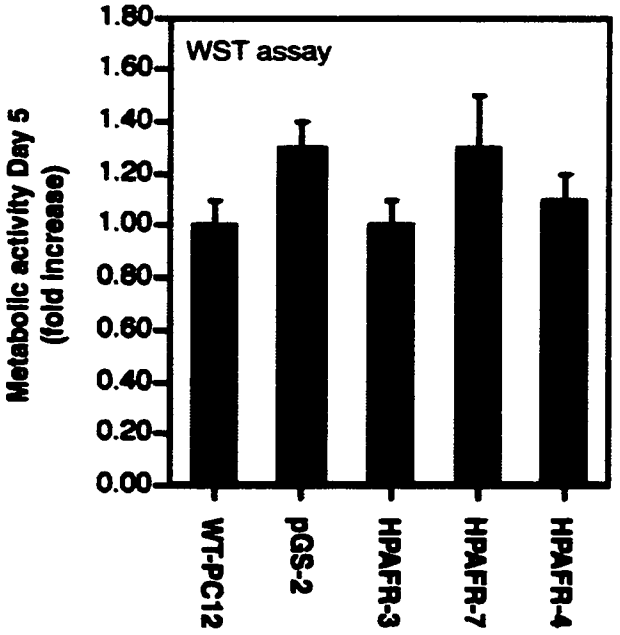
WST assay
Metabolic activity Day 5
(fold increase)
1.80
1.60
1.40
1.20
1.00
0.80
0.60
0.40
0.20
0.00
WT-PC12
pGS-2
HPAFR-3
HPAFR-7
HPAFR-4

Expression of hPAFR-GPCR results in increased proliferation during NGF-induced differentiation to a neuronal phenotype

hPAFR-GPCR expression prevented the relative growth arrest associated with differentiation to a neuronal phenotype in PC12 cells (Figure 3.4). Increased cell proliferation correlated with the level of hPAFR-GPCR protein expression and was statistically significant in HPAFR clones expressing medium (HPAFR-7) and high (HPAFR-4) levels of hPAFR-GPCR protein (Chapter 2). Data were standardized against WT-PC12 cells and expressed as percent cell number (cell counts) or fold increase in metabolic activity (WST assay). Transfection with empty vector or expression of low levels of hPAFR-GPCR protein (HPAFR-3) had no effect on cell proliferation (Figure 3.4). Gross morphology and neurite extension was comparable in all cultures (data not shown). In addition hPAFR-GPCR expression did not alter immunoreactivity of the neuronal differentiation marker MAP2 (Figure 3.5). To confirm that the increase in cell number observed in hPAFR-GPCR transfectants was the result of enhanced cell proliferation, empty vector pGS-2 and HPAFR-7 cells cultures were incubated in low serum media in the presence of NGF (50 ng/ml). Fluorescence microscopy demonstrated PCNA immunoreactivity in essentially all empty vector control cells consistent with low levels of proliferation throughout NGF-induced differentiaton (Figure 3.6). Expressed throughout the cell cycle PCNA is a 36 kD nuclear protein. While multiple cellular roles have been described, PCNA is best characterized as a marker of cellular proliferation. PCNA is required for DNA replication. Expression increases during G1 and is most abundant during S phase, functioning as an auxiliary protein for DNA polymerase delta and epsilon

Figure 3.4: Transfection of hPAFR-GPCR results in increased proliferation during NGF-induced differentiation to a neuronal phenotype.

Cultures were maintained in low serum media supplemented with NGF. Cell number was assessed on day 5 of culture by (A) trypan blue hemocytometer cell counts and by (B) WST cell proliferation assay to measure metabolic activity. Data are standardized against control cultures to represent percent (A) and fold (B) changes in cell proliferation relative to untransfected control WT-PC12 cells. Note that exogenous PAF is not added to the media during differentiation. It can be observed that proliferation is dependent upon the level of hPAFR-GPCR expression in transfectants. Low levels of hPAFR-GPCR (HPAFR-3, Chapter 2) had no effect on cell proliferation. HPAFR-7 and HPAFR-4, medium and high expressors of hPAFR-GPCR respectively, failed to undergo relative growth arrest during differentiation. Gross morphology and neurite extension was comparable in all cultures (data not shown). Results reported as means ± SEM (n= 5-15 per data point) details as described in materials and methods. [*$p<0.05$, ** $p<0.01$, ANOVA, *post-hoc* Dunnett's *t*-test]

A)

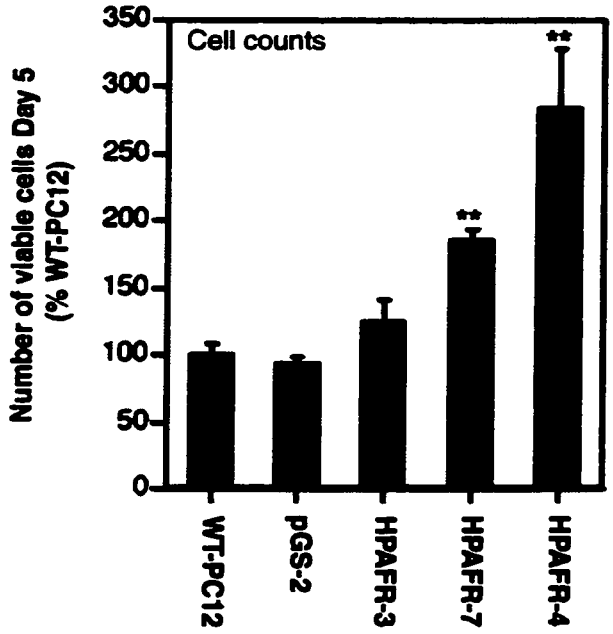
Cell counts
Number of viable cells Day 5
(% WT-PC12)
350
300
250
200
150
100
50
0
WT-PC12
pGS-2
HPAFR-3
HPAFR-7
HPAFR-4

B)

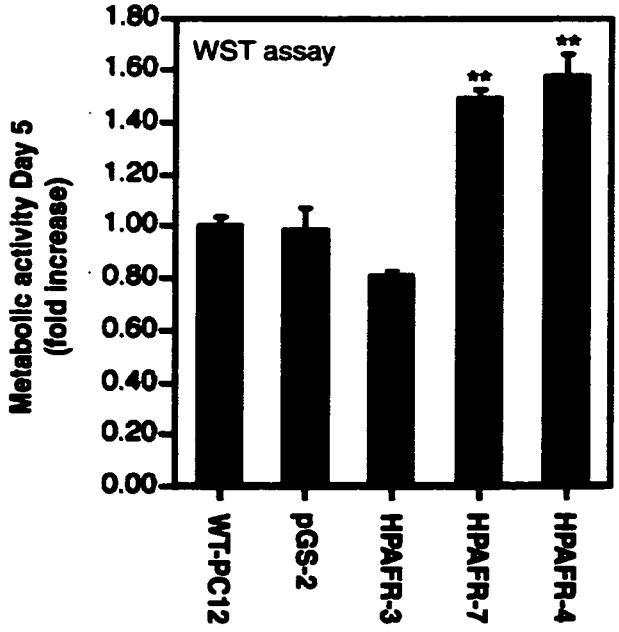
WST assay
Metabolic activity Day 5
(fold increase)
1.80
1.60
1.40
1.20
1.00
0.80
0.60
0.40
0.20
0.00
WT-PC12
pGS-2
HPAFR-3
HPAFR-7
HPAFR-4

Figure 3.5: Expression of the neuronal intermediate filament MAP2 following NGF-induced differentiation is not significantly affected by hPAFR-GPCR expression.

Development of a neuronal-like phenotype was confirmed immunocytochemically using anti-MAP2. Expression of MAP2 was unaffected by hPAFR-GPCR expression. Quantitation of the fluorescence intensity/cell after 5 days of NGF-treatment was not significantly reduced in HPAFR-7 cells relative to empty vector cells (n=15, 3 fields x 5 replicates).

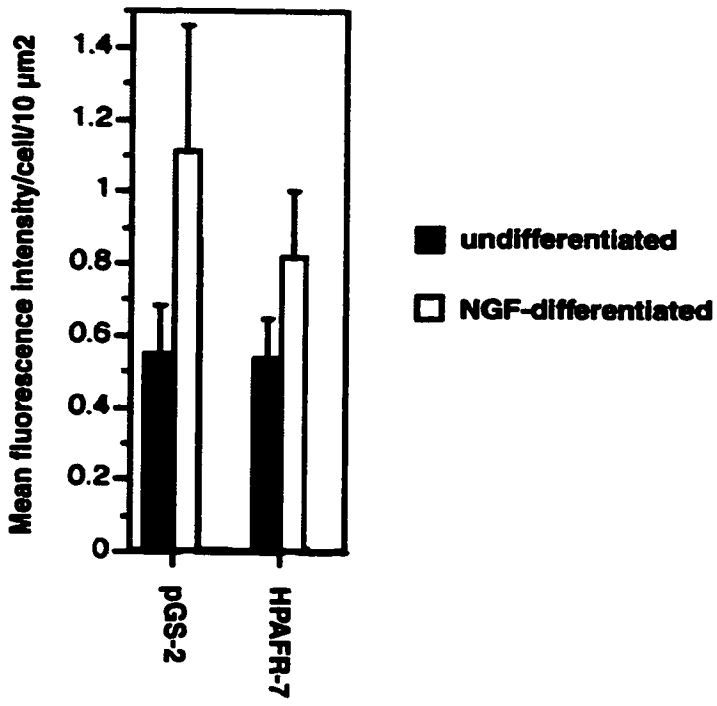
Mean fluorescence intensity/cell/10 µm2
1.4
1.2
1
0.8
0.6
0.4
0.2
0
pGS-2
HPAFR-7
undifferentiated
NGF-differentiated

(Prosperi, 1997). Thus, the intensity of PCNA immunoreactivity can be used as a measure of how recently a cell has progressed through S phase. Increased intensity of PCNA immunoreactivity was striking in HPAFR-7 cells in comparison to pGS-2 empty vector control cells. Quantitation of the mean fluorescent intensity per cell revealed an approximate 20-fold increase in PCNA staining in HPAFR-7 cells relative to empty vector transfectants (Figure 3.6). These results are consistent with the interpretation that hPAFR-GPCR transfectants continue to proliferate during NGF-induced differentiation.

Proliferation of hPAFR-GPCR transfected cells during NGF-induced differentiation is inhibited by the PAFR-GPCR specific antagonist CV3988

It is important to note that proliferation of HPAFR-7 and HPAFR-4 was stimulated without addition of exogenous PAF. These data imply an interaction with endogenous PAF synthesized by PC12 cells. To block putative hPAFR-GPCR activation during differentiation, the PAFR-GPCR specific antagonist CV3988 or vehicle (0.1% DMSO) was added to the differentiation media. Administration of CV3988 (0.2 –2 μM) had no effect on cell number or metabolic activity of WT-PC12 or pGS-2 empty vector cells in comparison to vehicle treated cultures (Figure 3.7). Treatment of HPAFR-7 cells with the PAFR-GPCR antagonist CV3988 (0.2-2 μM) blocked the observed NGF-induced proliferation (Figure 3.7).

Figure 3.6: NGF elicits cell proliferation in hPAFR-GPCR expressing cells. PCNA is expressed more intensely in HPAFR-7 cells.

Empty vector pGS-2 and HPAFR-7 cultures were maintained in low serum media supplemented with NGF for 5 days. (A) Immunocytochemical analysis demonstrated a 20-fold increase of PCNA staining in comparison to empty vector control cells (n= 15, 3 fields x 5 replicates). [**$p<0.01$, student's *t*-test] (B) Representative images 800x.

A)

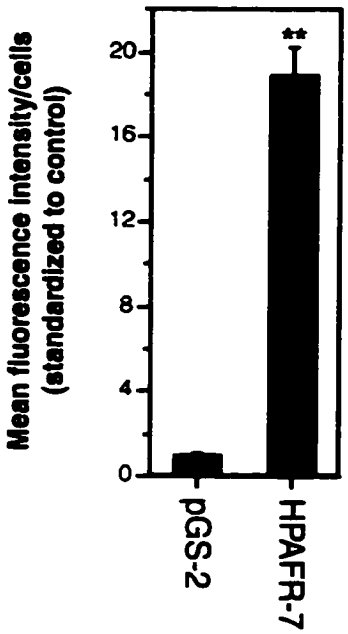
Mean fluorescence intensity/cells
(standardized to control)
20
16
12
8
4
0
pGS-2
HPAFR-7

B)

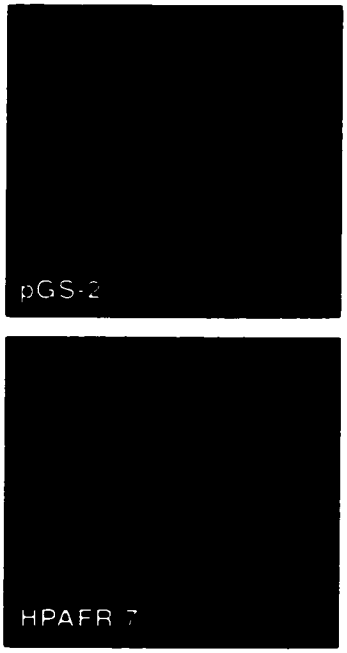
pGS-2
HPAFR-7

Figure 3.7: Increased cell proliferation during NGF-induced differentiation is mediated by PAF/PAFR-GPCR interaction. The PAFR-GPCR specific antagonist CV3988 blocks increased proliferation during NGF-induced differentiation in HPAFR-7.

Cultures were maintained in low serum media supplemented with NGF in the presence of CV3988 (0.2-2 μM) or vehicle (DMSO). Cell number was assessed on day 5 of culture by (A) trypan blue hemocytometer cell counts and by (B) WST cell proliferation assay to measure metabolic activity. Inhibition of proliferation by the PAF antagonist CV3988 was observed in both A and B. Data are standardized against control cultures to represent percent (A) and fold (B) changes in cell proliferation relative to untransfected control WT-PC12 cells. Note that exogenous PAF is not added to the media during differentiation. Results reported as means ± SEM (n=5-100 cell counts; n=5-40 WST per data point) details as described in materials and methods. [*$p<0.05$, ** $p<0.01$, significant reduction in proliferation compared to vehicle treatment; †† $p<0.01$, significant increase in proliferation relative to WT-PC12 cells, ANOVA, *post-hoc* Dunnett's *t*-test]

A)

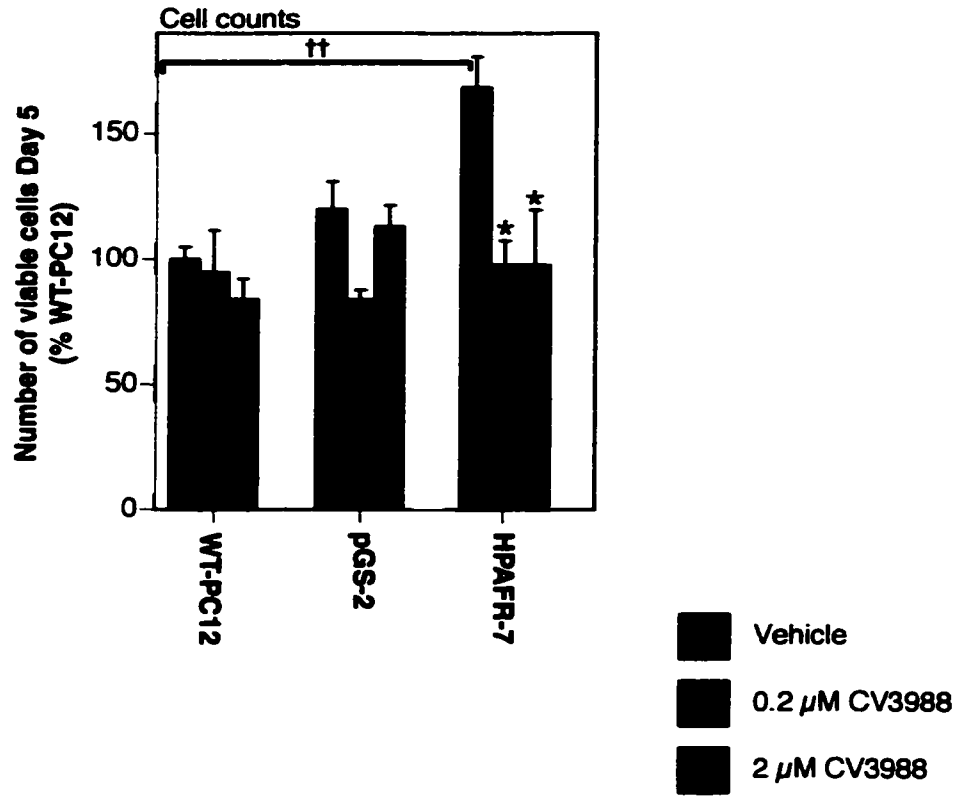
Cell counts
††
Number of viable cells Day 5
(% WT-PC12)
150
100
50
0
*
*
WT-PC12
pGS-2
HPAFR-7
Vehicle
0.2 μM CV3988
2 μM CV3988

B)

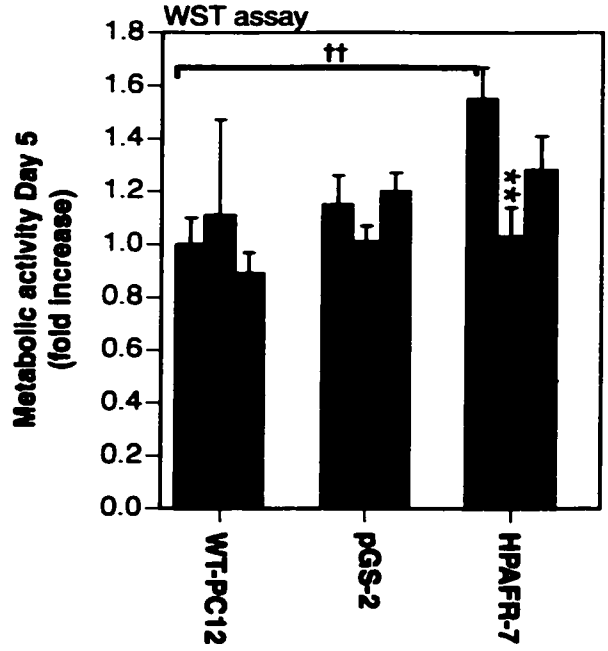
WST assay
††
Metabolic activity Day 5
(fold increase)
1.8
1.6
1.4
1.2
1.0
0.8
0.6
0.4
0.2
0.0
**
WT-PC12
pGS-2
HPAFR-7

Exogenous PAF administration stimulates proliferation of hPAFR-GPCR expressing cells in low serum media

To test the hypothesis that PAF/PAFR-GPCR interaction can directly stimulate cell growth in low serum media, cultures were treated with exogenous PAF (10 nM – 1 μM) or *lyso*-PAF (100 nM – 1 μM) over a five day period (Figure 3.8). Note that cells were not treated with NGF in these experiments. PAF elicited a dose-dependent increase in proliferation of HPAFR-7 cells with maximal activation at 100 nM and 1μM PAF (Figure 3.8; A, B). PAF treatment had no effect on WT-PC12 or empty vector controls (Figure 3.8; A, B). Proliferation in response to lyso-PAF was not distinguishably different in any of the assays from that of vehicle-treated cultures (Figure 3.8; C, D).

To confirm that PAF stimulates cell proliferation in low serum media, PCNA immunolabelling was performed as described above. The mean fluorescence intensity per cell was increased by approximately 35-fold following PAF treatment in HPAFR-7 cells relative to vehicle treatment (Figure 3.9). Fluorescence intensity was comparable in PAF and vehicle-treated empty vector controls. These results are consistent with the interpretation that the increase in cell number and metabolic activity observed in PAF-treated HPAFR-7 cells is the result of enhanced cell proliferation.

***In vitro* migration assay**

As indicated in Table 3.1, expression of hPAFR-GPCR had no net effect on the net migration of NGF-differentiated PC12 cells. Both WT-PC12 and HPAFR-7 cells demonstrated equivalent migration indices.

Figure 3.8: Proliferation is dependent upon PAF/PAFR-GPCR interaction.

Cells were maintained in low serum media and treated (A) exogenous PAF (0, 0.01, 0,1, 1 μM) in the absence of NGF or (B) exogenous *lyso*-PAF (0, 0.1, 1 μM) in the absence of NGF. Following five days of culture cell proliferation was assessed as described. Note that in comparison to WT-PC12 and empty vector control cells, proliferation in HPAFR-7 was observed in PAF treated cultures but not in vehicle or *lyso*-PAF treated cultures. Results reported as means ± SEM (n= 5-55 per data point) details as described in materials and methods. [*$p<0.05$, ** $p<0.01$, ANOVA, *post-hoc* Dunnett's *t*-test]

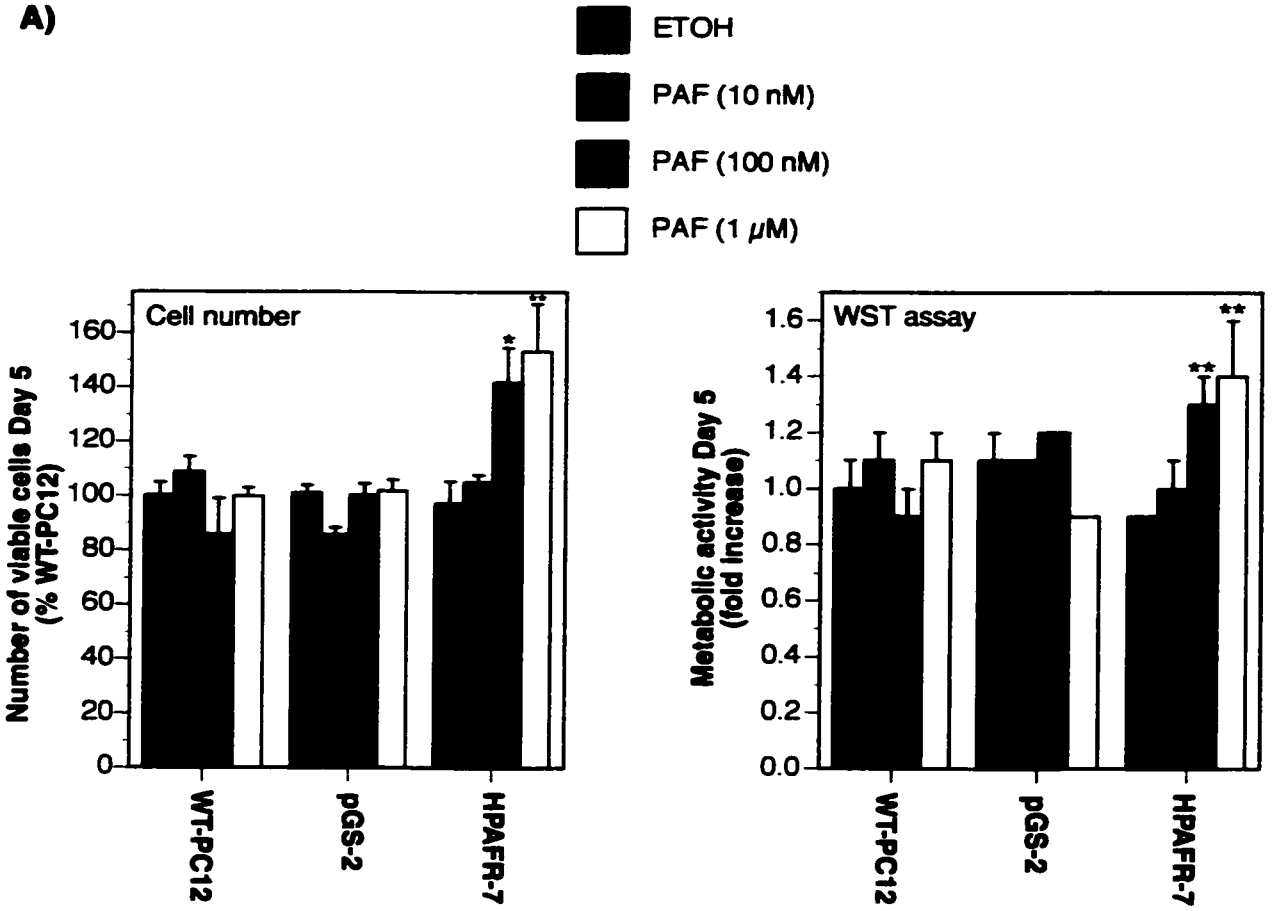
A)
ETOH
PAF (10 nM)
PAF (100 nM)
PAF (1 μM)
Cell number
Number of viable cells Day 5 (% WT-PC12)
0
20
40
60
80
100
120
140
160
*
**
WT-PC12
pGS-2
HPAFR-7
WST assay
Metabolic activity Day 5 (fold increase)
0.0
0.2
0.4
0.6
0.8
1.0
1.2
1.4
1.6
**
WT-PC12
pGS-2
HPAFR-7

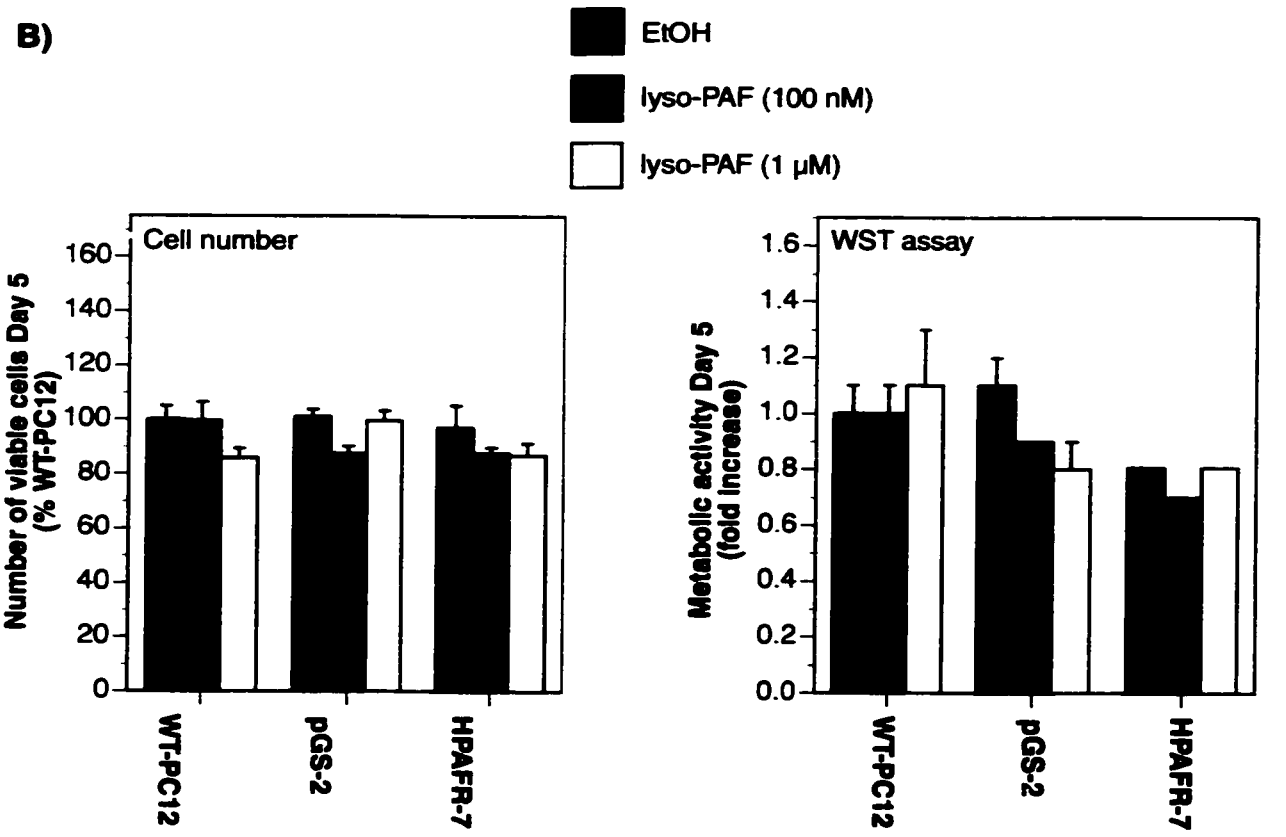
B)
EtOH
lyso-PAF (100 nM)
lyso-PAF (1 μM)
Cell number
Number of viable cells Day 5 (% WT-PC12)
0
20
40
60
80
100
120
140
160
WT-PC12
pGS-2
HPAFR-7
WST assay
Metabolic activity Day 5 (fold increase)
0.0
0.2
0.4
0.6
0.8
1.0
1.2
1.4
1.6
WT-PC12
pGS-2
HPAFR-7

Figure 3.9: Exogenous PAF administration elicits cell proliferation in hPAFR-GPCR expressing cells. PCNA is expressed more intensely in HPAFR-7 cells.

Empty vector pGS-2 and HPAFR-7 cultures were maintained in low serum media supplemented with PAF (100 nM) for 5 days. (A) Immunocytochemical analysis demonstrated a 35-fold increase of PCNA staining in comparison to empty vector control cells (n=15, 3 fields x 5 replicates). [**$p<0.01$, Student's *t*-test] (B) Representative images 800x.

A)

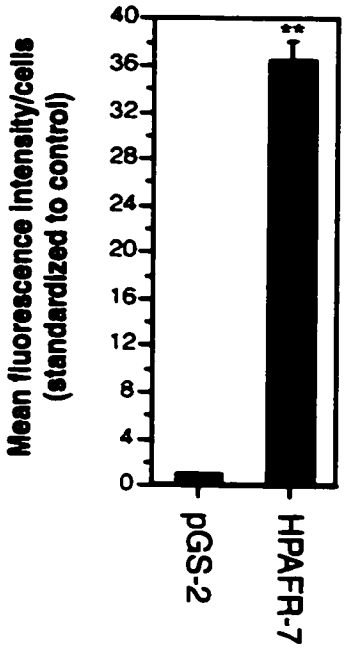
Mean fluorescence intensity/cells
(standardized to control)
40
36
32
28
24
20
16
12
8
4
0
**
pGS-2
HPAFR-7

B)

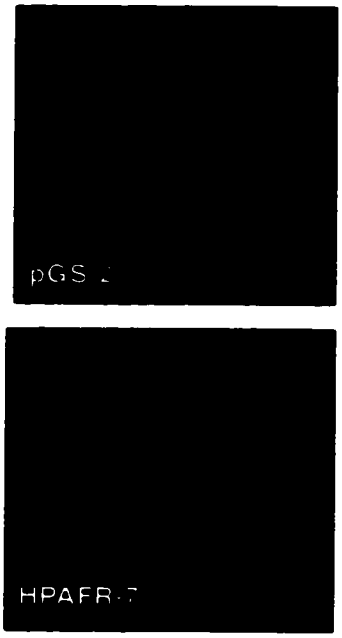
pGS-2
HPAFR-7

Table 3.1: Effect of hPAFR-GPCR expression on the net migration of differentiating PC12 cells.

Cultures were maintained in low serum media supplemented with NGF. Cell migration was assessed on day 5 of culture as described in materials and methods. Cell migration is represented as the migration index (see text). The migration indices between WT-PC12 and HPAFR-7 cells were comparable. Results reported as means ± SEM (n= 8-10 per data point).

	WT-PC12	HPAFR-7
Migration index (µm/cell)	0.159	0.153
SEM	0.04	0.04

PAF acetylhydrolase activity increases during NGF-induced differentiation

PAFAH activity was measured in cytosolic fractions prepared from WT-PC12, pGS-2 empty vector, and HPAFR-7 cells cultured for 5 days under undifferentiated or NGF-differentiated culture conditions. In Chapter 2, it was demonstrated that undifferentiated and NGF-differentiated WT-PC12 cells express PAFAH1b α1, PAFAH1b α2, and LIS-1 transcript and that the trimeric enzyme is functional. Table 3.2 shows a 2-fold increase in PAFAH activity in NGF-differentiated cultures relative to undifferentiated cells. PAFAH activity was not affected by hPAFR-GPCR expression. There was no detectable variance in PAFAH activity amongst WT-PC12, pGS-2 empty vector, and HPAFR-7 cells.

Table 3.2: Comparison of PAF acetylhydrolase activity in cytosolic fractions from undifferentiated cultures.

WT-PC12, pGS-2, and HPAFR-7 cytosolic fractions were prepared from undifferentiated and NGF-differentiated cultures as described in materials and methods. The catalytic activity of samples containing 50 µg of cytosolic protein was measured using the PAF acetylhydrolase assay kit (Caymen Chemical). PAFAH activity was comparable across all cell lines. Note the 2-fold increase in PAFAH activity in NGF-differentiated cultures as compared to undifferentiated cultures. In all assays, blanks without protein and no substrate controls with protein were run in parallel and subtracted from the experimental values (n=6 per data point). [**$p<0.01$, Student's *t*-test, note pGS-2 approaches significance at $p=0.058$]

	PAF acetylhydrolase activity (nmol/min/μg)	
	Undifferentiated	**NGF-differentiated**
WT-PC12	0.062±0.008	0.126±0.008**
pGS-2	0.064±0.017	0.130±0.064
HPAFR-7	0.051±0.003	0.159±0.045**

Discussion

Prolonged exposure to elevated levels of PAF during embryogenesis is implicated in MDS-a developmental brain disorder characterized by type 1 lissencephaly. Afflicted individuals are faced with mental retardation, enhanced seizure susceptibility and reduced life expectancy (Dobyns et al., 1991). Murine models of LIS-1 haploinsufficiency, the genetic determinant of MDS, have demonstrated two primary pathologies: (1) delayed neuronal migration resulting in cerebral malformation and (2) premature neurogenesis between embryonic days 11-14.5 (Hirotsune et al., 1998; Cahana et al., 2001; Fleck et al., 2000). Because LIS-1 codes for the regulatory subunit of PAFAH1b, these pathologies likely result from impaired PAF catabolism resulting in protracted exposure to elevated concentrations of PAF. This hypothesis predicts that the differentiation of neural precursor cells expressing a PAF receptor will be preferentially affected in MDS.

As reviewed in Chapter 1, a PAFR-GPCR has been cloned. mRNA is expressed by rodent neurons and microglia as early as embryonic day 18 and into adulthood (Bennett et al., 1998; Mori et al., 1996; Bito et al., 1992). Expression at earlier embryonic stages is currently being determined in our laboratory. The effect of receptor activation on neural precursors is not known but receptor activation has been shown to stimulate growth and migration of non-neuronal cells (described below). In the present study, we sought to test the hypothesis that PAF/PAFR-GPCR interaction mediates on neural precursor proliferation, neuronal differentiation, and/or migration using the PC12 cell model.

As described in Chapter 2, stable hPAFR-GPCR and empty vector transfectants were developed to evaluate the effect of PAF/PAFR-GPCR interaction on the growth and differentiation of WT-PC12 cells. Recall that PC12 cells, a rodent pheochromocytoma-derived cell line, can be differentiated to a neuronal-like phenotype by NGF in the presence of low serum media (Greene and Tischler, 1976). Neither undifferentiated nor NGF-differentiated WT-PC12 cells express endogenous rodent PAFR-GPCR (Chapter 2). In this series of experiments, ectopic expression of hPAFR-GPCR had no effect on the growth kinetics of undifferentiated cells but did interfere with NGF-induced differentiation of PC12 cells. When treated with NGF, WT-PC12 cells extend neurites and undergo relative growth arrest resulting in a measurable decrease in cell proliferation. By contrast, hPAFR-GPCR transfectants failed to undergo relative growth arrest when treated with NGF continuing to proliferate at a rate comparable to that seen in complete media. Proliferation of hPAFR-GPCR transfectants was inhibited by treatment with CV3988 implying that activation of PAFR-GPCR by endogenous PAF, synthesized over the course of NGF-induced differentiation, mediates cell growth.

To further test the hypothesis that PAF/PAFR-GPCR interaction is responsible for cell growth in hPAFR-GPCR transfectants, cultures were treated with exogenous PAF in the absence of NGF. PAF administration stimulated cell growth in hPAFR-GPCR expressing cells but not in empty vector clones or WT-PC12 cells. The specificity of this response was further verified by treatment of cultures with *lyso*-PAF, the biologically inactive PAF metabolite. Treatment with

lyso-PAF had no effect on the growth of hPAFR-GPCR transfectants, empty vector cell lines, or WT-PC12 cells. To confirm that the increase in cell number was, in fact, the result of cell proliferation, immunocytochemical analysis demonstrated that the intensity of PCNA staining was substantially higher in NGF- or PAF-treated hPAFR-GPCR expressing cells in comparison to NGF- or PAF-treated empty vector control cells. These data substantiate the hypothesis that PC12 neural precursor proliferation can be stimulated by PAF/PAFR-GPCR interaction.

Our findings are consistent with previous reports that PAF administration promotes proliferation of cells from non-neuronal origin *in vitro*. Examples include human T and B lymphocytes (Behrens and Goodwin 1990; Leprince et al 1991), human and guinea pig bone marrow cells (Denizot et al 1996; Kato et al 1988; Kudo et al 1991), human lung fibroblasts (Roth et al 1996), rodent lung pericytes (Khoury and Langleben, 1996), and primary human fibroblasts (Bennett and Birnboim, 1997). The mitogenic effects of PAF have also been reported in a number of human breast cancer cell lines (Bussolati et al 2000), the human immature K562 erythroid cell line (Dupuis et al., 1997), and the endometrial adenocarcinoma cell line HEC-1A (Bonaccorsi et al., 1997). Proliferative abnormalities are also observed in the skin of transgenic mice overexpressing guinea pig PAFR-GPCR (Ishii et al., 1997; Sato et al., 1999). These mice were designed as a model to study PAF/PAFR-GPCR interaction *in vivo*. Robust PAFR-GPCR transgene expession is consistently detected in skin (Ishii et al., 1997). A propensity for skin tumor formation of the ears and/or tails was

observed in aged animals (Ishii et al., 1997). Histological examination revealed epidermal hyperthickening in the ears, tails, and abdomen with an increase in the thickness of keratinocyte layers over time (Ishii et al., 1997; Sato et al., 1999). Skin analysis demonstrated accelerated proliferation of epidermal keratinocytes in PAFR-GPCR transgenic animals with otherwise normal differentiation through successive keratinocyte layers (Sato et al., 1999). These results, from mice overexpressing PAFR-GPCR, correlate with our findings. In the present study, WT-PC12 cells engineered to overexpress hPAFR-GPCR demonstrate accelerated proliferation during differentiation yet develop a normal neuronal-phenotype. Gross morphology and neuritic extension following NGF-induced differentiation was comparable in all cell lines. Development of a neuronal-like phenotype was confirmed immunocytochemically using anti-MAP2. Expression of this intermediate filament is routinely used as a marker of neuronal differentiation (Bernhardt et al., 1985). As anticipated, MAP2 levels increased significantly following five days of NGF treatment in empty vector transfectants and WT-PC12 cells. hPAFR-GPCR expression did not alter the expression profile of MAP2 expression following NGF treatment. These data implicate PAF/PAFR-GPCR in aberrant neural precursor proliferation but suggest that PAFR-GPCR activation does not block other phenotypic or biochemical markers of differentiation.

MDS is associated with two mechanistic pathologies: (1) aberrant neural precusor proliferation and (2) impaired neuronal migration. Our data indicate that PAFR-GPCR activation by PAF is likely involved in neural precursor proliferation.

The effects of PAFR-GPCR on neural precursor proliferation are observed when cells are treated with NGF or with exogenous PAF. Because cell growth in NGF-treated cells can be blocked by co-administration of the PAFR-GPCR specific antagonist CV3988, these data lead us to hypothesize that endogenous PAF synthesis increases over the course of PC12 differentiation to a neuronal phenotype. Ectopic expression of hPAFR-GPCR protects cells from PAF-induced apoptosis presumably mediated by a novel PAF receptor (Chapter 2) and enhances cell proliferation during NGF-induced differentiation. In Chapter 2, we also demonstrate that PAF is inactivated by functional PAFAHs expressed by PC12 cells. These data raise the question: If PAF is synthesized during NGF-induced differentiation, why do WT-PC12 cells not undergo apoptosis as a result of PAF-induced apoptogenic signal transduction? In the present series of experiments, a 2-fold increase in PAFAH activity was measured in all NGF-differentiated cultures (WT-PC12, empty vector, and hPAFR-GPCR transfectants). Increases in PAFAH activity have been used as marker of PAF and PAF-like lipids (Albrecht et al., 1998). We conclude that PAF is likely metabolized by the PAFAH1b enzyme complex in PC12 cells. This conclusion is based upon expression of the PAFAH1b subunits (alpha 1, alpha 2, and LIS-1) by PC12 cells (Chapter 2) and that the majority of neural PAFAH activity is attributed to the PAFAH1b isozyme (Hattori et al., 1993). As described in Chapter 1, the emerging body of evidence clearly demonstrates the importance of PAFAH1b activity during cortical development. Presumably, this activity protects cells from prolonged PAF signaling as demonstrated in Chapter 2.

However, recall from Chapter 1 that a link between neuronal migration and PAF hydrolysis has been established (Albrecht et al., 1996). In the present study, PAF/PAFR-GPCR interaction had no effect on the net cellular migration of differentiating PC12 cells. Transfectants did not exhibit reduced or enhanced migration relative to WT-PC12 cells. It should be noted that the assay employed detects migration of cells away from a colony. It does not measure directed migration (chemotaxis) of cells towards a source of PAF ligand. Thus, we cannot definitively state that PAFR-GPCR does not affect migration. PAFR-GPCR activation has been repeatedly associated with migration of peripheral inflammatory and carcinoma cells (Haribabu et al., 2001; Bussolati et al., 2000; Boccellino et al., 2000). In CNS, PAFR-GPCR expression in primary microglia is required for PAF-induced chemotaxis (Aihara et al., 2000). While we can state that gene expression in PC12 cells does not increase or decrease overall motility, more refined studies are required to definitely establish whether PAFR-GPCR plays a role in mediating neuronal migration. Therefore, an alternative hypothesis, is that the increased PAFAH1b activity may result in initiation of downstream migration signaling pathways. Salient to this hypothesis is evidence that inhibition of PAFAH1b activity represses neural cell migration (Adachi et al., 1997), suggesting that PAF-mediated neuronal migration occurs via a PAFR-GPCR independent pathway. Sustained PAF exposure in vitro has been reported to collapse neuronal growth cones by eliciting cytoskeletal alterations (Clark et al 1995; McNeil et al 1999) and inhibit neuronal cell motility (Bix and Clark 1998). Careful examination of these reports reveals that (1) none of the

studies screened for PAFR-GPCR expression and (2) conclusions were drawn based on exclusive use of mc-PAF. The use of mc-PAF, a non-hydrolyzable PAF analogue, resistant to inactivation by PAFAHs, is wide spread and provides potent PAFR-GPCR activation (O'Flaherty et al 1987). However mc-PAF is also an inhibitor of PAFAH1b activity (Adachi et al., 1997). The authors themselves acknowledge that PAF at high doses elicits erratic and transient growth cone collapse likely a result of rapid hydrolysis by PAFAHs. It is tempting to speculate that PAF-mediated migration and motility deficits are the result of PAF/Lis-1 interaction as postulated in Chapter 1[2].

Our phenotypic data provide circumstantial evidence for our speculation that PAF is synthesized during NGF-induced differentiation. There are precedents in the literature to indicate that PAF synthesis is increased in neuronal cultures during differentiation and neurite extension (Francescangeli et al., 1997). The last enzymatic step in the remodeling pathway for PAF synthesis is via *lyso*-PAF acetyltransferase. Increases in *lyso*-PAF acetyltransferase activity have been demonstrated during neuronal and glial differentiation in culture (Francescangeli et al., 1997). In human neutrophils, activation of *lyso*-PAF acetyltransferase is catalyzed by direct interaction with activated p38 MAPK (Nixon et al., 1999). It has been demonstrated that NGF induces sustained activation of p38 MAPK, which is required for neuritic extension of PC12 cells (Morooka and Nishida, 1998). Therefore, a similar mechanism may facilitate PAF synthesis following NGF treatment. A graduate student in the Bennett

---

[2] Please refer to page 12, Chapter 1.

laboratory, Fanny Bonin, is currently optimizing a biochemical assay to determine empirically whether PAF is synthesized through the remodeling pathway during NGF-induced differentiation of PC12 cells.

In summary, WT-PC12 cells and hPAFR-GPCR transfectants have proved to be a pertinent model for elucidation of receptor-mediated PAF events. We have successfully assessed whether or not sustained PAFR-GPCR activation impacts on pathological neural precursor proliferation and, to a lesser extent, migration consistent with the MDS phenotype. PAF/ PAFR-GPCR activation stimulates neural precursor proliferation consistent with MDS. Unrefined analysis of PC12 cell migration during differentiation demonstrated no effect of hPAFR-GPCR expression. However, further testing is required to definitively rule out a role for PAFR-GPCR signaling in neuronal migration. These data lead us to speculate that chronic exposure to PAF, as a result of reduced PAF catabolism in MDS and related disorders, may delay the ability of neural precursors expressing PAFR-GPCR to exit the cell cycle and thereby inhibit the appropriate timing of migration of neurons.

CHAPTER 4: CHARACTERIZATION OF A NEW PAFR-GPCR ANTIBODY DEVELOPED IN THE BENNETT LABORATORY

Introduction

Knowledge with respect to PAFR-GPCR activation, regulation, and localization at the protein level is limited. Using modern genetic and immunological techniques, mechanisms of PAFR-GPCR regulation and molecular details of the signaling pathways in which PAFR-GPCR is involved can be explored. To date new insights have been hindered by the lack of commercially available molecular tools to study PAFR-GPCR. Only a few laboratories have reported generation of peptide antibodies against PAFR-GPCR for use following Western Blot and immunohistochemical protocols (Muller et al., 1993; Ihida et al., 1999; Predescu et al., 1996). Therefore, the lack of commercially available antibodies accounts for the widespread use of epitope tags in PAFR-GPCR transfection studies. We sought to characterize a new human PAFR-GPCR polyclonal antibody developed in our laboratory. Positive fusion protein controls were created by transfection of WT-PC12 cells with a green fluorescent protein (GFP)-tagged hPAFR-GPCR fusion construct.

Materials and Methods

Production of polyclonal anti-hPAFR-GPCR antiserum

The hPAFR-GPCR antiserum was produced by Lampire Biological Laboratories using a peptide designed by Dr. Bennett. Briefly, a peptide was

synthesized corresponding to amino acid residues 125-138 (TAQANTRKRGISLS) of the predicted hPAFR-GPCR protein sequence representing a segment of the second intracellular loop. A nonencoded cysteine residue was included at the C-terminal amino acid to facilitate covalent coupling of the peptide to myoglobulin. An adult rabbit was immunized by intraperitoneal (IP) injection with 1 mg of peptide mixture in Ribi adjuvant system (RAS). Additional immunizations were performed 4 and 8 weeks after the first injection. Serum was collected before, during, and after immunization. The polyclonal antibody was affinity purified from the terminal bleed by standard chromatography on protein A-Sepharose (Amersham Pharmacia Biotech).

Generation of WT-PC12 expressing GFP-hPAFR-GPCR fusion construct

A positive fusion protein control for hPAFR-GPCR antibody characterization was created by transfection of WT-PC12 cells with a green fluorescent protein (GFP)-tagged to the N-terminus of hPAFR-GPCR. An insert encoding Flag-hPAFR-GPCR was excised from the pCDM8 construct kindly provided by Dr. C Gerard, Harvard Medical School. Insertion into the multiple cloning site of the pEGFP-C1 vector (Clonetech) permitted construction of GFP-Flag-hPAFR-GPCR fusion receptor cDNA within this expression vector.

Transfections of WT-PC12 cells were performed using Transfast reagent according to the manufacturer's specifications (Promega). Clonal lines resistant to 400 µg/ml G418 (Life Technologies) were expanded after 14 days of culture and maintained in 200 µg/ml G418.

Western Blot analysis of hPAFR-GPCR antibody

Total protein lysates were prepared from sub-confluent cultures as described in Chapter 2. For Western Blotting, protein samples (20 µg) were separated on 12% SDS-PAGE gels and transferred onto PDVF membranes (Immobilon-P, Millipore). Western analysis was performed using polyclonal anti-GFP (1:100, Clonetech), polyclonal hPAFR-GPCR (1:500), and rabbit pre-immune serum (1:500). Antibodies were diluted and membranes were blocked in 10 mM PBS containing 1% heat-denatured casein. Membranes were washed repeatedly between incubations with PBS containing 0.05% Tween-20. All primary antibodies were detected by incubation with horseradish peroxidase-conjugated goat anti-rabbit IgG (1:800; Jackson Immunolabs). Immunoreactive bands were visualized using SuperSignal West Pico (Pierce) chemiluminescent substrate according to the protocol provided by the manufacturer and exposed to Biomax X-Ray film (Kodak).

Proteomics performed on GFP-hPAFR-GPCR fusion protein

Online ExPASy Proteomic tools (http://www.expasy.ch/tools/) were used to translate GFP-hPAFR-GPCR cDNA sequence, predict molecular weights, and identify potential cleaved peptide fragments.

Results

Biochemical analysis of GFP-hPAFR-GPCR stably transfected into WT-PC12 cells and validation of hPAFR-GPCR polyclonal antibody

Western analysis of GFP-hPAFR-GPCR stably transfected into WT-PC12 cells is demonstrated in Figure 4.1. Control reactions performed with rabbit pre-immune serum detected three prominent non-specific bands at 70, 67, and 43 kD in both WT-PC12 cells and GFP-hPAFR-GPCR transfected cells (Figure 4.1, panel A). The same non-specific bands were detected using hPAFR-GPCR antibody. No additional bands were detected in WT-PC12 cells. The hPAFR-GPCR antibody detected multiple species of GFP-hPAFR-GPCR in transfected cells; bands with apparent molecular masses of 69, 65, 61, and 58 kD were detected (Figure 4.1, panel C). To identify these bands as GFP-hPAFR-GPCR fusion products, Western analysis was performed using commercially available polyclonal anti-GPF antibody. While no immunoreactive bands were detected in WT-PC12 cells, anti-GFP detected multiple GFP-hPAFR-GPCR species in transfected cells at apparent molecular masses of 65, 61, 58, and 27 kD (Figure 4.1, panel B)

Proteomic analysis of GFP-hPAFR-GPCR

ExPASy proteomic tools were used to translate the coding cDNA sequence for GFP-hPAFR-GPCR (Figure 4.1, panel D). Translation of the nucleotide sequence predicted a 604 amino acid fusion protein with a potential molecular weight of 69 kD. The hPAFR-GPCR polyclonal antibody raised

against residues 125-138 of hPAFR-GPCR, corresponds to residues 387-400 of GFP-hPAFR-GPCR (Figure 4.1, panel D). A number of potential serine endopeptidase cleavage sites were identified within the GFP-hPAFR-GPCR fusion protein (Figure 4.1D). Recorded in Figure 4.1, panel E are the predicted GFP-hPAFR-GPCR peptide fragments, their predicted molecular weights and the likelihood of recognition by hPAFR-GPCR polyclonal antibody and/or polyclonal anti-GFP.

Figure 4.1: Characterization of an hPAFR-GPCR antibody raised against a synthetic peptide corresponding to residues 125-138 of the human PAFR-GPCR.

Representative immunoblots from undifferentiated protein samples from WT-PCR cells and GFP-hPAFR-GPCR transfectant. Protein samples were separated by SDS-PAGE, transferred to PVDF membrane and detected using (A) rabbit preimmune serum, (B) anti-GFP polyclonal antibody, or (C) hPAFR-GPCR polyclonal antibody as described in materials and methods. Migration of molecular mass markers is indicated. The bands in (A) are non-specific binding of preimmune serum (N/S). Panel D depicts the amino acid sequence of GFP-hPAFR-GPCR fusion protein indicating N-terminal EGFP (green), hPAFR-GPCR antibody epitope (blue) and potential serine protease cleavage sites (red). (E) predicted characteristics of fusion protein cleavage peptides. Note the sizes of bands in (C) and (D) correspond to the GFP-hPAFR-GPCR fusion protein and potential cleavage peptides identified.

A)

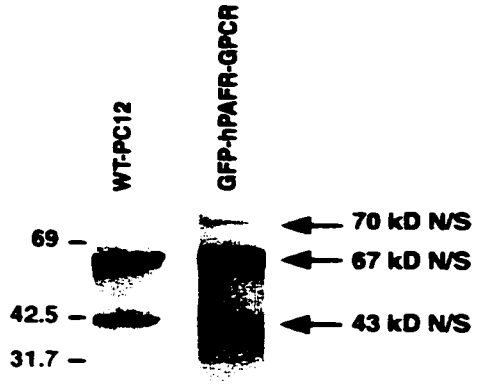

pre-immune serum

B)

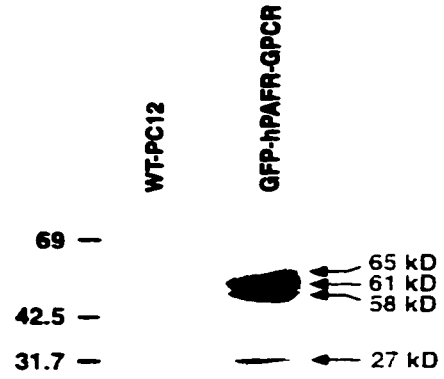

anti-GFP

C)

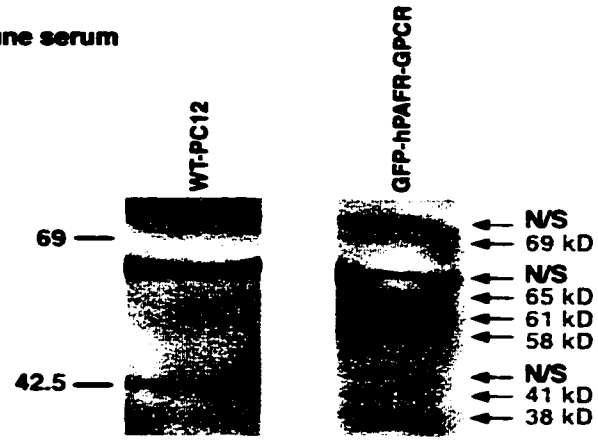

anti-hPAFR-GPCR

D)

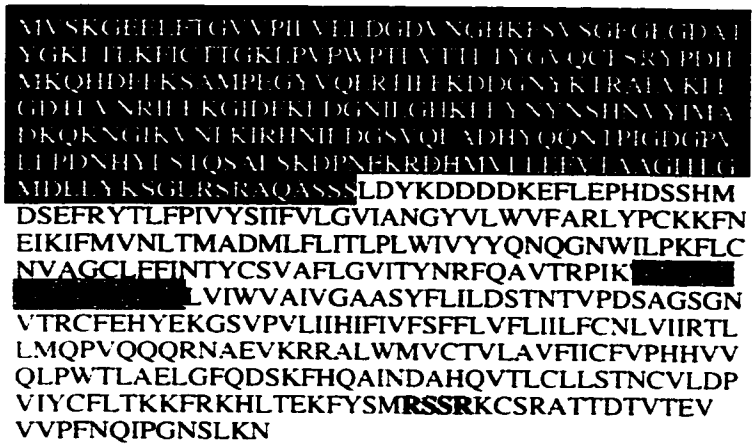

E)

Potential peptide fragments	Corresponding GFP-hPAFR-GPCR residues	Predicted molecular weight (kD)	Potential antibody recognition
#1	1-604 (full length)	69	GFP and HPAFR
#2	1-574	65	GFP and HPAFR
#3	74-604	61	GFP and HPAFR
#4	74-574	58	GFP and HPAFR
#5	244-604	41	HPAFR
#6	244-574	38	HPAFR
#7	1-243	27	GFP

Discussion

Initial characterization of a new anti-hPAFR-GPCR antibody has been demonstrated. To provide a standard, WT-PC12 cells were transfected with a GFP-hPAFR-GPCR expression construct. Western analysis using anti-hPAFR-GPCR raised against a synthetic peptide corresponding to residues 125-138 of hPAFR-GPCR confirmed detection of GFP-hPAFR-GPCR fusion protein.

The detection of multiple bands, possibly linked to endopeptidase activity, indicates that translated GFP-hPAFR-GPCR is degraded. We conclude that adding the GFP-tag to the N-terminus of hPAFR-GPCR is not an appropriate strategy. The large size of GFP and the extracellular location of the hPAFR-GPCR N-terminus likely obstruct proper post-translational processing of this fusion protein and result in degradation. For example, although hPAFR-GPCR detected a band corresponding to the predicted size of full length unmodified GFP-hPAFR-GPCR fusion protein (69 kD), the commercially available anti-GFP antibody did not detect a corresponding protein band. An antibody to hPAFR-GPCR, raised against residues 164-173 of the receptor, has been reported to detect a single protein band at 69 kD (Muller et al., 1993). The significance of this finding and the identity of the 69 kD band has been discussed in the literature and is addressed below. At present the consensus is that the molecular mass of unmodified hPAFR-GPCR is approximately 39 kD; post –translational modifications including modification of the N-linked consensus glycosylation sequence in the second extracellular loop required for efficient membrane trafficking of hPAFR-GPCR (Kunz et al., 1992; Garcia Rodriguez et

al., 1995) likely result in a fully-processed 69 kD protein. The few other laboratories that have raised antibodies to synthetic peptides of hPAFR-GPCR have reported various sizes of hPAFR-GPCR by Western analysis. Two main immunoreactive species have repeatedly been identified at molecular masses of approximately 39 and 69 kD. These bands have been detected singly at approximately 39 kD (Ihida et al., 1999; Predescu et al., 1996) or at approximately 69 kD (Tiemann et al., 2001; Muller et al., 1993). Other groups have detected both bands on the same blot (Ishii et al., 1998, Garcia Rodriguez et al., 1995). This leads us to speculate that the 69 kD band, detected by hPAFR-GPCR polyclonal antibody, is hPAFR-GPCR and the GFP tag was cleaved prior to proper post-translational processing. Further evidence for degradation of the fusion protein was observed by detection of a 27 kD band by anti-GFP that corresponds to the molecular weight of GFP.

While these results are promising, further characterization of this antibody is necessary to validate reactivity. Control reactions performed with the rabbit pre-immune serum identified 3 prominent non-specific bands. The primary concern was such that these bands at 70, 67, and 43 kD migrate in proximity to the predicted sizes of hPAFR-GPCR. As a result, we solicited new antisera from Lampire Biologicals. Unfortunately, assessment of this new preparation will follow submission of this manuscript. In anticipation of these studies, recall that an attractive feature of the pcDNA3.1/GS vector used in Chapter 2 and 3 is the presence of a C-terminal tagged V5 epitope. This epitope was successful in determination of hPAFR-GPCR expression (Chapter 2) and we are satisfied that

these hPAFR-GPCR transfected WT-PC12 cells will be more suitable as a positive control to characterize hPAFR-GPCR antisera.

CHAPTER 5: GENERAL DISCUSSION AND CONCLUSIONS

The studies presented in this thesis were designed to add to our understanding of how PAF initiates neurotoxicity and affects neuronal differentiation. A neuronal *in vitro* model system capable of dissociating the effects of the cloned PAFR-GPCR from putative intracellular binding sites (iPAFRs) was identified and characterized. PAF elicited apoptotic cell loss of WT-PC12 cells. Cell death, however, was not initiated by PAFR-GPCR, given that WT-PC12 cells do not express endogenous rodent PAFR-GPCR mRNA. Recall that two high affinity binding sites, localizing to intracellular membranes (iPAFRs) have been identified pharmacologically. It is not known whether these binding proteins are coded for by distinct genes or represent internalized PAFR-GPCR. Given that PAFR-GPCR transcript is not present in WT-PC12 cells, the present data suggest that WT-PC12 cells express distinct intracellular iPAFRs that initiate PAF-induced cell loss. In addition, it was demonstrated that WT-PC12 cells can be used effectively to determine the specificity of PAF antagonist for iPAFRs and may be used to screen a wide variety of PAF antagonists for therapeutic potential.

Surprisingly, exogenous hPAFR-GPCR expression protected cells following apoptogenic challenge with PAF. These data strengthen our conclusion that PAFR-GPCR is not the PAF death receptor. Thus, therapeutic strategies should be directed toward identifying iPAFRs at the molecular level to more effectively target PAF-mediated cytotoxicity. As well, it was demonstrated that sustained PAF exposure to active ligand is required for protracted cell loss.

Given that functional PAF acetylhydrolase activity was detected in WT-PC12 cultures, these data are consistent with previous reports that exogenous administration of PAF acetylhydrolase inhibits PAF-mediated neurotoxicity (Hirashima et al., 2000 and Ogden et al., 1998). These studies represent a first step in providing a mechanistic understanding of the how PAF-mediated cytotoxicity is initiated in HIV-dementia, ischemia-reperfusion injury, and epileptic seizure and support the hypothesis that PAF antagonists and/or recombinant PAF acetylhydrolase may reduce neuronal damage associated with these conditions.

WT-PC12 cells and hPAFR-GPCR transfectants have proved to be a pertinent model for investigation of the role of PAFR-GPCR activation in neuronal differentiation. We have successfully assessed whether or not sustained PAFR-GPCR activation impacts on pathological neural precursor proliferation and have begun to address whether PAFR-GPCR mediates the abberant neuronal migration consistent with clinical MDS cases and murine MDS models. PAF/PAFR-GPCR interaction stimulates neural precursor proliferation consistent with the abnormal proliferation observed in LIS-1 heterozygous mice (Hirotsune et al., 1998; Fleck et al., 2000; Cahana et al., 2001) in which PAF levels are likely increased during corticogenesis as a result of defective PAF catabolism. A basic analysis of WT-PC12 cell migration during differentiation, however, demonstrated no effect of hPAFR-GPCR expression. Further testing is required to definitively rule out a role for PAFR-GPCR signaling in neuronal migration. These data lead us to speculate that chronic exposure to PAF, as a result of reduced PAF

catabolism in MDS and related disorders, may delay the ability of neural precursors expressing PAFR-GPCR to exit the cell cycle and thereby inhibit the appropriate timing of neuronal migration. These data support existing literature implicating PAFR-GPCR signaling in mitogenic pathways in other cell systems (Behrens and Goodwin, 1990; Leprince et al., 1991; Denizot et al., 1996; Kato et al., 1988; Kudo et al., 1991; Roth et al., 1996; Khoury and Langleben, 1996; Bennett and Birnboim, 1997, Bennett et al., 1993; Bussolati et al., 2000; Dupuis et al., 1997; Bonaccorsi et al., 1997). While further experimentation is required, two studies may be sufficient to validate our speculation. Firstly, what is the expression profile of PAFR-GPCR in the developing nervous system? These data would confirm that PAFR-GPCR is expressed during corticogenesis. Secondly, a quantitative analysis of PAFR-GPCR expression and PAF levels in LIS-1 heterozygous mice in comparison to WT-littermates could establish the likelihood of sustained PAFR-GPCR activation during corticogenesis. This would be particularly informative data given that low concentrations of PAF have been demonstrated to induce neuronal differentiation (Herrick-Davis et al., 1991; Kornecki and Ehrlich, 1988) and an age-dependent decrease in PAF concentration has been reported coinciding with terminal neuronal differentiaton (Tokumura et al., 1992). These studies provide circumstantial evidence that PAF signaling is tightly regulated during cerebral development. In this study, we demonstrate that PAF catabolism increases during NGF-induced differentiation of WT-PC12 cells, which we cautiously interpret to be indicative of an increase in PAF synthesis. Ecotopic expression of hPAFR-GPCR prevented relative growth

arrest associated with differentiation to a neuronal phenotype suggesting that sustained PAF/PAFR-GPCR interaction may be responsible for the increase in neural precursor proliferation observed in MDS murine models. In conclusion, this thesis expands upon research that PAF is neurotoxic and demonstrates that it has the potential to induce both cell growth and cell death. These paradoxical biological activities appear to be mediated by distinct PAF receptors. To further address how PAF initiates biological activity, it will be necessary to identify the apoptogenic PAF binding protein at the molecular level and characterize the expression of this putative receptor and PAFR-GPCR at the protein level. To assist in these studies, a PAF receptor antibody was developed and preliminary characterization was performed in this thesis. These studies constitute the first comparison of PAF signal initiator proteins in neurons and provides insight into the molecular mechanisms underlying PAF control of neural cell fate. These data and subsequent studies are essential if we are to intervene in PAF-mediated neuropathology.

REFERENCES

Adachi T, Aoki J, Manya H, Asou H, Arai H, Inoue K (1997) PAF analogues capable of inhibiting PAF acetylhydrolase activity suppress migration of isolated rat cerebellar granule cells. Neurosci Lett 235:133-136.

Aicardi J (1994) The place of neuronal migration in child neurology. Can J Neurosci 21:185-193.

Aihara M, Ishii S, Kume K, Shimizu T (2000) Interaction between neurone and microglia mediated by platelet-activating factor. Genes Cells 5:397-406.

Akisu M, Kultursay N, Coker I, Huseyinov A (1998) Platelet-activating factor is an important mediator in hypoxic ischemic brain injury in the newborn rat. Flunarizine and Ginkgo biloba extract reduce PAF concentration in the brain. Biol Neonate 74:439-444.

Albrecht U, Abu-Issa R, Ratz B, Hattori M, Aoki J, Arai H, Inoue K, Eichele G (1996) Platelet-Activating Factor Acetylhydrolase Expression and Activity Suggest a Link between Neuronal Migration and Platelet-Activating Factor. Dev Biol 180:579-593.

Ali H, Fisher I, Haribabu B, Richardson RM, Snyderman R (1997) Role of Phospholipase $C^{\beta}3$ Phosphorylation in the Desensitization of Cellular Responses to Platelet-activating Factor. J Biol Chem 272:11706-11709.

Ali H, Richardson RM, Tomhave ED, DuBose RA, Haribabu B, Snyderman R (1994) Regulation of stably transfected platelet activating factor receptor in RBL-2H3 cells. Role of multiple G proteins and receptor phosphorylation. J Biol Chem 269:24557-24563.

Alloatti G, Montrucchio G, Camussi G (1994) Role of platelet-activating factor (PAF) in oxygen radical-induced cardiac dysfunction. J Pharmacol Exp Ther 269:766-771.

Baker RR (1995) Enzymes of platelet activating factor synthesis in brain. Neurochem Res 20:1345-1351.

Barber LA, Spandau DF, Rathman SC, Murphy RC, Johnson CA, Kelley SW, Hurwitz SA, Travers JB (1998) Expression of the platelet-activating factor receptor results in enhanced ultraviolet B radiation-induced apoptosis in a human epidermal cell line. J Biol Chem 273:18891-18897.

Barth PG (1987) Disorders of neuronal migration. Can J Neurol Sci 14:1-16

Bazan NG (1998) The neuromessenger platelet-activating factor in plasticity and neurodegeneration Prog Brain Res 118:281-291.

Behrens TW, Goodwin JS (1990) Control of human T cell proliferation by platelet-activating factor. Int J Immunopharmacol 12:175-184.

Bennett SAL, Chen J, Brewer C, Stevens WD, Davidson CM, Holden D, Fortin T, Franks DJ, Pappas BA (2001) Loss of retinal ganglion cells expressing platelet activating factor receptor following chronic hypoperfusion. Invest Ophthalmol Vis Sci, submitted for publication.

Bennett SAL, Chen J, Pappas BA, Roberts DCS, Tenniswood M (1998) Platelet activating factor receptor expression is associated with neuronal apoptosis in an in vivo model of excitotoxicity. Cell Death Differ 5:867-875.

Bennett SAL, Birnboim HC (1997) Receptor-mediated and protein kinase-dependent growth enhancement of primary human fibroblasts by platelet-activating factor. Mol Carcinog 20:366-375.

Bennett SAL, Chen JH, and Birnboim HC (1994) Recovery of a rare clone from a population of unstable retroviral vector-expressing mammalian cells using a new RNA extraction and slot-blot protocol. J Virol Methods 50: 245-255.

Bennett SAL, Leite LC, Birnboim HC (1993) Platelet activating factor, an endogenous mediator of inflammation, induces phenotypic transformation of rat embryo cells. Carcinogenesis 14:1289-1296.

Benveniste J, Hensen PM, Cochrane CG (1972) Leukocyte-dependent histamine release from rabbit platelets. The role of IgE, basophils and platelet-activating factor. J Exp Med 136:1356-1377.

Benveniste J, Tence M, Varenne P, Bidault J, Boullet C, Polonsky J (1979) Semi-synthese et structure purposee du facteur activant les plaquettes (PAF); PAF-acether, un alkyl ether analogue de la lysophophatidylcholine. CR Hebd Seances Acad Sci Ser D Sci Nat 289:1037-1040.

Bernhardt R, Huber G, Matus A (1985) Differences in the developmental patterns of three microtubule-associated proteins in the rat cerebellum. J Neurosci 5:977-991.

Berthou C, Bourge JF, Zhang Y, Soulie A, Geromin D, Denizot Y, Sigaux F, Sasportes M (2000) Interferon-gamma-induced membrane PAF-receptor expression confers tumor cell susceptibility to NK perforin-dependent lysis. Blood 95:2329-2336.

Birkle DL, Kurian P, Braquet P, Bazan NG (1988) Platelet-Activating Factor Antagonist BN52021 Decreases Accumulation of Free Polyunsaturated Fatty Acid in Mouse Brain During Ischemia and Electroconvulsive Shock. J Neurochem 51:1900-1905.

Bito H, Honda Z, Nakamura M, Shimizu T (1994) Cloning, expression and tissue distribution of rat platelet-activating-factor-receptor cDNA. Eur J Biochem 221:211-218.

Bito H, Nakamura M, Honda Z, Izumi T, Iwatsubo T, Seyama Y, Ogura A, Kudo Y, Simizu T (1992) Platelet-activating factor (PAF) receptor in rat brain: PAF mobilizes intracellular Ca2+ in hippocampal neurons. Neuron 9:285-294.

Bix GJ and Clark GD (1998) Platelet-activating Factor Receptor Stimulation Disrupts Neuronal Migration In vitro. J Neurosci 18:307-318.

Blank ML, Lee TC, Fitzgerald V, Snyder F (1981) A Specific Acetylhydrolase for 1-Alkyl-2-acetyl-sn-glycero-3-phosphocholine (a Hypotensive and Platelet-activating Lipid). J Biol Chem 256:175-178.

Blank MI, Snyder F, Byers LW, Brooks B, Muirehead EE (1979) Antihypertensive activity of an alkyl ether analog of phosphatidylcholine. Biochem Biophys Res Commun 90: 1194-1200.

Bliss TV and Collingridge GL (1993) A synaptic model of memory: long-term potentiation in the hippocampus. Nature 361:31-39.

Boccellino M, Biancone L, Cantaluppi V, Ye RD, Camussi G (2000) Effect of Platelet-Activating Factor Receptor Expression on CHO Cell Motility. J Cell Physiol 183:254-264.

Bonaccorsi L, Luconi M, Maggi M, Muratori M, Forti G, Serio M, Baldi E (1997) Protein tyrosine kinase, mitogen-activated protein-kinase and protein kinase C are involved in the mitogenic signaling of platelet-activating factor (PAF) in HEC-1A cells. Biochim Biophys Acta 1355:155-166.

Braquet P, Rola-Pleszczynski M (1987) The role of PAF in immunological responses: a review. Prostaglandins 34:143-148.

Braquet P, Touqui L, Shen TY, Vargaftig BB (1987) Perspectives in platelet-activating factor research. Pharmacol Rev 39:97-145.

Bussolati B, Biancone L, Cassoni P, Russo S, Rola-Pleszczynski M, Montrucchio G, Camussi G (2000) PAF Produced by Human Breast Cancer Cells Promotes Migration and Proliferation of Tumor Cells and Neo-Angiogenesis. Am J Pathol 157:1713-1725.

Cahana A, Escamez T, Nowakowski RS, Hayes NL, Giacobini M, von Holst A, Shmueli O, Sapir T, McConnell SK, Wurst W, Martinez S, Reiner O (2001) Targeted mutagenesis of Lis1 disrupts cortical development and LIS1 homodimerization. Proc Natl Acad Sci USA 98:6429-6434.

Calcerrada MC, Perez-Alvarez MJ, Catalan RE, Martinez AM (1999a) Modulation of protein kinase C isoforms by PAF in cerebral cortex. Prostaglandins Other Lipid Mediat 58:19-27.

Calcerrada MC, Catalan RE, Perez-Alvarez MJ, Miguel BG, Martinez AM (1999b) Platelet-activating factor stimulation of p125(FAK) and p130(Cas) tyrosine phosphorylation in brain. Brain Res 835:275-281.

Calcerrada MC, Catalan RE, Martinez AM (1999c) Glutamate release is involved in PAF-increased cyclic GMP levels in hippocampus. Biochem Mol Biol Int 47:529-535.

Carlson SA, Chatterjee TK, Fisher RA (1996) The third intracellular domain of the platelet-activating factor receptor is a critical determinant in receptor coupling to phosphoinositide pphospholipaseC-activating G proteins. Studies using intracellular domain minigenes and receptor chimeras. J Biol Chem 271:23146-23153.

Carmody RJ, Cotter TG (2001) Signalling apoptosis: a radical approach. Redox Rep 6:77-90.

Catalan RE, Martinez AM, Aragones MD, Fernandez I, Lombardia M, Miguel BG (1992) PAF-induced activation of polyphosphoinositied-hydrolyzing phospholipase C in cerebral cortex. Biochem Biophys Res Commun 183:300-305.

Chase PB, Yang JM, Thompson FH, Halonen M, Regan JW (1996) Regional mapping of the human platelet-activating factor receptor gene (PTAFR) to 1p35-p34.3 by fluorescence in situ hybridization. Cytogenet Cell Genet 72:205-207.

Chen C and Bazan NG (1999) Platelet-activating factor inhibits ionotropic GABA receptor activity in cultured hippocampal neurons. Neuroreport 20: 3831-3835.

Chong SS, Pack SD, Roschke AV, Tanigami A, Carrozzo R, Smith AC, Dobyns WB, Ledbetter DH (1997) A revision of the lissencephaly and Miller-Dieker syndrome critical regions in chromosome 17p13.3. Hum Mol Genet 6:147-155.

Clark GD, Zorumski CF, McNeil RS, Happel LT, Ovella T, McGuire S, Bix GJ, Swann JW (2000) Neuronal platelet-activating factor receptor signal transduction involves a pertussis toxin-sensitive G-proteins. Neurochem Res 25:603-611.

Clark GD, McNeil RS, Bix GJ, Swann JW (1995) Platelet-activating factor produces neuronal growth cone collapse. Neuroreport 6:2569-2575.

Clark GD, Happel LT, Zorumski CF, Bazan NG (1994) The role of platelet-activating factor in the release of excitotoxic neurotransmitters. J Lipid Mediat 10:95-97.

Clark GD, Happel LT, Zorumski CF, Bazan NG (1992) Enhancement of hippocampal excitatory synaptic transmission by platelet-activating factor. Neuron 9;1211-1216.

DeFeudis FV, Drieu K (2000) Ginkgo biloba extract (EGb 761) and CNS functions: basic studies and clinical applications. Curr Drug Targets 1:25-58.

Demopouolos CA, Pinckard RN, Hanahan DJ (1979) Platelet-activating factor evidence for 1-O-alkyl-2-acetyl-sn-glycero-3-phosphorylcholine as the active component (a new class of lipid chemical mediators). J Biol Chem 54:9355-9358.

Denizot Y, Dupuis F, Trimoreau F, Verger C, Allegraud A, Praloran V (1996) PAF and haematopoiesis: IX. Platelet-activating factor increases DNA synthesis in human bone marrow cells. J Lipid Mediat Cell Signal 15:1-4.

Dieker H, Edwards RH, Zurhein G, Chou SM, Hartman HA, Opitz JM (1969) The lissencephaly syndrome. The clinical delineation of birth defects. II. Malformation syndromes. New York: National Foundation-March of Dimes pp53-64.

Dobyns WB, Reiner O, Carrozzo R, Ledbetter DH (1993) Lissencephaly. A human brain malformation associated with deletion of the LIS1 gene located at chromosome 17p13. JAMA 270:2838-2842.

Dobyns WB, Curry CJR, Hoyme HE, Turlington L, Ledbetter DH (1991) Clinical and Molecular Diagnosis of Miller-Dieker Syndrome. Am J Hum Genet 48:584-594.

Domingo MT, Spinnewyn B, Charbrier PE, Braquet P (1994) Changes in [3H]PAF binding and PAF concentrations in gerbil brain after bilateral common carotid artery occlusion: a quantitative autoradiographic study. Brain Res 640:268-276.

Dupuis F, Levasseur S, Jean-Louis F, Dulery C, Praloran V, Denizot Y, Michel L (1997) Production, metabolism and effect of platelet-activating factor on the growth of the human K562 erythroid cell line. Biochim Biophys Acta 1359:241-249.

Faulkner NE, Dujardin DL, Tai C-Y, Vaughan KT, O'Connell CB, Wang Y, Vallee RB (2000) A role for the lissencephaly gene LIS1 in mitosis and cyoplasmic dynein function. Nat Cell Biol 2:784-791.

Feng Y, Olson EC, Stukenberg PT, Flanagan LA, Kirschner MW, Walsh CA (2000) LIS1 regulates CNS lamination by interacting with mNudE, a central component of the centrosome. Neuron 28:665-679.

Feuerstein G, Yue G, and Lysko R (1990) Platelet activating factor: a putative mediator in central nervous system injury? Stroke 21 (suppl III): III-90-III-94.

Fleck MW, Hirotsune S, Gambello MJ, Phillips-Tansey E, Suares G, Mervis RF, Wynshaw-Boris A, McBain CJ (2000) Hippocampal Abnormalities and Enhanced Excitability in a Murine Model of Human Lissencephaly. J Neurosci 20:2439-2450.

Francescangeli E, Boila A, Goracci G (2000) Properties and regulation of microsomal PAF-synthesizing enzymes in rat brain cortex. Neurochem Res 5:705-713.

Francescangeli E, Lang D, Dreyfus H, Boila A, Freysz L, Goracci G (1997) Activities of enzymes involved in the metabolism of platelet-activating factor in neural cell cultures during proliferation and differentiation. Neurochem Res 22:1299-1307.

Garcia-Higuera I, Fenoglio J, Li Y, lewis C, Panchenko MP, Reiner O, Smith TF, Neer EJ (1996) Folding of proteins with WD-repeats: Comparison of six members of the WD-repeat superfamily to the G protein β subunit. Biochemistry 35:13985-13994.

Garcia Rodriguez C, Cundell DR, Tuomanen EI, Kolakowski LF Jr, Gerard C, Gerard NP (1995) The role of N-glycosylation for functional expression of the human platelet-activating factor receptor. Glycosylation is required for efficient membrane trafficking. J Biol Chem 270:25178-25184.

Gelbard HA, Nottet HS, Swindells S, Jett M, Dzenko KA, Genis P, White R, Wang L, Choi Y-B, Zhang D, Lipton SA, Tourtellotte WW, Epstein LG, Gendelman HE (1994) Platelet-Activating Factor: a Candidate Human Immunodeficiency Virus Type 1-Induced Neurotoxin. J Virol 68:4628-4635.

Gilboe DD, Kintner D, Fitzpatrick JH, Emoto SE, Esanu A, Braquet PG, Bazan NG (1991) Recovery of Postischemic Brain Metabolism and Function Following Treatment with a Free Radical Scavenger and Platelet-Activating Factor Antagonists. J Neurochem 56:311-319.

Goldman R, Moshonov S, Zor U (1999) Calcium-dependent PAF-stimulated generation of reactive oxygen species in a human keratinocyte cell line. Biochim Biophys Acta 1438:349-358.

Grassi S, Francescangeli E, Goracci G, Pettorossi VE (1998) Role of platelet-activating factor in long-term potentiation of the rat medial vestibular nuclei. J Neurophysiol 79:3266-3271.

Greene LA, Tischler AS (1976) Establishment of a noradrenergic clonal line of rat adrenal pheochromocytoma cells which respond to nerve growth factor. Proc Natl Acad Sci USA 73:2424-2428.

Haribabu B, Richardson RM, Verghese MW, Barr AJ, Zhelev DV, Snyderman R (2001) Function and regulation of chemoattractant receptors. Immunol Res 22:271-279.

Haribabu B, Zhelev DV, Pridgen BC, Richardson RM, Ali H, Snyderman R (1999) Chemoattractant receptors activate distinct pathways for chemotaxis and secretion. Role of G-protein usage. J Biol Chem 274:37087-37092.

Hattori K, Hattori M, Adachi H, Tsujimoto M, Arai H, Inoue K (1995) Purification and characterization of platelet-activating factor acetylhydrolase II from bovine liver cytosol. J Biol Chem 270:22308-22313.

Hattori M, Adachi H, Tsujimoto M, Arai H, Inoue K (1994) Miller-Dieker lissencephaly gene encodes a subunit of brain platelet-activating factor. Nature 370:216-218.

Hattori M, Arai H, Inoue K (1993) Purification and Characterization of Bovine Brain Platelet-activating Factor Acetylhydrolase. J Biol Chem 268:18748-18753.

Herrick-Davis K, Camussi G, Bussolino F, Baglioni C (1991) Modulation of neurite outgrowth in neuroblastoma cells by protein kinase C and platelet-activating factor. J Biol Chem 266:18620-18625.

Hershkkowitz M, Adunsky A (1996) Binding of platelet-activating factor to platelets of Alzheimer's disease and multi-infarct dementia patients. Neurobiology of Aging 17:865-868.

Hirashima Y, Ueno H, Karasawa K, Yokoyama K, Setaka M, Takaku A (2000) Transfection of the plasma-type platelet-activating factor acetylhydrolase gene attenuates glutamate-induced apoptosis in cultured rat cortical neurons. Brain Res 885:128-132.

Hirotsune S, Fleck MW, Gambello MJ, Bix GJ, Chen A, Clark GD, Ledbetter DH, McBain CJ, Wynshaw-Boris A (1998) Graded reduction of Pafah1b1 (Lis1) activity results in neuronal migration defects and early embryonic lethality. Nat Genet 19:333-339.

Ho YS, Swenson L, Derewenda U, Serre L, Wei Y, Dauter Z, Hattori M, Adachi T, Aoki J, Arai H, Inoue K, Derewenda ZS (1997) Brain acetylhydrolase that inactivates platelet-activating factor is a G-protein-like trimer. Nature 385:89-93.

Honda Z, Takano T, Gotoh Y, Nishida E, Ito K, Shimizu T (1994) Transfected platelet-activating factor receptor activates mitogen-activated protein (MAP) kinase and MAP kinase kinase in Chinese hamster ovary cells. J Biol Chem 269:2307-2315.

Honda Z, Nakamura M, Miki I, Minami M, Watanabe T, Seyama Y, Okado H, Toh H, Ito K, Miyamoto T, Shimizu T (1991) Cloning by functional expression of platelet-activating factor receptor from guinea-pig lung. Nature 349:342-346.

Horn F, Weare J, Beukers MW, Horsch S, Bairoch A, Chen W, Edvardsen O, Campagne F, Vriend G (1998) GPCRDB: an information system for G protein-coupled receptors. Nucleic Acids Res 26:275-279.

Hwang S (1990) Specific receptors of platelet-activating factor, receptor heterogeneity, and signal transduction mechanisms. J Lipid Mediators 2:123-158.

Hwang SB, Lam MH (1991) L-659,989: a useful probe in the detection of multiple conformational states of PAF receptors. Lipids 26:1148-1153.

Ihida K, Predescu D, Czekay RP, Palade GE (1999) Platelet activating factor receptor (PAF-R) is found in a large endosomal compartment in human umbilical vein endothelial cells. J Cell Sci 112:285-295.

Ishii I, Saito E, Izumi T, Ui M, Shimizu T (1998) Agonist-induced sequestration, recycling and resensitization of platelet-activating factor receptor. J Biol Chem 273:9878-9885.

Ishii I, Izumi T, Tsukamoto H, Umeyama H, Ui M, Shimizu T (1997) Alanine exchange of polar amino acids in the transmembrane domains of a platelet-activating factor receptor generate both constitutively active and inactive mutants. J Biol Chem 272:7846-7854.

Ishii S, Nagase T, Tashiro F, Ikuta K, Sato S, Waga I, Kume K, Miyazaki J, Shimizu T (1997) Bronchial hyperactivity, increased endotoxin lethality and melanocytic tumorigenesis in transgenic mice overexpressing platelet-activating factor receptor. EMBO J 16:133-142.

Ishii S, Matsuda Y, Nakamura M, Waga I, Kume, Izumi T, Shimizu T (1996) A murine platelet-activating factor receptor gene: cloning, chromosomal localization and up-regulation of expression by lipopolysaccharide in peritoneal resident macrophages. Biochem J 314:671-678.

Kajihara A, komooka H, Kamiya K, Yoneda T, Nakamura M, Shimizu T, Umeyama H (1994) Three-dimensional model of the human PAF receptor. J Lipid Mediat Cell Signal 9:185-196.

Kato K, Clark GD, Bazan NG (1994) Platelet-activating factor as a potential retrograde messenger in CA1 hippocampal long term potentiation. Nature 367:175-179.

Kato T, Kundo I, Hayashi H, Onozaki K, Inoue K (1988) Augmentation of DNA synthesis in guinea pig bone marrow cells by platelet-activating factor (PAF). Biochem Biophys Res Commun 157:563-568.

Khoury J and Langleben D (1996) Platelet-activating factor stimulates lung pericyte growth in vitro. Am J Physiol 270 (2 Pt 1):L298-304.

Kornecki E and Ehrlich YH (1988) Neuroregulatory and Neuropathological Actions of the Ether-Phospholipid Platelet-Activating Factor. Science 240:1792-1794.

Kudo I, Kato T, Hayashi H, Yanoshita R, Ikizawa K, Uda H, Inoue K (1991) Guinea pig bone marrow cells treated with platelet-activating factor generate factor(s) which affects their DNA synthesis and microbicidal activity. Lipids 26:1065-1070.

Kuijpes TW, van den Berg JM, Tool AT, Roos D (2001) The impact of platelet-activating factor (PAF)-like mediators on the functional activity of neutrophils: anti-inflammatory effects of human PAF-acetylhydrolase. Clin Exp Immunol 123:412-420.

Kumar R, Harvey SA, Kester M, Hanahan DJ, Olson MS (1988) Production and effects of platelet-activating factor in the rat brain. Biochim Biophys Acta 963:375-383.

Kunz D, Gerard NP, Gerard C (1992) The Human Leukocyte Platelet-activating Factor Receptor; cDNA cloning, cell surface expression, and construction of a novel epitope-bearing analog. J Biol Chem 267:9101-9106.

Langley SM, Chai PJ, Jaggers JJ, Ungerleider RM (1999) Platelet-activating factor receptor antagonism improves cerebral recovery after circulatory arrest. Ann Thorac Surg 68:1578-1584.

Lave D, James C, Rajoharison H, Floch A, Robaut C, Sedivy P (1990) [PAF-acether antagonistic pyrrolo[1,2-c]thiazoles: from RP 48740 to RP 59227]. J Pharm Belg 45:219-223.

Le Gouill C, Parent JL, Rola-Pleszczynski M, Stankova J (1997) Role of the Cys^{90}, Cys^{95} and Cys^{173} residues in the structure and function of the human platelet-activating factor receptor. FEBS Lett 402:203-208.

Leprince C, Vivier E, Treton D, Galanaud P, Benveniste J, Richard Y, Thomas Y (1991) Immunoregulatory functions of paf-acether. VI. Dual effect on human B cell proliferation. Lipids 26:1204-1208.

Levi A, Alema S (1991) The mechanism of action of nerve growth factor. Annu Rev Pharmacol Toxicol 31:205-228.

Liu Z, Steward R, Luo L (2000) Drosophila Lis1 is required for neuroblast proliferation, dendritic elaboration and axonal transport. Nat Cell Biol 2:776-783.

Loucks EB, Symersky P, Qayumi AK (1997) Platelet-activating factor antagonism: a new concept in the management of regional myocardial ischemia-reperfusion injury. J Invest Surg 10:321-338.

MacLennan KM, Smith PF, Darlington CL (1996) Platelet-Activating Factor in CNS. Prog Neurobiol 50:585-596.

Marcheselli VL and Bazan NG (1994) Platelet-activating factor is a messenger in the electroconvulsive shock-induced transcriptional activation of c-fos and zif-268 in hippocampus. J Neurosci Res 37: 54-61.

Marcheselli VL, Rossowska MJ, Domingo MT, Braquet P, Bazan NG (1990) Distinct platelet-activating factor binding sites in synaptic endings and in intracellular membranes of rat cerebral cortex. J Biol Chem 265:9140-9145.

Matsuo Y, Kihara T, Ikeda M, Ninomiya M, Onodera H, Kogure K (1996) Role of platelet-activating factor and thromboxane A2 in radical production during ischemia and replerfusion of the rat brain. Brain Res 709:296-302.

McNeil RS, Swann JW, Brinkley BR, Clark GD (1999) Neuronal Cytoskeletal Alterations Evoked by a Platelet-Activating Factor (PAF) Analogue. Cell Motility and the Cytoskeleton 43:99-113.

Miller JQ (1963) Lissencephaly in 2 siblings. Neurology 13:841-850.

Milligan G (2000) Receptors as kissing cousins. Science 288:65-67.

Mori M, Aihara M, Kume K, Hamanoue M, Kohsaka S, Shimizu T (1997) Localization of PAF receptor in the rat brain. Adv Exp Med Biol 407:357-363.

Mori M, Aihara M, Kume K, Hamanoue M, Kohsaka S, Shimizu T, (1996) Predominant expression of platelet-activating factor receptor in rat brain microglia. J Neurosci 16:3590-3600.

Morooka T and Nishida E (1998) Requirement of p38 mitogen-activated protein kinase for neuronal differentiation in PC12 cells. J Biol Chem 273:24285-24288.

Morris AJ, Malbon CG (1999) Physiological Regulation of G Protein-Linked Signaling. Physiological Reviews 79:1373-1430.

Muirhead EE Leach BE, Byers LW, Brooks B, Rightsel WA, Pitcock JA (1976) Anti-hypertensive lipid tissue from the culture of renomedullary interstitial cells of the rat. Clin Sci Mol Med Supp 3:2878-2908

Mukherjee PK, DeCoster MA, Campbell FZ, Davis RJ, Bazan NG (1999) Glutamate receptor signaling interplay modulates stree-sensitive mitogen-activated protein kinases and neuronal cell death. J Biol Chem 274:6493-6498.

Muller E, Dagenais P, Alami N, Rola-Pleszczynski M (1993) Identification and functional characterization of platelet-activating factor receptors in human leukocyte populations using polyclonal anti-peptide antibody. Proc Natl Acad Sci 90:5818-5822.

Mutoh H, Bito H, Minami M, Nakamura M, Honda Z, Izumi T, Nakata R, Kurachi Y, Terano A, Shimizu T (1993) Two different promoters direct expression of two distinct forms of mRNAs of human platelet-activating factor receptor. FEBS 322:129-134.

Nakamura M, Honda Z, Izumi T, Sakanaka C, Mutoh H, Minami M, Bito H, Seyama Y, Matsumoto T, Noma M, Shimizu T (1991) Molecular cloning and expression of platelet-activating factor receptor from human leukocytes. J Biol Chem 266:20400-20405.

Neer EJ, Schmidt CJ, Nambudripad R, Smith T (1994) The ancient regulatory-protein family of WD-repeat proteins. Nature 371:297-300.

Niethammer M, Smith DS, Ayala R, Peng J, Ko J, Lee MS, Morabito M, Tsai LH (2000) NUDEL is a novel cdk5 substrate that associates with LIS1 and cytoplasmic dynein. Neuron 28:697-711.

Nishida K, Markey SP (1996) Platelet-activating factor in brain regions after transient ischemia in gerbils. Stroke 27:514-518.

Nishida K, Markey SP, Kustova Y, Morse HC, Skolnick P, Basile AS, Sei Y (1996) Increased brain levels of platelet activating factor in a murine acquired immune deficiency syndrome are NMDA receptor-mediated. J Neurochem 66:433-435.

Nixon AB, O'Flaherty JT, Salyer JK, Wykle RL (1999) Acetyl-CoA:1-O-alkyl-2-lyso-sn-glycero-3-phosphocholine acetyltransferase is directly activated by p38 kinase. J Biol Chem 274:5469-5473.

Nogami K, Hirashima Y, endo S, Takaku A (1997) Involvement of platelet-activaing factor (PAF) in glutamate neurotoxicity in rat neuronal cultures. Brain Res 754:72-78.

Nothwang HG, Kim HG, Aoki J, Geisterfer M, Kubart S, Wegner RD, van Moers A, Ashworth LK, Haaf T, Bell J, Arai H, Tommerup N, Ropers HH (2001) Functional hemizygosity of PAFAH1B3 due to a PAFAH1B3-CLK2 fusion gene in a female with mental retardation, ataxia and atrophy of the brain. Hum Mol Genet 10:797-806.

O'Flaherty JT, Redman Jr JF, Schmitt JT, Ellis M, Surles JR, Marx MH, Piantadosi C, Wykle RL (1987) A biologically potent, non-metabolizable analog of platelet-activating factor. Biochem Biophys Res Commun 147:18-24.

Ogden F, DeCoster MA, Bazan NG (1998) Recombinant Plasma-Type Platelet-Activating Factor Acetylhydrolase Attenuates NMDA-Induced Hippocampal Neuronal Apoptosis. J Neurosci Res 53:677-684.

Okamoto M, Yoshida K, Uchida I, Nishikawa M, Kohsaka M, Aoki H (1986) Studies of platelet activating factor (PAF) antagonists from microbial products. I. Bisdethiobis(methylthio)gliotoxin and its derivatives. Chem Pharm Bull (Tokyo) 34:340-344.

Panetta T, Marcheselli VL, Braquet P, Spinnewyn B, Bazan NB (1987) Effects of a platelet-activating factor antagonist (BN 52021) on free fatty acids, diacylglycerols, polphosphoinositides, and blood flow in the gerbil brain: inhibition of ischemia/reperfusion-induced cerebral injury. Biochem Biophys Res Commun 149:580-587.

Parent JL, Le Gouill C, Rola-Pleszczynski M, Stankova J (1996a) Mutation of an aspartate at position 63 in the human platelet-activating factor receptor augments binding affinity but abolishes G-protein-coupling and inositol phosphate production. Biochem Biophys Res Commun 219:968-975.

Parent JL, Le Gouill C, Escher E, Rola-Pleszczynski M, Stankova J (1996b) Identification of Transmembrane Domain Residues Determinant in the Structure-Function Relationship of the Human Platelet-activating Factor Receptor by Site-directed Mutagenesis. J Biol Chem 271:23298-23303.

Parent JL, Le Gouill C, de Brum-Fernandes AJ, Rola-Pleszczynski M, Stankova J (1996c) Mutations of Two Adjacent Amino Acids Generate Inactive and Constitutively Active Forms of the Human Platelet-activating Factor Receptor. J Biol Chem 271:7949-7955.

Perry SW, Hamilton JA, Tjoelker LW, Dbibo G, Dzenko KA, Epstein LG, Hannum Y, Whittaker JS, Dewhurst S, Gelbard HA (1998) Platelet-activating factor receptor activation – An initiator step in HIV-1 neuropathogenesis. J Biol Chem 273:17660-17664.

Piechaczyk M, Blanchard JM, Marty L, Dani C, Panabieres F, Sabouty SE, Fort P, and Jeanteur P (1984) Post-transcriptional regulation of glyceraldehyde-3-phosphate-dehydrogenase gene expression in rat tissues. Nucleic Acids Res. 12: 6951-6963.

Pinckard RN, Woodard DS, Showell HJ, Conklyn MJ, Novak MJ, McManus LM (1994) Structural and (patho)physiological diversity of PAF. Clin Rev Allergy 12:329-359.

Predescu D, Ihida K, Predescu S, Palade GE (1996) The vascular distribution of the platelet-activating factor receptor. Eur J Cell Biol 69:86-98.

Prescott SM, Zimmerman GA, Stafforini DM, McIntyre TM (2000) Platelet-Activating Factor and Related Lipid Mediators. Annu Rev Biochem 69:419-445.

Probst WC, Snyder LA, Schuster DI, Brosius J, Sealfon SC (1992) Sequence alignment of the G-protein coupled receptor superfamily. DNA Cell Biol 11:1-20.

Prosperi E (1997) Multiple roles of the proliferating cell nuclear antigen: DNA replication, repair and cell cycle control. Prog Cell Cycle Res 3:193-210.

Reiner O, Carrozzo R, Shen Y (1993) Isolation of a Miller-Dieker lissencephaly gene containing G protein β-subunit-like repeats. Nature 364:717-721.

Roth M, Nauck M, Yousefi S, Tamm M, Blaser K, Perruchoud AP, Simon HU (1996) Platelet-activating factor exerts mitogenic activity and stimulates expression of interleukin 6 and interleukin 8 in human lung fibroblasts via binding to its functional receptor. J Exp Med 184:191-201.

Sapir T, Cahana A, Seger R, Nekhai S, Reiner O (1999) LIS1 is a microtubule-associated phosphoprotein. Eur J Biochem 265:181-188.

Sapir T, Elbaum M, Reiner O (1997) Reduction of microtubule catastrophe events by LIS1, platelet-activating factor acetylhydrolase subunit. EMBO J 16:6977-6984.

Sasaki S, Shionoya A, Ishida M, Gambello MJ, Yingling J, Wynshaw-Boris A, Hirotsune S (2000) A LIS1/NUDEL/cytoplasmic dynein heavy chain complex in the developing and adult nervous system. Neuron 28:681-696.

Sato S, Kume K, Ito C, Ishii S, Shimizu T (1999) Accelerated proliferation of epidermal keratinocytes by the transgenic expression of the platelet-activating factor receptor. Arch Dermatol Res 291:614-621.

Schifitto G, Sacktor N, Marder K, McDermott MP, McArthur JC, Kieburtz K, Small S, Epstein LG and the Neurological AIDS Research Consortium (1999) Randomized trial of the platelet-activating factor antagonist lexipafant in HIV-associated cognitive impairment. Neurology 53:391-396.

Seyfried CE, Schweickart VL, Godiska R, Gray PW (1992) The human platelet-activating factor receptor gene (PTAFR) contains no introns and maps to chromosome 1. Genomics 13:832-834.

Shen TY, Hwang S-B, Doebber TW, Robbins JC (1987) The Chemical and Biological Properties of PAF Agonists, Antagonists, and Biosynthetic Inhibitors. In: Platelet Activating Factor and Related Lipid Mediators, Snyder F, ed., New York, Plenum Press, pp153-190.

Shi LC, Wang HY, Horwitz J, Friedman E (1996) Guanine nucleotide regulatory proteins, Gq and Gi1/2, mediate platelet-activating factor-stimulated phosphoinositide metabolism in immortalized hippocampal cells. J Neurochem 67:1478-1484.

Shmueli O, Cahana A, Reiner O (1999) Platelet-Activating Factor (PAF) Acetylhydrolase Activity, LIS1 Expression, and Seizures. J Neurosci Res 57:176-184.

Shukla SD (1992) Platelet-activating factor receptor and signal transduction mechanisms. FASEB J 6:2296-2301.

Smith DS, Niethammer M, Ayala R, Zhou Y, Gamvello MJ, Wynshaw-Boris A, Tsai L-H (2000) Regulation of cytoplasmic dynein behaviour and microtubule organization by mammalian Lis1. Nat Cell Biol 2:767-775.

Snyder F (1995) Platelet-activating factor: the biosynthetic and catabolic enzymes. Biochem J 305:689-705.

Snyder F (1994) Metabolic processing of PAF. Clin Rev Allergy 12:309-327.

Stafforini DM, McIntyre TM, Zimmerman GA, Prescott SM (1997) Platelet-activating Factor Acetylhydrolases. J Biol Chem 272:17895-17989.

Stremler KE, Stafforini DM, Prescott SM, McIntyre TM (1991) Human plasma platelet-activating factor acetylhydrolase. Oxidatively fragmented phospholipids as substrates. J Biol Chem 266:11095-11103.

Sweeney KJ, Clark GD, Prokscha A, Dobyns WB, Eichele G (2000) Lissencephaly associated mutations suggest a requirement for the PAFAH1B heterotrimeric complex in brain development. Mech Dev 92:263-271.

Takano T, Honda Z, Sakanaka C, Izumi T, Kameyama K, Haga K, Haga T, Kurokawa K, Shimizu T (1994) Role of cytoplasmic tail phosphorylation sites of platelet-activating factor receptor in agonist-induced desensitization. J Biol Chem 269:22453-22458.

Terasita Z, Imura Y, Takatani M, Tsushima S, Nishikawa K (1987) CV-6209, a highly potent antagonist of platelet activating factor in vitro and in vivo. J Pharmacol Exp Ther 242:263-268.

Terashita ZI, Tsushima S, Yoshioka Y, Nomura H, Inada Y, Nishikawa K (1983) CV-3988: a specific antagonist of platelet activating factor (PAF). Life Sci 32:1975-1982.

Tiemann U, Neels P, Pohland R, Walzel H, Lohrke B (1999) Influence of inhibitors on increase in intracellular free calcium and proliferation induced by platelet-activating factor in bovine oviductal cell. J Reprod Fertil 116:63-72.

Tokumura A, Yotsumoto T, Hoshikawa T, Tanaka T, Tsukatani H (1992) Quantitative analysis of platelet-activating factor in rat brain. Life Sci 51:303-308.

van Biesen T, Hawes BE, Raymond JR, Luttrell LM, Koch WJ, Lefkowitz RJ (1996) G(o)-protein alpha-subunits activate mitogen-activated protein kinase via a novel protein kinase C-dependent mechanism. J Biol Chem 271:1266-1269.

Ved HS, Gustow E, Pieringer RA (1991) Regulation of neuronal differentiation in neuron-enriched primary cultures from embryonic rat cerebra by platelet-activating factor and the structurally related glycerol ether lipid dodecylglycerol. J Neurosci Res 30:353-358.

Wang JH and Sun GY (2000) Platelet activating factor (PAF) antagonists on cytokine induction of iNOS and sPLA2 in immortalized astrocytes. Neurochem Res 25:613-619.

Wang X, Bae JH, Kim SU, McLarnon JG (1999) Platelet-activating factor induced Ca(2+) signaling in human microglia. Brain Res 42:159-165.

Wang DS, Shaw R, Hattori M, Arai H, Inoue K, Shaw G (1995) Binding of pleckstrin homology domains to WD40/β-transducing repeat containing segments of the protein product of the Lis-1 gene. Biochem Biophys Res Comm 209:622-629.

Watson S, Arkinstall S (1994) The G-Protein Linked Receptor Facts Book. Academic Press Inc., Toronto.

Westmoreland SV, Kolson D, Gonzalez-Scarano F (1996) Toxicity of TNFα and platelet activating factor for human NT2N neurons: a tissue culture model for human immunodeficiency virus dementia. J Neuro Vir 2:118-126.

Wieraszko A, Gang L, Kornecki E, Hogan MV, Ehrlich YH (1993) Long-term potentiation in the hippocampus induced by platelet-activating factor. Neuron 10:553-557.

Wynshaw-Boris A, Gambello MJ (2001) LIS1 and dynein motor function in neural migration and development. Genes Dev 15:639-651.

Yamakawa Y, Takano M, Patel M, Tien N, Takada T, Bulkley GB (2000) Interaction of platelet activating factor, reactive oxygen species generated by xanthine oxidase, and leukocytes in the generation of hepatic injury after shock/resuscitation. Ann Surg 231:387-398.

Ye RD, Prossnitz ER, Zou A, Cochrane CG (1991) Characterization of a human cDNA that encodes a functional receptor for platelet activating factor. Biochem Biophys Res Commun 180:105-111.

Yildrim G, Bastug M, Akcil IE, Ficicilar H, Koc E, Zaloglu N (2000) Does the platelet-activating factor affect the antioxidant defense system? The possible role of hyperbaric oxygenation. Biol Trace Elem Res 78:7-12.

Yoshikawa T, Naito Y, Kondo M (1999) Ginkgo biloba leaf extract: review of biological actions and clinical applications. Antioxid Redox Signal 1:469-480.

Yue TL and Feuerstein G (1994) Platelet-Activating-Factor - A Putative Neuromodulator and Mediator in the Pathophysiology of Brain Injury. Crit Rev Neurobiol 8: 11-24.

Yue TL, Gu JL, Feuerstein G (1992) Protein kinase C activator phorbol 12, 13-dibutyrate inhibits platelet activating factor –stimulated Ca2+ mobilization and phosphoinositide turnover in neurohybrid NG108-15 cells. Neurochem Res 17:997-1004.

APPENDIX A (CURRICULUM VITAE)

Cynthia Brewer
Email: cynthiabrewer10@hotmail.com

EDUCATION

University of Ottawa, M.Sc. Biochemistry, 2001
Thesis: Use of PC12 cells to characterize PAFR-GPCR-mediated activity in neural precursors.

Carleton University, B.Sc., Highest Honours in Biochemistry/Biotechnology, 1999
Awarded University Medal in Science

AWARDS/SCHOLARSHIPS

- Natural Sciences and Engineering Research Council of Canada Postgraduate Scholarship 2000
- Alzheimer Society of Canada Doctoral Training Award 2000 (declined)
- Ontario Graduate Scholarship in Science and Technology 1999
- Carleton University Medal in Science 1999
- Carleton University Scholarship 1995-1998

PUBLICATIONS

Books, Book Chapters, Published Reports

Brewer C, Bonin F, Imbeault S, Morin J, Nault M, Shen TY, Bennett SAL. Platelet activating factor-induced apoptotic loss is initiated independently of the platelet activating factor G-protein linked receptor in PC12 cells. *J Biol Chem*, submitted for publication.

Chen J, **Brewer C**, Stevens WD, Davidson CM, Holden D, Fortin T, Franks DJ, Pappas BA, Bennett SAL. Loss of retinal ganglion cells expressing platelet activating factor receptor following chronic hypoperfusion. *Invest Ophthalmol Vis Sci*, submitted for publication.

Bennett JA, **Brewer C**, Beyko S, and Bennett, SAL (1999) Cancer Control Strategies in Eleven OECD Countries (Health Canada, Ottawa).

Solicited WWW publication
Bennett JA, **Brewer C**, Beyko S, and Bennett SAL (1999) Cancer Control Strategies Report in OECD Countries, URL: http://www.hc-sc.gc.ca/hppb/cscc/background/scan.html

Published Abstracts and Presentations

Brewer C, Bonin F, Chen J, Bennett SAL (2001) Effect of Platelet Activating Factor Receptor Expression on Nerve Growth Factor Induced Differentiation of PC12 Cells. Canadian Federation of Biological Societies Annual Meeting (Ottawa, Canada, Poster presentation).

Brewer C, and Bennett SAL (2000) Use of PC12 Cells Expressing Recombinant Platelet Activating Factor Receptor to Investigate Neuronal Differentiation. Proceedings of the Ottawa Life Sciences Research Conference (Ottawa, Canada, Poster presentation).

Brewer C, and Bennett SAL (1999) Use of PC12 Cells Expressing EGFPhPAFR Fusion Proteins to Characterize a New Platelet Activating Factor Receptor Antibody. Proceedings of the Ottawa Life Sciences Research Conference (Ottawa, Canada, Poster presentation).

EMPLOYMENT HISTORY

University of Ottawa, Neural Regeneration Laboratory
2001-1999 Supervisor: Dr. S.A.L. Bennett **M.Sc. Research**

- employed a variety of molecular biology and cell culture strategies to (1) develop and characterize an *in vitro* model to address the influence of platelet activating factor receptor signaling in neuronal differentiation and migration (2) characterize a new antibody to platelet activating factor receptor
- involved in supervision and training of undergraduate students performing laboratory research

1999 (3mths) Supervisor: Dr. S.A.L. Bennett **Research Assistant**

- member of team reporting Cancer Control Strategies in OECD Countries to Health Canada

Industrial Hygiene Laboratory, Human Resources Development Canada
1999 and 1998 (summer) **Technologist**

- maintained and calibrated instruments for use in monitoring hazardous substances at sites across Canada

Carleton University, Chemistry Department
1997 (May-September) Supervisor: Dr. R. Wightman **Research Assistant**

- assisted with experiments involving the synthesis and analysis of Polychlorinated Naphthalenes using NMR, GC-MS, HPLC, FTIR

1996 (May-September) Supervisor: Dr. R. Burk **Research Assistant**

- assisted with chemical extraction and detection experiments using Solid-Phase Microextraction and GC-ECD